Evaluation of Residual Starch Determination Methods for Dried Distillers' Grains with Solubles (DDGS)

by

Desmond Koel Reed

A thesis submitted to the Faculty of Graduate Studies and Research

in partial fulfillment of the requirements for the degree of

Master of Science

in

Bioresource and Food Engineering

Agricultural, Food & Nutritional Science

Spring 2012

Edmonton, Alberta

Abstract

A co-product of ethanol production is known as dried distillers' grains with solubles (DDGS). DDGS contains residual starch that escaped hydrolysis under ideal conditions during ethanol production; therefore, residual starch in DDGS is expected to include enzyme-resistant starch. Common starch analysis methods involve enzymatic or chemical hydrolysis, but these methods may be unable to access resistant starch leading to an underestimation of the residual starch in DDGS. This study used several enzymatic starch analysis methods, with or without chemical pre-treatment, in an attempt to find an appropriate methodology for the measurement of residual starch in DDGS. Alternatively, an acid hydrolysis method that is commonly used by industry was also attempted for comparison. It was determined that the addition of a chemical solubilization step prior to enzymatic hydrolysis was necessary to access resistant starch present in DDGS samples. Chemical hydrolysis using dilute acid vastly overestimated the amount of residual starch in DDGS.

Acknowledgements

I want to sincerely thank my supervisors Dr. David Bressler and Dr. Thava Vasanthan for all of their help during my entire program, their patience and guidance was much appreciated. I would also like to thank them for giving me the opportunity to study in a laboratory with great equipment. I feel very fortunate to have studied under two very knowledgeable professors during my tenure as a graduate student.

I would like to acknowledge the funding sources that helped make this thesis possible. I owe a lot of thanks to the Biorefining Conversions Network, Alberta Innovates Biosolutions Corporation, and the University of Alberta. Without their support I would not have been able to complete my program.

I also want to thank the lab members of 2-38 for all their support and ideas regarding my project. It was a pleasure to work with you all over the course of my program. I wish you all the best in the future.

Lastly, I would like to express the utmost gratitude for my friends and family. I am lucky to have such a great group of people that are there to lend a helping hand whenever I may need it.

Table of Contents

CHAPTER 1: INTRODUCTION.....1
1.1 PROJECT BACKGROUND.....1
1.2 OBJECTIVES.....1
1.3 SIGNIFICANCE.....1

CHAPTER 2: LITERATURE REVIEW.....2
2.1 CEREAL GRAINS.....2
2.1.1 Proximate composition.....2
2.1.2 Kernel structure.....4
2.1.3 Starch.....8
2.1.3.1 Botanical origin.....8
2.1.3.2 Amylose.....8
2.1.3.3 Amylopectin.....10
2.1.3.4 Granular structure.....12
2.1.3.5 Crystallinity.....15
2.1.3.6 Starch-protein matrix.....16
2.1.3.7 Gelatinization and retrogradation.....18
2.2 ETHANOL AND DDGS PRODUCTION.....20
2.2.1 Grain milling.....20
2.2.1.1 Wet-milling.....20
2.2.1.2 Dry-grind process.....22
2.2.2 Mashing.....23
2.2.3 Conventional liquefaction.....24
2.2.4 Raw starch hydrolysis.....27
2.2.5 Simultaneous saccharification and fermentation.....29
2.2.6 Distillation.....30
2.2.7 Dryhouse technologies.....32
2.3 DDGS COMPOSITION.....33
2.3.1 Starch.....35
2.3.1.1 Soluble starch.....35
2.3.1.2 Resistant starch.....35
2.3.1.2.1 Resistant starch type I.....36
2.3.1.2.2 Resistant starch type II.....36
2.3.1.2.3 Resistant starch type III.....37
2.3.1.2.4 Resistant starch type IV.....38
2.3.1.2.5 Resistant starch type V.....38
2.3.2 Protein.....39
2.3.2 Lipids.....40
2.3.4 Non-starch polysaccharides.....41
2.4 STARCH DETERMINATION.....43

2.4.1 Enzymatic hydrolysis.....43
2.4.2 Acid hydrolysis.....46
2.4.3 Glucose analysis.....47
2.4.3.1 Glucose oxidase peroxidase enzyme.....47
2.4.3.2 Calculation to convert sample absorbance to % starch.....48

CHAPTER 3: MATERIALS AND METHODS.....49
3.1 MATERIALS.....49
3.1.1 DDGS.....49
3.1.2 Chemicals and other materials.....51
3.2 EXPERIMENTAL METHODS.....51
3.2.1 DDGS sieving.....51
3.2.2. Benchmarking residual starch analysis methods.....51
3.2.2.1 Megazyme method.....52
3.2.2.2 Megazyme method (DMSO format).....53
3.2.2.3 Acid hydrolysis.....54
3.2.2.4 Testing the effect of α-amylase concentration.....55
3.2.3 Alternative methods for residual starch analysis.....56
3.2.3.1 Buffer optimization experiments.....56
3.2.3.2 Megazyme method (KOH format).....57
3.2.3.3 Megazyme method + NaOH.....58
3.2.4 Moisture analysis.....59
3.2.5 Hydrolysis of non-starch polysaccharides.....59
3.2.6 Glucose reactivity.....60

CHAPTER 4: RESULTS AND DISCUSSION.....60
4.1 EVIDENCE OF RESIDUAL STARCH IN DDGS.....60
4.2 CHALLENGES OF RESIDUAL STARCH ANALYSIS.....62
4.3 BENCHMARKING RESIDUAL STARCH ANALYSIS METHODS.....63
4.3.1 Acid hydrolysis of non-starch polysacchardies.....69
4.3.2 Effect of α-amylase dilution.....70
4.4 ALTERNATIVE METHODS FOR RESIDUAL STARCH DETERMINATION.....71
4.4.1 Buffer optimization for the Megazyme + KOH method.....71
4.4.2 Buffer optimization for the Megazyme + NaOH methods.....72
4.4.3 Alternative methods for residual starch analysis in DDGS.....73
4.4.3.1 Effect of KOH and NaOH on non-starch polysaccharides.....79
4.4.3.2 Effect of KOH and NaOH on pure glucose.....81
4.5 DISCUSSION.....82

CHAPTER 5: CONCLUSIONS.....83
CHAPTER 6: BIBLIOGRAPHY.....85
APPENDIX 1: METHODS USED FOR THE FERMENTATION OF CEREAL GRAINS.....95

APPENDIX 2: METHODS USED FOR CONFOCAL MICROSCOPY.....96
APPENDIX 3: STATISTICAL ANALYSIS METHODS.....96

List of Tables

Table 2-1: Proximate composition of cereal grains

Table 2-2: Summary of the structural components of cereal grains (by % weight)

Table 2-3: Branch chain length distributions of amylopectin and amylose content of wheat, triticale, and barley granules

Table 2-4: Physical characteristics of cereal grain starch granules

Table 2-5: Gelatinization temperatures of corn, wheat, triticale, and barley

Table 2-6: The proximate composition of DDGS as determined by various studies

Table 3-1: Background information about the cereal grains used to produce DDGS

Table 3-2: Chemicals and materials used in thesis experiments

List of Figures

Figure 2-1: Summary of Osborne fractions and their functions within cereals

Figure 2-2: Cross section of a mature barley kernel

Figure 2-3: Stained cereal grain kernels

Figure 2-4: Glycosidic linkages in amylose

Figure 2-5: Glycosidic linkages in amylopectin

Figure 2-6: The proposed chain architecture of amylopectin; Hizukuri model

Figure 2-7: The structure of an A-type double helix

Figure 2-8: Radial orientation of starch granules

Figure 2-9: Alternating crystalline and amorphous lamellae

Figure 2-10: The crystallinity pattern in starch granules

Figure 2-11: Scanning electron micrographs of the starch-protein matrix

Figure 2-12: Confocal microscopy of the starch-protein matrix in barley flour

Figure 2-13: Scanning electron micrographs of native corn starch and gelatinized corn starch

Figure 2-14: Proposed model of amylose gel

Figure 2-15: Counter-current extraction process

Figure 2-16: Corn wet-milling process flow diagram

Figure 2-17: Corn dry-grinding process flow diagram

Figure 2-18: α-amylase hydrolysis of starch into dextrins

Figure 2-19: Laboratory scale jet-cooker

Figure 2-20: Mechanism of the Amadori rearrangement

Figure 2-21: Scanning electron micrographs of native corn starch granules and raw starch hydrolyzed corn starch granules

Figure 2-22: Synergism of α-amylase and amyloglucosidase

Figure 2-23: A simplified distillation column

Figure 2-24: Highly ordered regions of amylopectin that constitute resistant starch type II

Figure 2-25: Structure of furfural

Figure 2-26: Structure of 5-hydroxymethylfurfural

Figure 2-27: Proposed structure of melanoidins

Figure 2-28: Structure of repeating β-glucan molecules (β-1-4 linkages) in cellulose

Figure 2-29: Structure of repeating β-glucan molecules (β-1-3 and β-1-4 linkages) in β-glucan cellotriosyl and cellotetraosyl units

Figure 2-30: Interaction between cell wall polysaccharides

Figure 2-31: GOPOD reactions

Figure 3-1: Generalized flow-chart of the processing and drying conditions used to produce DDGS samples

Figure 3-2: A flow-chart of two enzyme hydrolysis methods used for residual starch benchmarking

Figure 3-3: A flow-chart of the acid hydrolysis method used for residual starch benchmarking

Figure 3-4: A flow-chart of the alternative residual starch analysis methods

Figure 4-1: Confocal microscopy images of residual starch in wheat DDGS

Figure 4-2: Benchmarking of residual starch analysis methods for barley DDGS samples

Figure 4-3: Benchmarking of residual starch analysis methods for corn DDGS samples

Figure 4-4: Benchmarking of residual starch analysis methods for triticale DDGS samples

Figure 4-5: Benchmarking of residual starch analysis methods for wheat DDGS samples

Figure 4-6: Measurement of glucose released from non-starch polysaccharides using acid hydrolysis

Figure 4-7: Effect of α-amylase concentration on starch hydrolysis of a known corn starch sample

Figure 4-8: Buffer optimization experiment for the Megazyme + KOH method using different DDGS grain types

Figure 4-9: Buffer optimization experiment for the Megazyme + NaOH method using wheat DDGS

Figure 4-10: Measurement of residual starch in barley DDGS using alternative analysis methods

Figure 4-11: Measurement of residual starch in corn DDGS using alternative analysis methods

Figure 4-12: Measurement of residual starch in triticale DDGS using alternative analysis methods

Figure 4-13: Measurement of residual starch in wheat DDGS using alternative analysis methods

Figure 4-14: Amount of glucose released from non-starch polysaccharides exposed to 2M KOH

Figure 4-15: Amount of glucose released from non-starch polysaccharides exposed to NaOH

Figure 4-16: Reactivity of glucose with KOH and NaOH

List of Equations

Equation 2-1: Calculation for conversion of sample absorbance into starch content

Equation 3-1: Calculation to determine sample moisture content

List of Abbreviations

DDGS = dried distillers' grains with solubles

DMSO = dimethylsulfoxide

KOH = potassium hydroxide

NaOH = sodium hydroxide

HCl = hydrochloric acid

GOPOD = glucose oxidase-peroxidase reagent

SSF = simultaneous saccharification and fermentation

DP = degree of polymerization

1. Introduction

1.1 Project background

First generation ethanol production involves the utilization of cereal grains that are milled, mashed, liquefied, saccharified, and fermented into ethanol. These industrial processes are necessary because yeast cannot absorb or utilize cereal starch in its native form. The starch must be hydrolyzed into small saccharides such as maltose or glucose using externally added enzymes. The produced sugars are small enough to be absorbed through yeast membranes where they can be used for yeast growth and for ethanol production.

First generation ethanol installations use a process commonly referred to as dry-grinding. As of 2007, 82% of existing ethanol production plants used a dry-grind process (Renewable Fuels Association, 2007), which produces two co-products: ethanol and distillers' grains with solubles (DDGS). DDGS is comprised of unhydrolyzed cereal grain components such as protein, fibre, lipid, and other minor compounds. The DDGS also contains yeast biomass and any residual glucose that was not absorbed by the yeast. During the process of dry-grinding, the majority of starch in the cereal grain is hydrolyzed into glucose and is utilized during fermentation by the yeast; however, some starch escapes hydrolysis and remains in the DDGS. The remaining starch in DDGS is referred to as residual starch. This project aims to accurately and reliably measure the residual starch in DDGS.

1.2 Objectives

This thesis had two main objectives including:

I) The benchmarking of existing residual starch determination methods

II) The improvement of existing residual starch determination methods

OR the development of new residual starch determination methods

1.3 Significance

Many studies have provided conflicting reports about the correlation between grain starch content and ethanol yield (Zhao *et al.*, 2009, Swanston *et al.*, 2007, Kindred *et al.*, 2008). It was suggested by Kindred *et al.* (2008) that inconsistent results are due to inherent variability and difficulty of starch measurements. Residual starch measurement is expected to be even more difficult than for native cereal grains due to the structure of the remaining starch and the high proportion of non-starch substrates in DDGS. It is important to find a method that is accurate and reliable so that true and consistent values are reported in the literature.

Residual starch in DDGS is often reported in academic studies (Belyea *et al.*, 2004, Hall *et al.*, 2001, Kim *et al.*, 2008, Zhao *et al.*, 2009); however, it is commonly determined with different methodologies. This thesis attempted to benchmark existing methodologies, develop modifications to existing methodologies, and test new methodologies used for residual starch measurement in order to recommend the most appropriate method. Consistent reporting of residual starch in DDGS would allow for improved comparisons between fermentation studies using different techniques. Furthermore, residual starch determination is used heavily in the enzyme production industry for starch hydrolysis optimization studies (Whitworth *et al.*, 2011); the favoured method identified during this study has the potential to support the production of better industrial enzymes.

2. Literature Review

2.1 Cereal grains

2.1.1 Proximate composition

Cereals are grouped as part of the grass family (*Poaceae*) and produce grains that are rich in carbohydrates. Cereal grains range from 70-85% carbohydrate by weight, depending on the type of grain (MacGregor and Bhatty, 1993; Matz, 1991). The most abundant carbohydrate stored in cereal grains are long polymer chains of α-linked glucose molecules, known as starch. There are two polymeric forms of starch: amylose and amylopectin. Another type of carbohydrate, broadly classed as fibre, is responsible for the structural features of the grain. These cell wall polysaccharides represent over 10% of the grain weight (MacGregor and Bhatty, 1993) and consist mainly of cellulose, hemi-cellulose, and β-glucan. Finally, another class of carbohydrate in cereal grains are simple sugars such as monosaccharides, disaccharides, and short chain oligosaccharides accounting for 2-4% of the cereal grain (Matz, 1991)-(see Table 2-1).

Cereal proteins are broadly classified based on solubility. The solubility classes are known as Osborne fractions (Ullrich, 2011) and are referred to as albumins, globulins, prolamins, and glutelins. The most abundant fractions in cereal grains are the prolamins and globulins which are soluble in either water or salt solutions respectively. The fraction type is also associated with certain physiological functions within the cereal grain (see Figure 2-1). Subclasses within these Osborne fractions are unique to each cereal grain type. For example, hordeins, zein, and gliadin (prolamins) are the major storage proteins in barley, corn, wheat & triticale respectively (Ullrich, 2011; Peterson, 1965; Matz, 1991; Siriamornpun *et al.*, 2004; Salmanowicz and Nowak, 2009).

Table 2-1: Proximate composition of cereal grains (% dwb)

Cereal	Starch	Protein	Lipids	Fibre	Ash	Sugars	Reference
Wheat	63-70	7-18	2-2.5	2-2.5	2-2.5	2-3.5	Peterson, 1965‡; Matz, 1991
Corn	67-75	8-12	3-6	8-12	1-3	2-3	Watson, 2003; Jane, 2009
Triticale	55-60	10-13	3-5	12-17	2-3	ND	Matz SA, 1991;
Barley (Hulled)	57-60	12-15	2-2.5	19-23	2-3	2.5-3.5	Newman and Newman, 2008
Barley (Hulless)	60-65	12-17	2.5-4	12-16	2-3.5	2-4	Newman and Newman, 2008

‡ Converted to dry weight basis (dwb)

ND = not determined

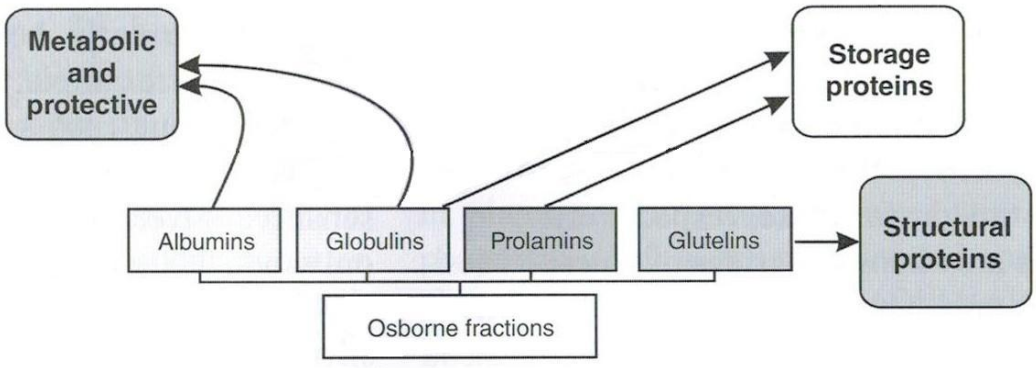

Figure 2-1: Summary of Osborne fractions and their functions within cereals

Adapted from: "Barley: Production, Improvement, and Uses. Ullrich SE. Copyright (2011) John Wiley and Sons. Reprinted by permission of John Wiley and Sons via Rightslink."

Lipids are classified into two groups in cereal grains: nonstarch and starch lipids (Newman and Newman, 2008). The nonstarch lipids exist as oil droplets sometimes referred to as spherosomes (MacGregor and Bhatty, 1993; Newman and Newman, 2008), which are composed of nonpolar lipids such as triacylglycerol, diacylglycerol, monoacylglycerol, and free fatty acid (MacGregor and Bhatty, 1993). In general, nonpolar lipids account for 75% of the total cereal lipids and the remaining 25% of lipids are polar (Newman and Newman, 2008). The polar lipids are located on the outer membranes of spherosomes and consist of glycolipids and phospholipids (Newman and Newman, 2008). A portion of the polar lipids also exist within, or adsorbed onto, starch granules and are referred to as starch lipids. Starch lipids are almost exclusively

lysophospholipid within wheat, barley, corn, and triticale grains (MacGregor and Bhatty, 1993; Morrison *et al.*, 1993). The lysophospholipids come in various forms and are capable of binding starch molecules.

Minor components in cereals such as minerals, vitamins, and phenolic compounds are limited to <3% of the cereal grain composition. The proportion of these compounds within barley, corn, wheat, and triticale are labelled in Table 2-1 as the ash content. Cereal grains are high in the minerals potassium, magnesium, phosphorus, manganese, and selenium and in the vitamins thiamine, niacin, and B_6. These compounds help complete physiological functions within the cereal grain and also provide physiological health benefits to humans and livestock (Ullrich, 2011).

2.1.2 Kernel structure

Cereal grains, such as barley, wheat, corn, and triticale are produced either by self-pollination or cross-pollination (Newman and Newman, 2008; Peterson, 1965; Kiesselbach, 1999). Once fertilization is complete, the kernel will develop over a period of weeks. The mature barley kernel consists of a hull (~13%), pericarp (~3%), aleurone (~5%), endosperm (~76%), and germ (~3%) - (Newman and Newman, 2008). Some barley genotypes are hulless and alter the kernel composition (see Figure 2-2). Variations in kernel structure composition exist between the cereal grains and the differences are summarized in Table 2-2.

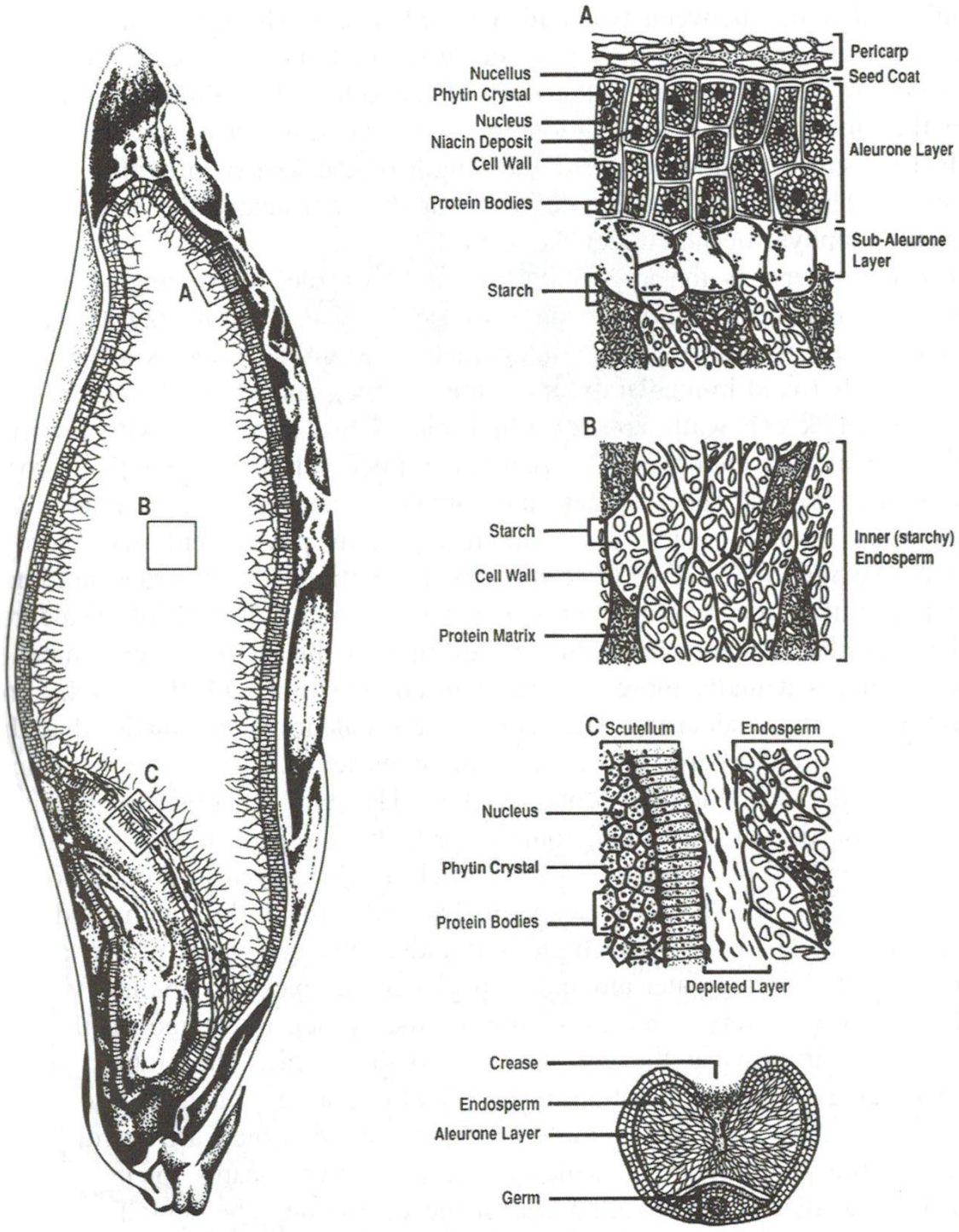

Figure 2-2: Cross section of a mature barley kernel

Table 2-2: Summary of the structural components of cereal grains (by % weight)

Cereal grain	Endo-sperm	Pericarp	Nucleus & Seed coat	Aleurone	Hull	Germ	Reference
Wheat	84	4	3	6	N/A	3	Peterson, 1965
Corn	85	2	1	2	N/A	10	Kiesselbach, 1999
Barley	76	2	1	5	13	3	Newman and Newman, 2008; Ullrich, 2011

Hulls, which are distinctive of barley, oat, rice, and millet cereal grains are an outer protective layer for the grain and consist mainly of cellulose, lignin, and silica (Newman and Newman, 2008). Hull-less varieties of barley or other cereal grains have been produced via plant breeding programs. For other cereal grains, the pericarp, seed coat, nucellus, and lipoid layers form the outer protective layer. The pericarp is the outermost layer (in hull-less varieties) and contains four to five layers of elongated cells (Peterson, 1965). The seed coat, comprised mainly of cellulose, lies beneath the pericarp and encloses nearly the whole kernel (Newman and Newman, 2008). Next is a thin lipoid layer, known as the epidermis nucellus which helps minimize nutrient loss from the endosperm, as well as functioning to reduce parasitic attack (Peterson, 1965). These outer layers are responsible for protecting the viability of the kernel for the growth of a new generation (Newman and Newman, 2008).

Inside the outer protective layers exists a layer of thick-walled cells rich in lipids, proteins, and minerals. For wheat, triticale, and corn kernels this layer is one cell thick, but barley contains two or three layers of thick-walled cells. These cells make up what is known as the aleurone layer (Ullrich, 2011). The aleurone layer is situated between the outer protective layers and the inner starchy endosperm and acts as a storage enclosure for the grain (Ullrich, 2011). Once activated by the hormone giberellin during germination, the aleurone layer releases enzymes to hydrolyze the starchy endosperm and utilize the energy stores for the growth of the plant.

The pericarp and germ are responsible for starch biosynthesis of the developing grain kernel (Ullrich, 2011), but at maturation little or no starch exists in any tissues except for the endosperm. Within the endosperm, the starch is embedded into a protein matrix and enclosed by cell walls made mainly of polysaccharides: arabinoxylans, β-glucan, and/or cellulose (Matz, 1991)-(see Figure 2-3). The makeup of the cell wall polysaccharides varies depending on the botanical origin.

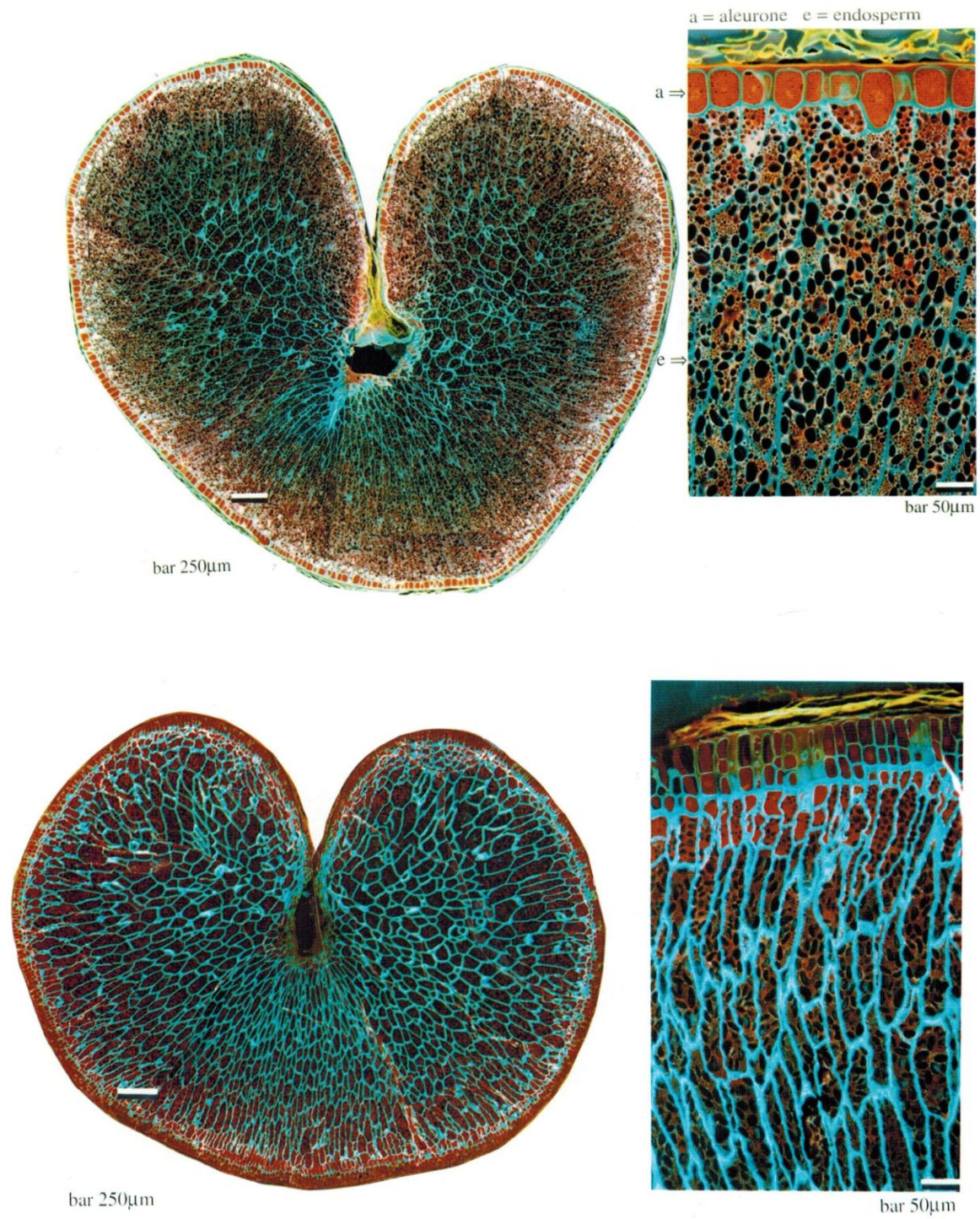

Figure 2-3: Stained cereal grain kernels (wheat and barley respectively; blue = cell walls; brown = protein; black = starch)

Lipids in cereals are concentrated in the germ and aleurone layer (Ullrich, 2011); however, the endosperm tissue contains higher amounts of total lipids (MacGregor and Bhatty, 1993). According to Bhatty (1982) lipids account for over 20% of the dry weight of the barley germ and up to 90% of barley germ lipids are triacylglycerols. In comparison, the barley endosperm contains monoacyl lipids (lysophatidylcholine, lysophosphatidylethanolamine, lysophosphatidylinositol, lysophosphatidylglycerol) comprising 1-3% by weight of the total endosperm, but 62-73% of the total lipids in the barley grain (MacGregor and Bhatty, 1993). The high lipid content in corn requires the majority of its lipids to be present in the germ. Up to 80% of all the lipids in corn are triacylglycerols and primarily inhabit the corn germ (Kohl, 2009; Matz, 1991).

2.1.3 Starch

2.1.3.1 Botanical origin

The two polymeric forms of starch are known as amylose (see Section 2.1.3.2) and amylopectin (see Section 2.1.3.3). The ratio of these starch polymers varies depending on botanical origin (Qiang, 2005). Plant breeding programs have also made adjustments to the amylose:amylopectin ratio. One type of cultivar, termed waxy, has been altered to contain nearly 100% amylopectin (Ullrich, 2011; Newman and Newman, 2008). Conversely, high amylose cultivars raise the amylose content to 40-70% (Newman and Newman, 2008). In general, native cereal starches contain approximately 75% amylopectin and 25% amylose. Other minor components of starch also vary according to botanical origin. For example, varying amounts of protein, lipids, and phosphorus are found in cereal grain starches (Qiang, 2005).

Regardless of the type of cereal grain, some structural characteristics of starches are similar. For instance, the α-linkages between glucose units in starch polymers (amylose and amylopectin) are consistent between all cereal grains. Certain levels of starch organization within granules are also consistent between starches of various origins. It has been recognized by Perez *et al.* (2009) that only very basic features of starch granules are ever consistent, which demonstrates the complexity of starch structure. The following sections will often identify examples of structural or physical properties using specific grains; however, differences may exist between starches from different grain types, cultivars, or even growing years.

2.1.3.2 Amylose

Amylose is a mainly linear polymer of repeating D-glucopyranose units with α-D-(1-4) linkages (see Figure 2-4). Some chains of amylose do have limited branching with α-D-(1-6) linkages (Jane, 2009). Amylose chains contain up to 6000 D-glucopyranose units, yet amylose is the smaller molecular weight (MW) starch polymer (10^5-10^6 MW)-(Wu *et al.*, 2006; Sharma *et al.*, 2006). Amylose is capable of complexing with many types of

compounds forming either single or double helices. Heating amylose in excess water followed by a period of cooling forms a rigid gel due to a rapid alignment of amylose chains upon cooling known as retrogradation.

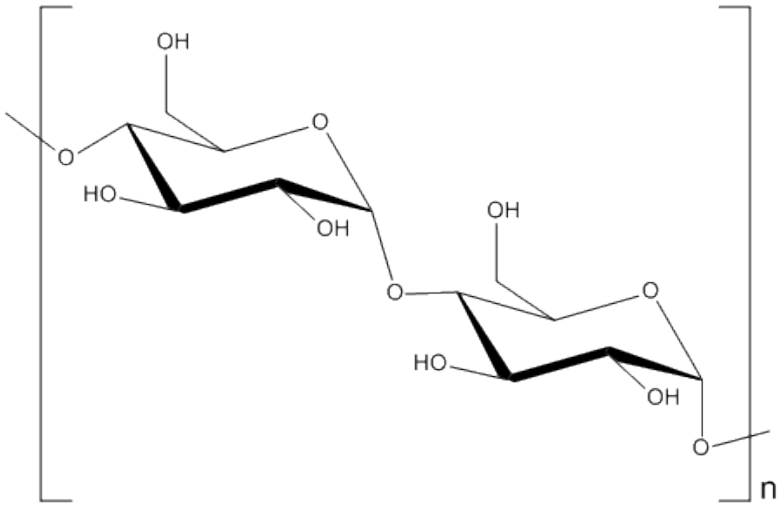

Figure 2-4: Glycosidic linkages in amylose (α-1-4 bonds)

A neutral, dilute, and aqueous solution of amylose will result in a flexible coil conformation (Miles *et al.*, 1985a). Each D-glucopyranose bond in the amylose molecule has a radius of gyration; therefore, many different conformations are possible as described by Wang and Cui (2005). The flexible coil structure of amylose favours precipitation due to instability in solution, but precipitation speed depends on the amylose concentration and molecular weight (Miles *et al.*, 1985a). Amylose prefers to exist in a complexed state, either with itself or with other compounds.

Formation of a single helix occurs when complexing agents are readily available (Bulpin *et al.*, 1982). Complexing agents capable of forming single helices with amylose include fatty acids, monoacylglycerol, dimethyl sulfoxide (DMSO), iodine, alcohols, and other small molecules (Bulpin *et al.*, 1982; MacGregor and Bhatty, 1993; Wang and Cui, 2005). The single helix is stabilized by both intra- and interchain hydrogen bonds (Wang and Cui, 2005) which creates a more favourable thermodynamic amylose configuration; however, the reaction is reversible as demonstrated by differential scanning calorimetry (Bulpin *et al.*, 1982).

When two amylose strands bind together a double helix is formed. Double helices are typically formed in retrogradated amylose gels (Wang and Cui, 2005). Because amylose molecules need to correctly align, this process requires a longer reaction time than single helix formation (Jane, 2009). Amylose chain length plays an important role formation of double helices. Gidley and Bulpin (1989) used oligosaccharides as a model for amylose double helix formation and concluded that a degree of polymerization (DP) of at least 10 is required for amylose double helix formation. Pfannemuller (1989) also

tested malto-oligosacchardies and confirmed Gidley and Bulpins conclusion. Others have shown that as the DP of amylose increases up to 110 increased retrogradation occurs, but the rate gradually declines when amylose chains have a DP over 250 (Gidley and Bulpin, 1989; Gidley, 1989; Gidley *et al.*, 1986). Interestingly, amylose below a DP of 110 has also been found to precipitate out of solution (Jane, 2009), likely the reason for increased retrogradation.

2.1.3.3 Amylopectin

Amylopectin is one of the largest known polymers in nature (10^6-10^8 MW), second only to cellulose (Qiang, 2005; MacGregor and Bhatty, 1993). Like amylose, repeating D-glucopyranose units with α-D-(1-4) linkages are present, but amylopectin also contains a larger proportion of α-D-(1-6) linkages (see Figure 2-5). The α-D-(1-6) linkages create branch points every 20-25 D-glucopyranose units and allow for the construction of a polymer with several thousand D-glucopyranose units (Qiang, 2005; Ullrich, 2011; MacGregor and Bhatty, 1993). The highly branched structure of amylopectin is commonly depicted by the cluster model proposed by Hizukuri (1986)-(see Figure2-6).

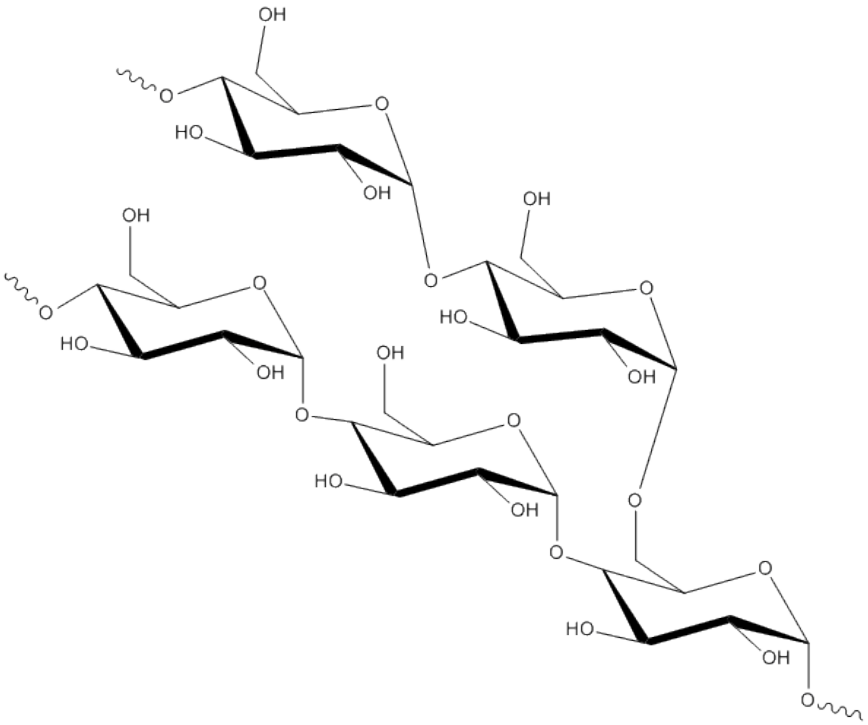

Figure 2-5: Glycosidic linkages in amylopectin (α-1-4 and α-1-6 bonds)

D-glucopyranose chains are classified according to their chain length and branching points (Qiang, 2005). A chains are on the outer region of the amylopectin molecule, are usually the most abundant chain type, have a chain length of 10-12 units, and contain no branch points (Qiang, 2005; Hanashiro *et al.*, 1996; MacGregor and Bhatty, 1993). B chains are the second most abundant chain type and are further classified into B1, B2,

B3, and B4 chains (MacGregor and Bhatty, 1993). B chains are grouped depending on their length, or more specifically, how many clusters the chain passes through. The B1, B2, B3, and B4 chains would pass through 1 through 4 clusters respectively (Hizukuri *et al.*, 1983). The C chain is the foundation chain and contains the sole reducing end of the amylopectin molecule (Qiang, 2005; Perez *et al.*, 2009). The distribution of amylopectin chain lengths are presented in Table 2-3 and the chain architecture is demonstrated in Figure 2-6.

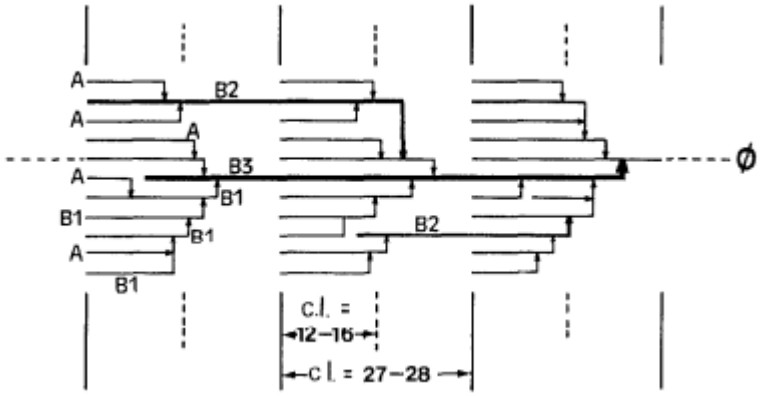

Figure 2-6: The proposed chain architecture of amylopectin; Hizukuri model

"Reprinted from Carbohydrate Research, 147 /2, Hizukuri S, Polymodal distribution of the chain lengths of amylopectins and its significance, 342-347, Copyright (1986), with permission from Elsevier."

Table 2-3: Branch chain length distributions of amylopectin and amylose content of wheat, triticale, and barley granules

Grain type	Amylose content (% dwb)	Amylopectin chain length distribution					Average chain length
		DP 6-9	DP 6-12	DP 13-24	DP 25-36	DP ≥ 37	
Wheat A granule	30.9	4.9	21.8	43.3	15.1	19.7	24.2
Wheat B granule	25.5	6.9	25.2	46.8	13.5	14.2	21.8
Triticale A granule	28.2	4.8	20	41.9	18.2	19.9	25
Triticale B granule	19.7	6.3	22.6	43.8	17.3	16.4	23.4
Barley A granule	28.1	3.7	15.3	40.3	21.4	22.9	26.7
Barley B granule	23	5.3	18.9	42.6	18.4	20	24.9

"Adapted from Carbohydrate Polymers, 67 /2, Ao Z and Jane J, Characterization and modelling of the A- and B- granule starches of wheat, triticale, and barley, 46-55, Copyright (2007), with permission from Elsevier."

Amylopectin chains also form double helices, specifically with chains 10-13 D-glucopyranose units in length (Imberty *et al.*, 1991). This chain length corresponds to the outer A chains in the amylopectin molecule. Double helices in cereal starches are aligned in a tight pseudo-hexagonal formation. The helix exhibits a repeating unit of maltotriose that leaves little space within the internal structure (Imberty *et al.*, 1991)- (see Figure 2-7). Double helices join together in both amorphous and crystalline regions of starch granules described in the following sections. Jane *et al.*, (1992) also discovered that amylose can also form a double helix with amylopectin chains.

Figure 2-7: The structure of an A-type double helix (repeating units of maltotriose)

2.1.3.4 Granular Structure

Starch granules vary in shape, size, texture, and other physical properties both between and within grain types. For example, barley, wheat, and triticale starches have a bimodal distribution of large and small granules (Jane, 2009; Dhital *et al.*, 2010); whereas, corn starch has a unimodal distribution (Dhital *et al.*, 2010). Barley, wheat, and triticale starch granules also have similar sizes and shapes (see Table 2-4). It has been reported that large barley granules account for ~10-20% of the total number of starch granules, but constitute 85-95% of the total starch weight (Vasanthan and Bhatty, 1996). Similarly, large wheat granules represent 10% of the total number of starch granules, but 70% of the total starch weight (Lindeboom *et al.*, 2004). See Table 2-4 for a detailed description of normal (native) wheat, barley, corn, and triticale granular features.

Starch granules are comprised of the two main starch polymers: amylose and amylopectin. The granules are organized with a radial orientation from the centre, or

hilum, of the starch granule (see Figure 2-8). Ordering of the starch polymers within the granular form leads to repeating sections of crystalline and semi-crystalline regions that resemble growth rings in trees (see Figure 2-9). This organization within starch granules is considered the lowest level of structure within starch granules. Depending on the botanical source of the starch, the alternating regions range from 120-400nm thick (Gallant *et al.*, 1997; Yamaguchi *et al.*, 1979).

Table 2-4: Physical characteristics of cereal grain starch granules

SEM	Grain	Large graunle size (μm)	Small granule size (μm)	Shape	Reference
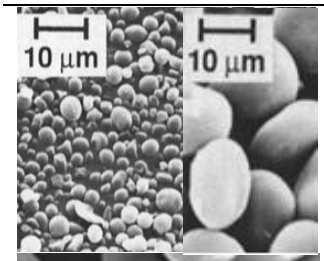	Barley	12-26	2-10	Large: disk Small: spherical	Vasanthan and Bhatty, 1996; Jane, 2009
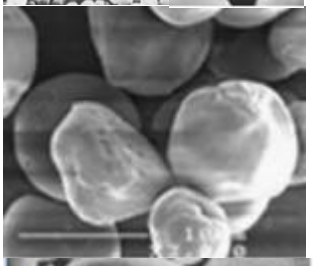	Corn	10-20	1-5	spherical to polygonal	Dhital *et al*. 2010; Jane, 2009; Jane *et al*., 1992b
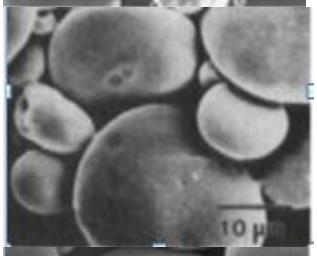	Wheat	22-36	2-3	Large: disk Small: spherical	Jane, 2009; Jane *et al*., 1994
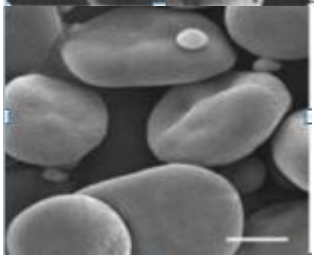	Triticale	22-36	5	Large: disk Small: spherical	Li *et al*., 2011; Jane, 2009; Jane *et al*., 1994

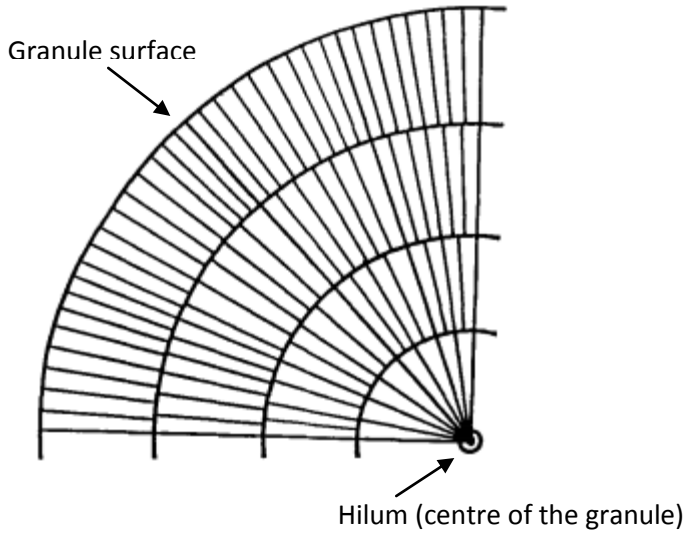

Figure 2-8: Radial orientation of starch granules

"A note on the gelatinization of starch. Hoseney RC, Zeleznak KJ, Yost DA. Starch 38(12) 407-409. Copyright (1986) John Wiley and Sons. Reprinted by permission of John Wiley and Sons via Rightslink."

The next level of organization in starch granules is related to the clustering and branching of amylopectin molecules (French, 1984). The radial alignment of these clusters results in an alternating crystalline and amorphous lamellae (see Figure 2-9). Crystalline lamellae in cereal starch are comprised of units containing 12 D-glucosyl units and 4 water molecules (Perez *et al.*, 2009). Amorphous regions contain amylopectin branch points, as well as free or complexed amylose (Imberty *et al.*, 1991; Gallant *et al.*, 1987). The crystalline and amorphous lamellae are reported to be 9-10nm thick (Jenkins *et al.*, 1993). Other structural features of granular structure incorporate amylose in close proximity to, or possibly co-crystallized with amylopectin (Jane *et al.*, 1992a; Kasemsuwan and Jane, 1994); high amylose concentrations near the interior of the starch granule (Schwartz, 1982); and longer amylopectin branch chains near the inner region of starch granules (Li *et al.*, 2007).

Internal cavities are known to be present within cereal grain starch granules. Findings presented by Baldwin (1994) propose a round internal cavity near the hilum of wheat starch granules. It was also concluded by Huber and BeMiller (1997) that corn starch granules have internal cavities, but are found as an irregular star shape. Another finding reported by Huber and BeMiller (1997) shows that channels connect the outer surface of corn granules to the internal cavity. More recently, internal channels were discovered in large (A-type) triticale starch granules using confocal imagery (Naguleswaran 2011).

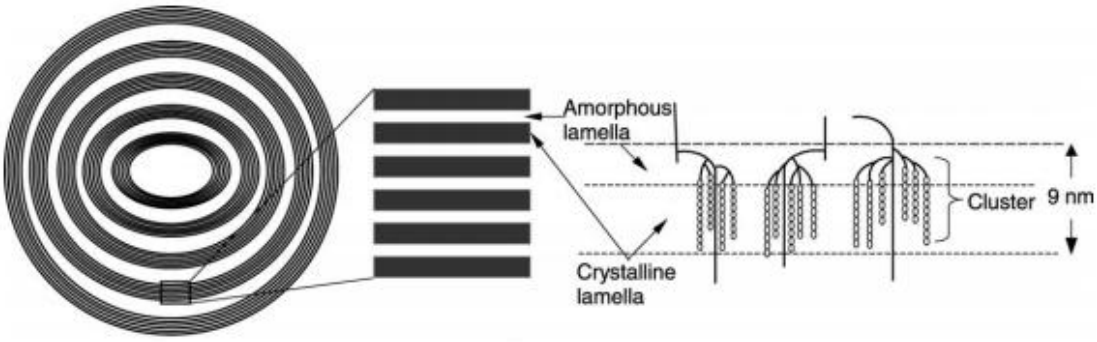

Figure 2-9: Alternating crystalline and amorphous lamellae

"Starch: structure and functionality. Frazier PJ. ISBN: 0854047425. Copyright (1997). Royal Society of Chemistry. Reprinted by permission of Woodhead Publishing."

2.1.3.5 Crystallinity

Cereal starch granules range in crystallinity from 20-45% (Yu and Chen, 2009), as determined by X-ray diffraction. The crystalline lamellae of amylopectin in starch granules lead to characteristic X-ray diffraction patterns (Perez *et al.*, 2009). Cereal grains are classified as A-type crystallinity due to the specific X-ray diffraction pattern observed by cereal starch crystallites (Imberty *et al.*, 1987)-(see Figure 2-10). When viewed under polarized light, starch granules exhibit a Maltese cross, also referred to as birefringence (Perez *et al.*, 2009). This phenomenon is observed due to a radial alignment of crystallites within starch granules (Perez *et al.*, 2009).

Amylose exposed to solvents (DMSO), fatty acids, monoacylglycerol, iodine, or alcohols adopt a left-handed, six-fold single helix conformation known as V-type amylose (Wang and Cui, 2005). The single helix has a low pitch in order to accommodate the complexing molecules (Wang and Cui, 2005). This conformation, or molecular ordering, results in V-type crystallinity named for the German word Verkieiterung, meaning gelatinization (Habibi and Dufresne, 2011). The process of gelatinization leaches amylose out of the starch granule where it can then form these complexes; described in more detail in Section 2.1.3.7.

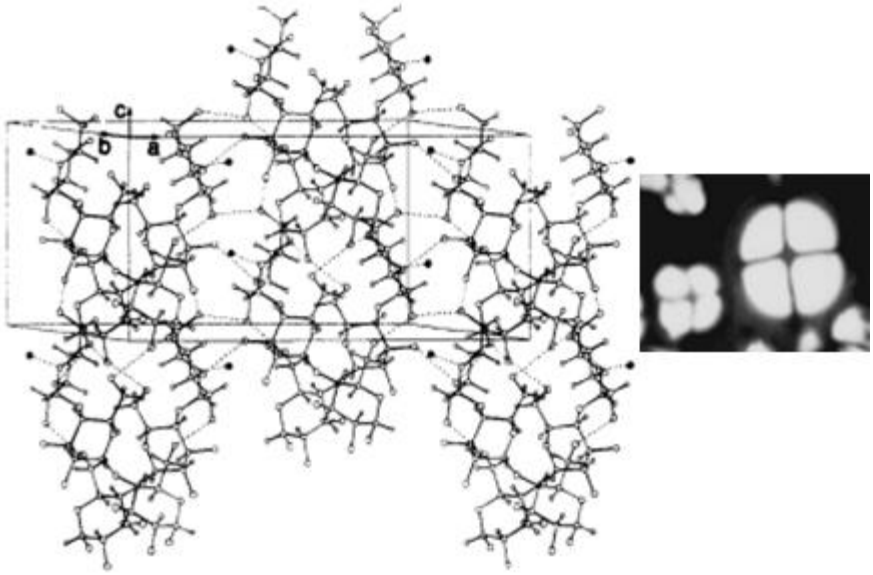

Figure 2-10: The crystallinity pattern in starch granules; subset shows birefringence (Maltese cross)

"Recent advances in knowledge of starch structure. Imberty A, Buleon A, Tran V, Perez S. Starch 43(10) 375-384. Copyright (1991) John Wiley and Sons. Reprinted by permission of John Wiley and Sons via Rightslink."

Other crystallinity patterns applicable to cereal grains include retrogradated amylose or amylose gel (see Section 2.1.3.7). Amylose chains crystallize during retrogradation to form double helices. The double helices in the amylose gel correspond to a B-type X-ray diffraction crystallinity pattern, which is usually associated with tuber starches (Imberty *et al.*, 1991; Miles *et al.*, 1985b).

2.1.3.6 Starch-protein matrix

Starch granules within cereal grains are embedded into a protein matrix (See Figures 2-11 and 2-12). Endosperm tissue is not always uniform and could be made up of both floury (soft) and vitreous (hard) starch. Floury starch can be described as endosperm tissue with lesser amounts of protein and vitreous starch contains more protein (Macrae *et al.*, 1993). In the wheat endosperm, factors such as cultivar type, environment, and protein content influence both the hardness and the accessibility of starch granules within the starch-protein matrix (Stenvert and Kingswood, 1977). Scanning electron micrography (see Figure 2-11) showed that higher protein content results in a more continuous protein matrix and a higher degree of structural order, or hardness (Stenvert and Kingswood, 1977). The protein in the matrix may influence the physical entrapment of starch granules and could influence starch hydrolysis rates.

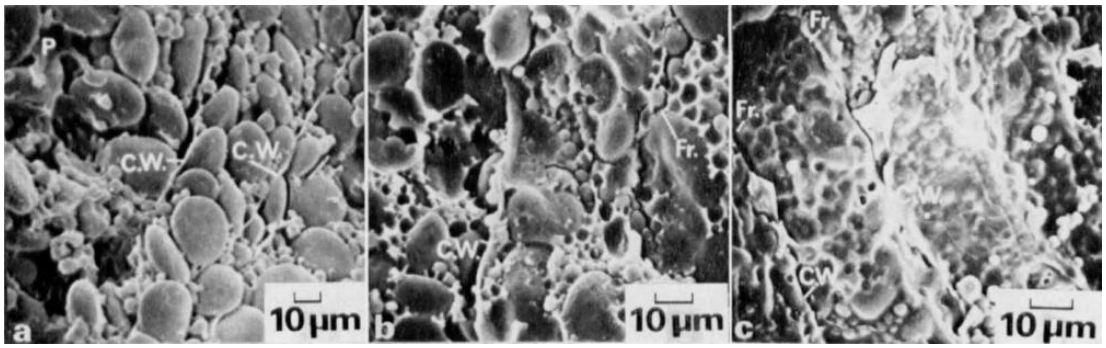

Figure 2-11: Scanning electron micrographs of the starch-protein matrix (wheat cultivar - Pride): a, mealy (9.1% protein); b, intermediate (10.4% protein); c, vitreous (11.4% protein). Abbreviations: cell wall (CW); protein (P); and lines of fracture (Fr).

"The influence of the physical structure of the protein matrix on wheat hardness. Stenvert NL and Kingswood K. Journal of the Science of Food and Agriculture 28(1): 11-19. Copyright (1977) John Wiley and Sons. Reprinted by permission of John Wiley and Sons via Rightslink."

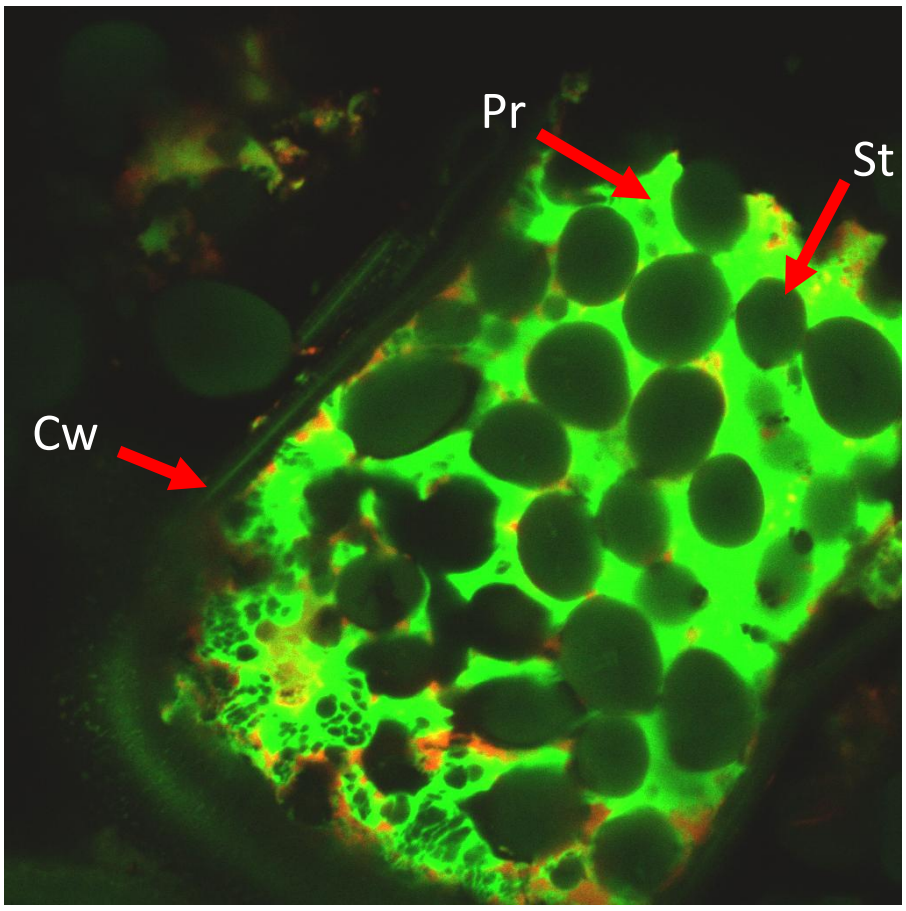

Figure 2-12: Confocal microscopy of the starch-protein matrix in barley flour; St = starch, Pr = protein, Cw= cell wall

2.1.3.7 Gelatinization and Retrogradation

When starch granules are exposed to high moisture they begin to swell (see Figure 2-13). This phenomenon is augmented by high heat which can swell the granules to many times their original size (Ring *et al.*, 1985). Swelling is a result of water molecules entering amorphous regions of starch granules (Macrae *et al.*, 1993) and is entirely reversible below the gelatinization temperature, which is different for each cereal grain (see Table 2-5). Gelatinization occurs over a temperature range and is not instantaneous. Type A starches, as exists in cereals, increase in gelatinization temperature with the increasing crystallinity of the granule (Perez *et al.*, 2009). Temperatures above the initial gelatinization point initiate a process that melts crystalline regions and amylopectin double helices in starch granules (Donovon, 1979). Loss of the crystalline regions of starch, also result in the loss of birefringence (Macrae *et al.*, 1993; Miles *et al.*, 1985b). Changes to starch structure as a result of gelatinization are irreversible (Macrae *et al.*, 1993).

Table 2-5: Gelatinization temperatures of corn, wheat, triticale, and barley

Grain type	T_o	T_p	T_c	Reference
Corn	66-69	70-74	75-80	Sandhu and Singh, 2007
Wheat	61.7	65.3	69.3	Ao and Jane, 2007
Triticale	60.7	64.2	68.4	Ao and Jane, 2007
Barley	57.9	62.6	67.9	Ao and Jane, 2007

To, Tp, Tc = Temperature (°C) of the onset, peak and conclusion of gelatinization

Another occurrence of gelatinization involves amylose leaching out of the granule into the surrounding water phase due to the hydrophilic nature of amylose hydroxyl groups (Qiang, 2005). Upon cooling, the leached amylose begins to align parallel to each other, forms hydrogen bonds, and precipitates out of solution (Qiang, 2005). This process is termed retrogradation. Amylose retrogradation results in a formation of a gel comprised of a 3D network of amylose chains (Leloup 1992). The gel contains amylose in double helix conformation and loosely associated amylose within amorphous regions (see Figure 2-14). Swollen gelatinized granules are also embedded in the amylose gel matrix (Miles *et al.*, 1985b). Retrogradated amylose is well known to be resistant to hydrolysis and will be discussed in more detail in Section 2.3.1.2.

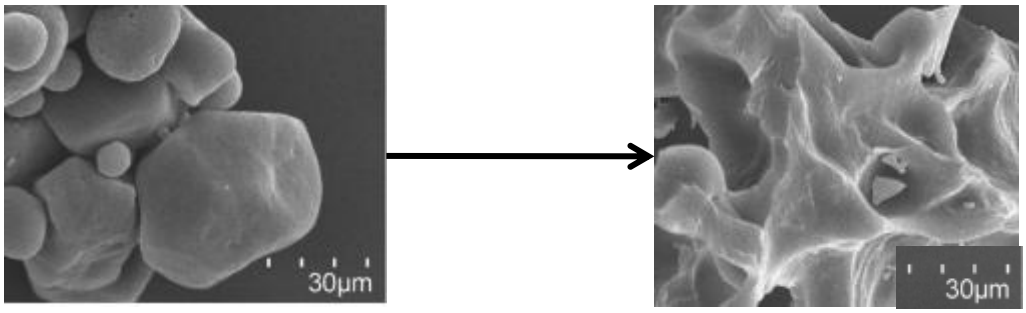

Figure 2-13: Scanning electron micrograph of native corn starch (1:5 slurry in distilled water) and gelatinized corn starch (1:5 slurry in distilled water; heated at 100°C for 60 minutes)

"Reprinted (adapted) with permission from (Xiaowen L, Lei W, Jing W, Junguo L, Yuchang Q. Characterization of water binding and dehydratation in gelatinized starch. Journal of Agricultural and Food Chemistry 59(1): 256-262). Copyright (2011) American Chemical Society."

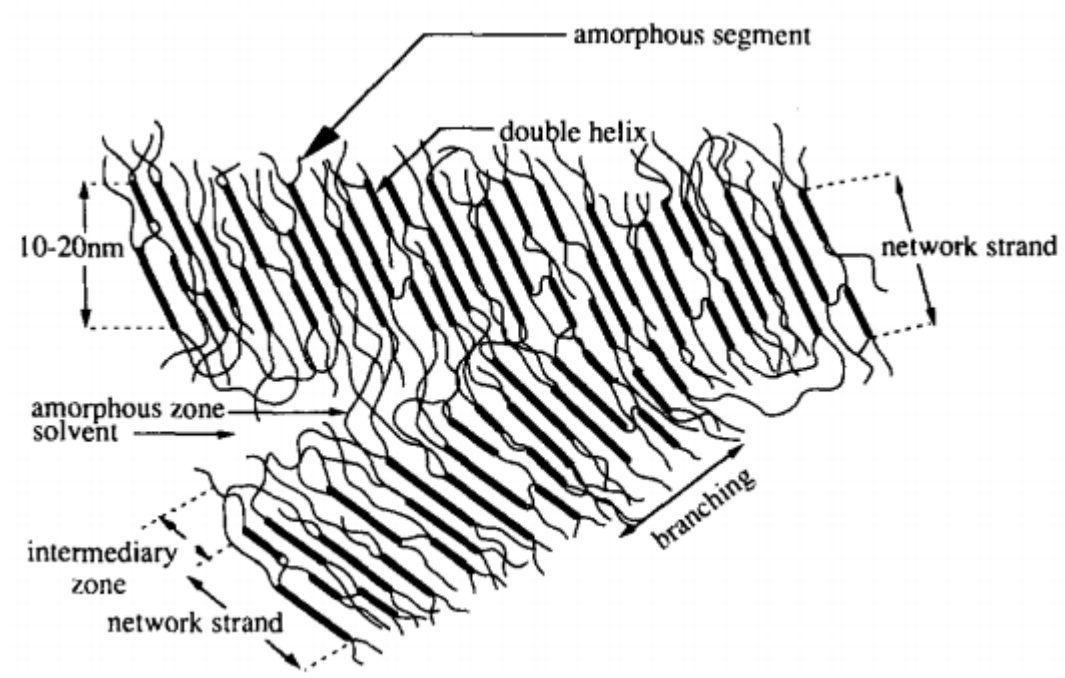

Figure 2-14: Proposed model of amylose gel

“Reprinted from Carbohydrate Polymers, 18 /3, Leloup VM, Colonna P, Ring SG, Roberts K, Wells B, Microstructure of amylose gels, 189-197, 1992, with permission from Elsevier.”

2.2 Ethanol and DDGS production

2.2.1 Grain milling

Grain milling in general is a required step for the production of ethanol due to the inherent inaccessibility of starch. Milling provides access to the inner endosperm region of cereal grains consisting of starch. The purpose of milling is to increase the surface area available for starch saccharification efficiency. Two main methods are utilized for this purpose: wet-milling and dry-grinding. The sub-sections below only describe the milling section of the process, while typically these terms refer to the entire ethanol production process. The remaining process steps are separated into their own sections and differences between each method will be outlined in those sections.

2.2.1.1 Wet-milling

Wet-milling allows for the separation of germ, fibre and protein prior to fermentation, thereby allowing for more co-products to be produced from cereal grains (see Figure 2-15). Corn is the most common cereal to undergo wet-milling; however, sorghum, wheat, rice, and cassava are also commercially wet-milled (Kohl, 2009; Matz, 1991). The rest of this section will focus on corn wet-milling specifically.

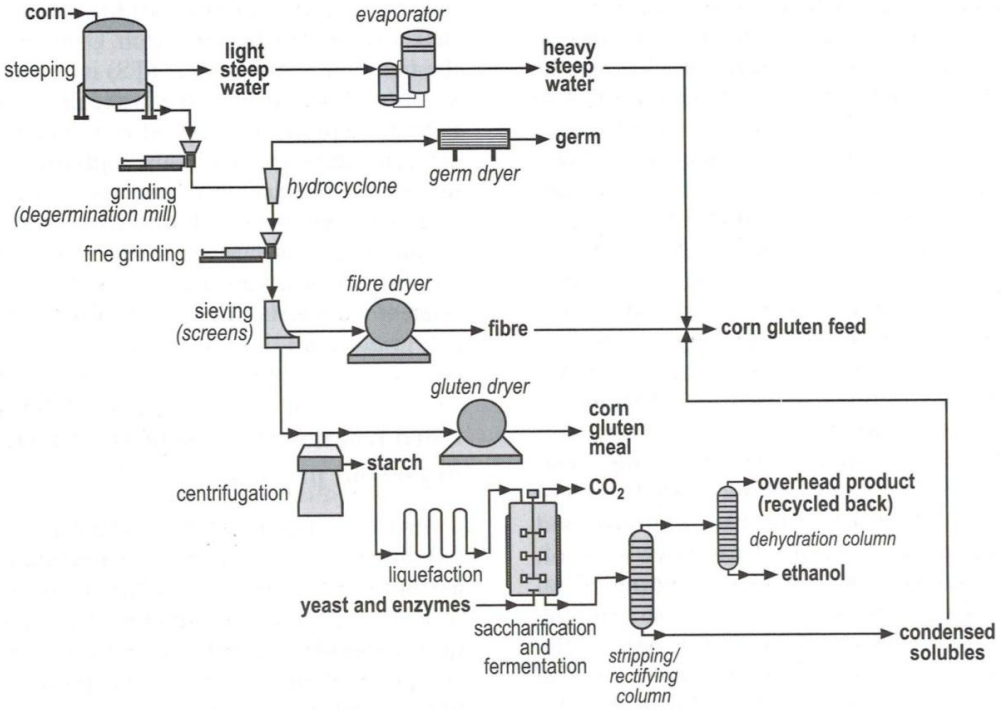

Figure 2-16: Corn wet-milling process flow diagram

Before milling, the corn is shelled, scraped, and screened to remove the husks, stover, and cobs (Kohl, 2009). The corn is then air classified by size to remove shrunken or damaged kernels. Cleaned corn is steeped in water for 36-48 hours at temperatures of 49-53°C prior to fractionation (Kohl, 2009; Matz, 1991). The steep water contains small amounts of sulfur dioxide to prevent both germination and fermentation of the corn (Matz, 1991). Following steeping, the steep water also contains soluble sugars and proteins, which are extracted to be used as animal feed. Corn kernels, once fully steeped, swell to double their original size and bonds within the starch-protein matrix are disrupted, giving the germ a rubbery consistency (Kohl, 2009).

The steep water solubles are extracted using a counter-current water flow, used to reduce water use in the wet-milling process. The counter-current system uses a multi-stage process that begins with the concentrated steep water (see Figure 2-16). Clean water is added to this extraction system in the opposite direction, which contains steep water with a lower concentration of soluble sugars and proteins. As the water passes through each stage it becomes more concentrated, but it is still able to extract more of the sugars and proteins because of the higher concentration of solubles.

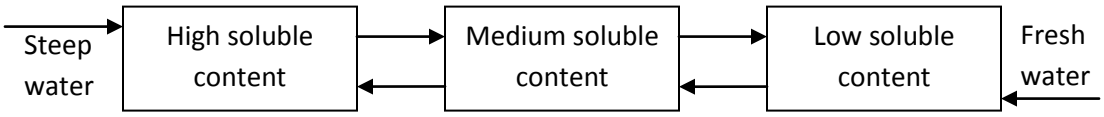

Figure 2-16: Counter-current extraction process

The rubbery consistency of the germ allows for germ removal from the kernel during the first milling step. Large circular plates with teeth, known as attrition mills, rotate and tear the germ from the rest of the kernel (Matz, 1991). The resulting slurry is further diluted in process water and sent to hydrocyclones (Matz, 1991). Hydrocyclones are designed to separate materials based on density; in this case the lighter germ spins to the top and the heavier carbohydrate and protein materials flow out the bottom. The crude germ is sent to an oil refinery, while the remaining slurry is further processed. At this point, the slurry still contains starch, protein (gluten), and fibre. A series of mesh screens filter the large fibre particles out of the slurry (Matz, 1991). Next, another milling step is used to remove any remaining starch or gluten from the fibre particles (Kohl, 2009). The slurry is then washed and sieved to separate the newly released starch and protein from the fibre (Kohl, 2009). Then large highly efficient continuous centrifuges are used to separate starch and gluten protein (Matz, 1991). A series of washing and centrifugation steps are used to obtain a good separation of starch and gluten protein (Kohl, 2009). Wet-milling generates product streams of corn starch, corn oil, gluten, and gluten feed (germ cake, fibre, and solubles combined)-(Matz, 1991). In ethanol plants, the starch is fermented to produce ethanol.

2.2.1.2 Dry-grind process

The dry-grind process is often incorrectly referred to as the dry-milling process (Singh and Johnston, 2009). Dry-milling refers to fractionation of corn into grits (endosperm), germ, pericarp fibre, and flour (Duensing *et al.*, 2003)-(see Figure 2-17). Dry-milling is used for the food and feed industry, whereas the dry-grind process refers specifically to the ethanol production industry. Modern dry-grind corn ethanol plants produce 345-436L ethanol/tonne of corn (Haefele and Ross, 2009). The low end of the range is a result of low quality corn and an average yield is considered to be 400L ethanol/tonne of corn.

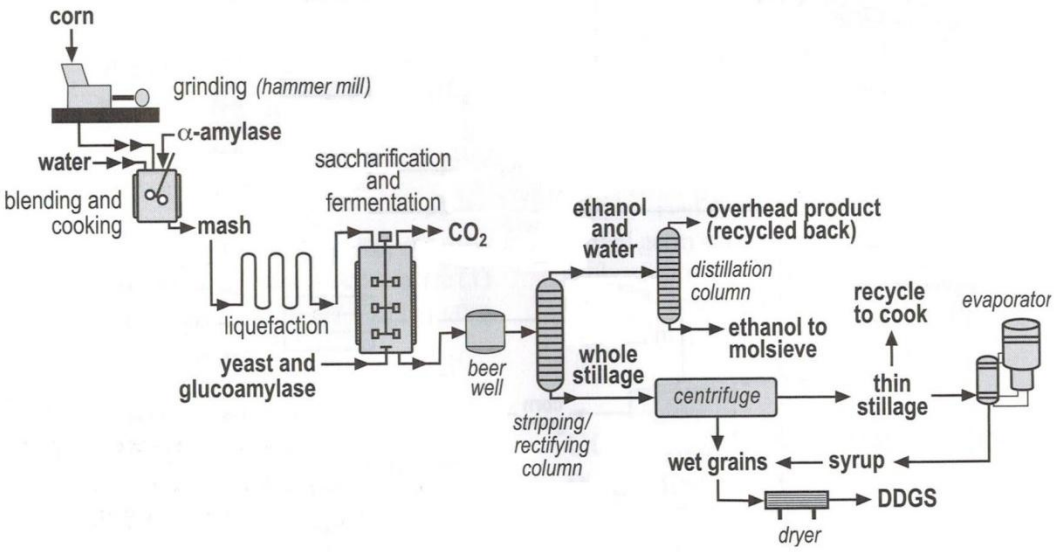

Figure 2-17: Corn dry-grinding process flow diagram

"Reprinted from The Alcohol Textbook, Chapter 15, Singh V and Johnston DB, Fractionation technologies for dry-grind corn processing, 196, Copyright (2009), with permission from Nottingham University Press."

In the dry-grind process, a hammer mill is used to grind the kernel to a diameter of approximately 1mm for the purpose of reducing the grains particle size (Rausch *et al.*, 2005). The milling generates more surface area, exposes the endosperm fraction of grain kernels, and allows access to starch-protein matrix. The resulting ground corn becomes a dry granular mixture of carbohydrate, protein, fibre, lipid, and other minor compounds. It has been reported that recent construction in the USA has predominantly been focused on dry milling due to the increased cost of capital expenditure for wet-mill facilities (Zhao *et al.*, 2010; Singh and Johnston, 2009). The two co-products produced from the dry-grind process include ethanol and DDGS (or wet distillers' grains). Drying the distillers' grains allows the producer to ship the feed to

cattle producers; whereas wet distillers' grains are produced when the ethanol production facility is in close proximity to cattle lots.

Laboratory modifications have attempted to fractionate corn prior to the dry-grind process. These modifications make use of dry or wet fractionation processes (Singh and Johnston, 2009). Wet fractionation processes include the quick germ process, the quick germ quick fibre process, and the enzymatic dry-grind (E-mill) process (Singh and Johnston, 2009). The above processes remove the germ, germ & pericarp fibre, and germ & pericarp fibre & endosperm fibre respectively. Dry fractionation also removes germ and pericarp fibre, but utilizes short tempering times with hot water or steam along with density based separations. Removal of these compounds provides another income stream to ethanol producers, especially for the high value germ fraction. Other benefits of fractionation include an increase in fermenter starch concentration and improved nutritional characteristics in the DDGS (Singh and Johnston, 2009).

2.2.2 Mashing

Mashing refers to the initial blending and cooking step for the dry-grind process only. Ground grain from the hammer mill is added to a large slurry tank followed by addition of water, backset water, and thermostable α-amylase. Backset water is the portion of thin stillage that is recycled to reduce the use of water during ethanol production. The mixture is blended and cooked at low temperatures, causing the starch granules to swell and an increase in viscosity of the mash (Ring *et al.*, 1985; Tester *et al.*, 2004). Thermostable α-amylase works at high temperatures to cleave α-1-4 bonds which reduces the viscosity of the mash by converting large starch molecules into shorter chain dextrins (Singh and Johnston, 2009)-(see Figure 2-18). Mixing and pumping of the mash would be challenging and energy consuming without the addition of α-amylase (Robertson *et al.*, 2006).

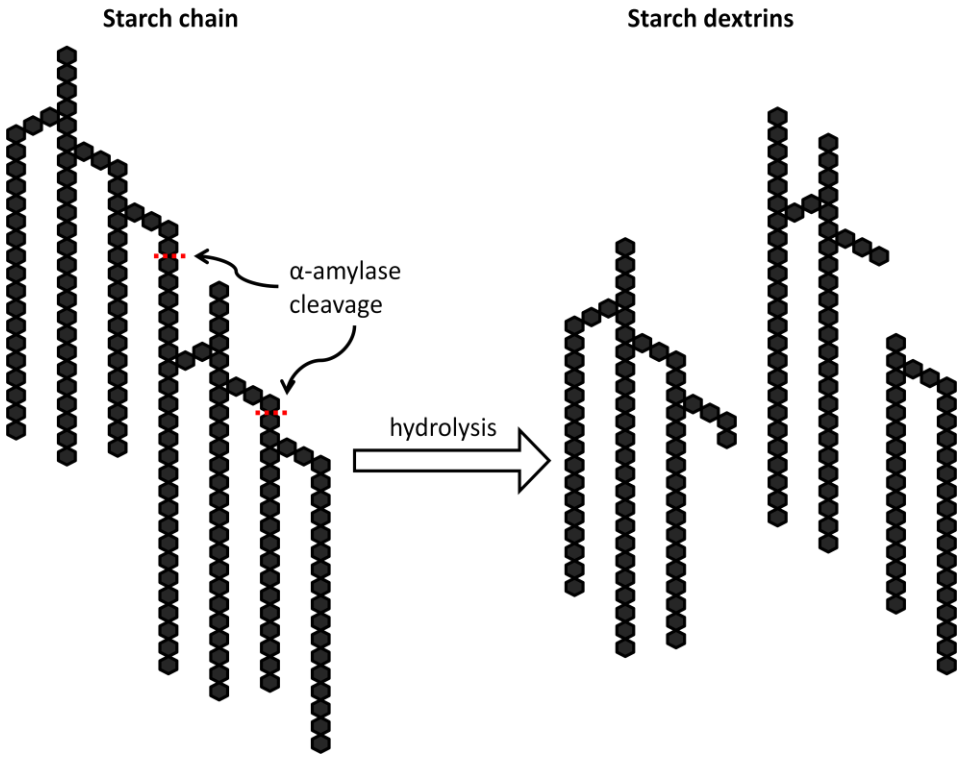

Figure 2-18: α-amylase hydrolysis of starch into dextrins

Commonly, mash consists of a solids content ranging from 20-24% (Thomas *et al.*, 1996). Raising the solids content is possible through a technique referred to as very high gravity fermentation (Kelsall and Lyons, 1999). Very high gravity fermentations are defined as mashes containing ≥27 grams of dissolved solids/100g of mash (Thomas *et al.*, 1993). Using very high gravity fermentations can increase plant throughput and productivity (Liu *et al.*, 2011), reduce energy and water consumption (Liu *et al.*, 2011), limit unwanted microbial growth (Pilgrim and Wright, 2009), and reduce the heat needed for distillation (Pilgrim and Wright, 2009).

2.2.3 Conventional liquefaction

Mash from the dry-grind process, or starch from wet-milling, is passed through a high temperature high pressure jet-cooker to liquefy the starch. Jet-cooking utilizes thermostable α-amylase and is commonly called liquefaction because α-amylase works to reduce the viscosity of the mash to a liquid consistency. The jet-cooker is a continuous process using high pressure steam to cook at temperatures up to 120°C (Singh and Johnston, 2009)-(see Figure 2-19). The high temperatures help to break down the crystalline structure of starch granules (Singh and Johnston, 2009) and to sterilize the mash, helping to reduce contamination during fermentation (Pilgrim and Wright, 2009). Wet-milling requires the α-amylase to be added prior to the jet-cooker; however, the dry-grind process adds the α-amylase during the mashing stage. Following

the jet-cooking stage, the mash enters a liquefaction tank for an incubation period of 30-60 minutes at 80-90°C (Kelsall and Piggot, 2009). It is important that the pH is controlled within the 5.5-6.5 range, so the α-amylase can continue to hydrolyze the cooked starch (Kelsall and Piggot, 2009). The liquefied mash is then cooled before being transferred into the fermentation vessel.

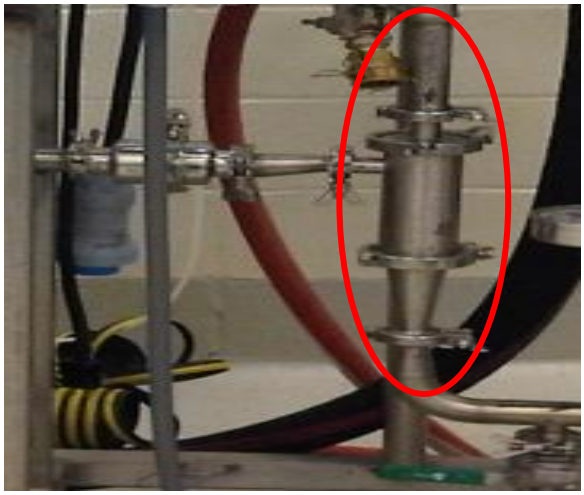

Figure 2-19: Laboratory scale jet-cooker (donated from Pick Heaters, Inc.; West Bend, WI)

High temperatures used during jet-cooking may result in a loss of fermentable sugars from the mash due to the Maillard reaction (non-enzymatic browning). Reducing sugars and nitrogenous compounds undergo a condensation reaction in the first step of Maillard reactions. The condensation reaction occurs between the α-amino-group of amino acids or proteins and the carbonyl group of reducing sugars (Izydorczyk, 2005). The resulting condensation compound is rapidly dehydrated to form a Schiff's base, which subsequently undergoes cyclization (Izydorczyk, 2005)-(see Figure 2-20). From this stage a series of complex reactions, known as the Amadori rearrangement, proceed and the reducing sugars are no longer available for yeast (Izydorczyk, 2005). Although Izydorczyk (2005) indicates that D-glucose is the slowest reacting hexose, Agu *et al.*(2008) showed that at high temperatures increased levels of Maillard reaction products were produced from cooked mash. Maillard reaction products were measured as a function of mash colour, tested with a Lovibond 2000 comparator (Hellige and Co., UK). Wu *et al.* (2006) also observed what they believed to be Maillard reactions when cooking above temperatures of 95°C. These findings are also supported by the fact that all wheat varieties tested by Agu *et al.* (2008) saw a significant decrease in alcohol yield when raising the processing temperature from 85°C to 140°C. Loss in yield was concluded to be due to a loss in reducing sugars via the Maillard reaction. Another significant effect of the Maillard reaction is due to the loss of nitrogenous compounds for yeast growth, which could affect the rate of fermentation (Agu *et al.*, 2008). Corn

samples in the same study showed inconsistent results, as alcohol yield varied from sample to sample regardless of processing temperature (Agu *et al*.,2008).

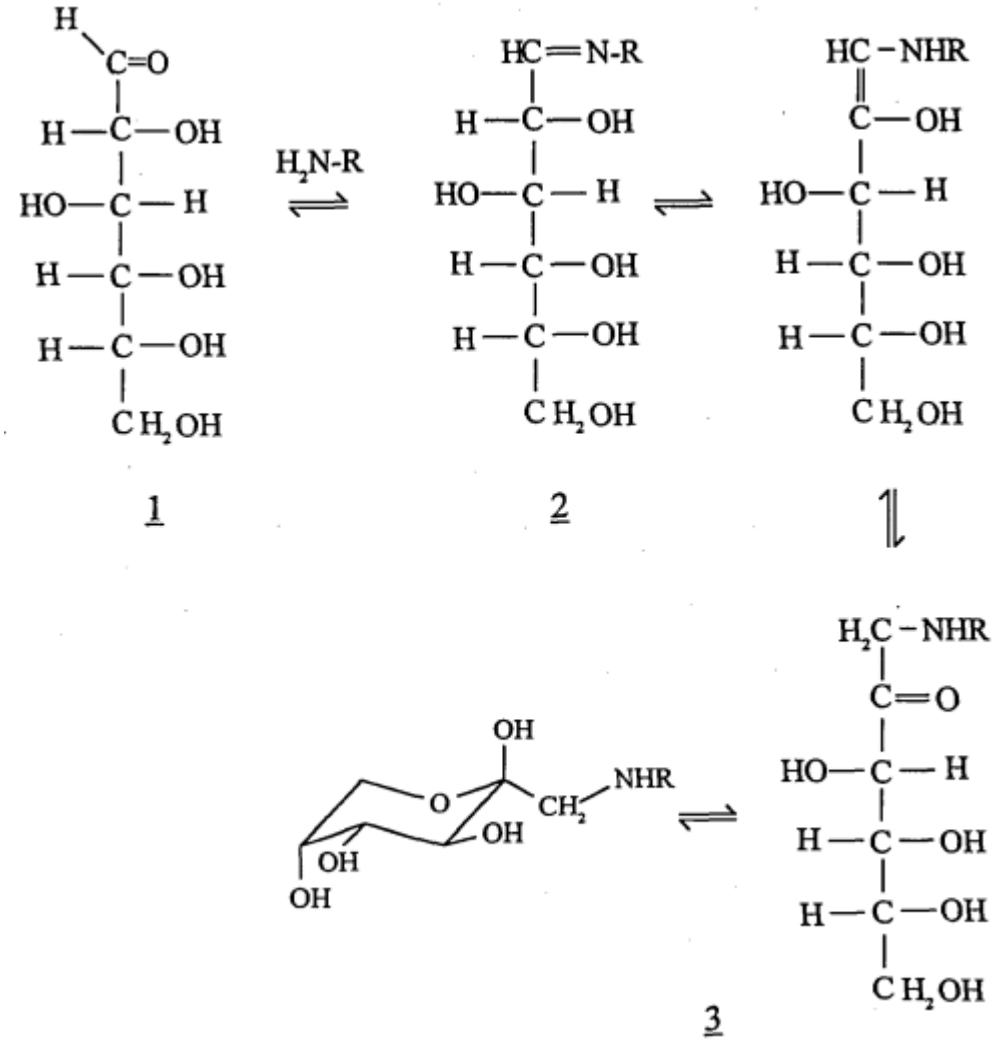

Figure 2-20: Mechanism of the Amadori rearrangement

"Reprinted from Critical Reviews in Food Science and Nutrition, 34/4, Yaylayan VA, Huyghues-Despointes A,Feather MS, Chemistry of Amadori rearrangement products: Analysis, synthesis, kinetics, reactions, and spectroscopic properties, 321-369, Copyright (1994), with permission from Taylor & Francis."

Starch structure is known to have a major impact on the starch hydrolysis process. This was confirmed by Wu *et al.* (2006) and Sharma *et al.* (2007) using model systems with altered amylose:amylopectin ratios using purified commercial starch varieties with known amylose and amylopectin values. Sharma *et al.* (2007) found a significantly higher ethanol concentration was produced with high amylopectin corn starch samples at the completion of a 72 hour shake flask fermentation. Dry-grind samples of waxy,

dent, and high amylose corn samples were also tested and again the same trends held; waxy and dent corn (<1% amylose and ~30% amylose respectively) had a significantly higher ethanol yield than high amylose corn (~65% amylose). Although Sharma *et al.* (2007) studied conventional amylases (α-amylase from *Bacillus licheniformis* [Liquozyme SC; Novozymes] and glucoamylase from *Aspergillis niger* [AMG 300L; Novozymes]), they were not able to combine the hydrolysis with temperatures commonly seen with jet-cooking. High temperatures may have melted amylose-complexes and made them available to conventional amylases resulting in improved high amylose fermentation yields. In fact, the study by Wu *et al.* (2006) used a high temperature reactor to heat samples of pure starch and dry-grind corn with various amylose:amylopectin ratios at 120, 140, and 160°C and found that higher temperatures significantly raised the conversion efficiency. The trend was particularly noticeable in high amylose dry-grind corn compared to high amylose corn starch. Later, similar results were reported for waxy and nonwaxy wheat (Zhao *et al.*, 2009).

2.2.4 Raw starch hydrolysis

Numerous enzymes have the ability to hydrolyze raw (ungelatinized) starch (see Figure 2-21). This process, also called the cold-cook process, is used alternatively to the high temperature liquefaction (Pilgrim and Wright, 2009). A short incubation time is used to begin the process of saccharification and additional raw starch hydrolyzing enzyme can be added during the fermentation. One type of raw starch hydrolyzing enzyme (Stargen 001) was used in the preparation of DDGS for this study.

Stargen 001 combines genetically engineered α-amylases, amyloglucosidases, and other enzymes in an enzyme cocktail used to saccharify raw starch. The exo-acting amyloglucosidases drill or expand existing pinholes in raw starch granules (Shariffa *et al.*, 2009). The endo-acting α-amylases then begin to widen the pinholes and interior cavity (Shariffa *et al.*, 2009). Advantages of raw starch hydrolysis include more nutritious DDGS (Pilgrim and Wright, 2009), substantial energy savings (Robertson *et al.*, 2006), reduced capital expenditure (Shetty *et al.*, 2005), and reduced viscosity issues. More detail on other raw starch hydrolyzing enzymes can be obtained from a widespread review published by Robertson *et al*. (2006).

Ethanol fermentation productivity with raw starch hydrolyzing enzymes is similar to conventional ethanol production. Wang *et al*. (2007) compared raw starch hydrolysis (with Stargen 001) to two traditional enzyme systems containing both α-amylase and amyloglucosidase, but found no difference in final ethanol concentration, ethanol yields, ethanol conversion efficiencies, or DDGS yields when using dry-grind corn. Sharma *et al*. (2007) determined that waxy corn ethanol yields were not significantly different when using raw starch hydrolysis (with Stargen 001) versus using conventional hydrolysis enzymes. Conversely, when high amylose corn (~65%) was used Sharma *et al*. (2007) found that raw starch hydrolysis resulted in a lower ethanol yield. Both studies used a

standard volume addition of enzymes, which was expected to be above the enzyme requirements needed commercially. While this did prove that raw starch hydrolysis is capable of producing the same ethanol yield as conventional enzymes, it failed to identify that higher enzyme loading with raw starch hydrolyzing enzymes is required (Vidal Jr. *et al.*, 2009). A higher enzyme loading, combined with the increased cost of these enzymes are two major limitations of the raw starch hydrolysis process.

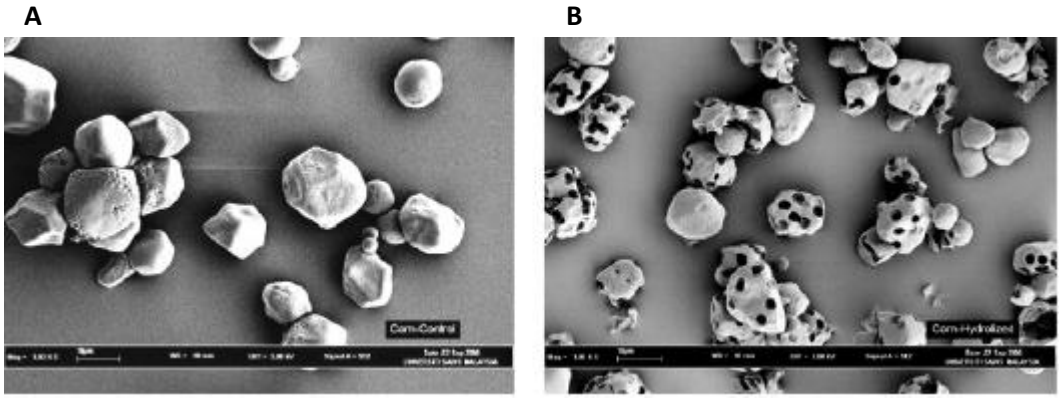

Figure 2-21: Scanning electron micrograph of native corn starch granules (A) and raw starch hydrolyzed corn starch granules (B)

"Reprinted from Food and Bioproducts Processing, 88/1, Uthumporn U, Zaidul ISM, Karim AA, Hydrolysis of granular starch at sub-gelatinization temperature using a mixture of amylolytic enzymes, 47-54, Copyright (2010), with permission from Elsevier."

Additional studies by Gibreel *et al*. (2009 & 2011) measured the fermentation efficiency of multiple grain types comparing laboratory scale dry-grinding (with jet-cooking) to raw starch hydrolysis. Between the two studies, the analysis of corn, wheat, barley, and triticale fermentation efficiencies were tested. It was concluded by the authors that the raw starch hydrolysis was 'comparable' to the jet-cooking process in terms of efficiency. It was also determined that higher amounts of potential by-products could be recovered from DDGS when using raw starch hydrolysis, likely due to the lower temperatures. Examples of these by-products include sterols, tocopherols, tocotrienols, and fatty acids. The possibility of multiple product streams resulting from raw starch hydrolysis could potentially provide a payoff for producers. This is an area that will require much further study, but it does provide another benefit to consider when taking into account increased costs for the enzyme technology.

It is important to note that a major drawback of raw starch hydrolysis is the lack of a sterilization step. Cereal grains are potentially contaminated with various microorganisms, so strategies are needed to limit their growth. Other sources of contamination include poorly cleaned transfer lines, tanks, and heat exchangers; yeast preparations; and poorly stored backset water (Narendranath and Brey, 2009). One

technique commonly used to limit the growth of contaminating organisms is referred to as simultaneous saccharification and fermentation (discussed in the following section). Other potential solutions involve improved cleaning and sanitation procedures, adjustment of the mash pH, and antimicrobial or antibiotic use (Narendranath and Brey, 2009). Even without sterilization, the levels of acids formed from contaminating lactic acid bacteria during raw starch hydrolysis are very low. Narendranath and Brey (2009) report that ≤0.12% w/v of lactic acid and ≤0.02% w/v of acetic acid are produced at commercial ethanol plants using raw starch hydrolysis technology.

2.2.5 Simultaneous saccharification and fermentation (SSF)

First generation ethanol fermentations use starch as a carbon source for yeast cell growth and ethanol production. Transportation of carbon molecules into yeast cells requires that the starch is hydrolyzed into smaller saccharrides, such as maltose or glucose. Industrial saccharification is achieved using purified microbial enzymes from specialized microorganisms. Extracellular enzymes allow for high temperature, liquid-phase starch hydrolysis (Robertson *et al.*, 2006). Alternatively dilute acid hydrolysis may be used to cleave glycosidic bonds; however, using acid at high temperatures causes corrosion of equipment and lead to undesired side reactions (Robertson *et al.*, 2006).

The objective of liquefaction and saccharification is to cause starch hydrolysis via enzymatic cleavage of the glycosidic bonds. Although liquefaction has been described in a previous section, it is well known that amylase enzymes used to hydrolyze starch work synergistically (Shariffa *et al.*, 2009; Wong *et al.*, 2007). As the liquefaction enzyme, α-amylase, cleaves α-1-4 bonds and creates dextrins (shorter glucose chains – see Figure 2-22), more reducing ends are created for the exo-action of another amylase known as amyloglucosidase. Amyloglucosidase is referred to as an exo-enzyme because it hydrolyzes from the reducing end of starch molecules. Saccharification typically occurs simultaneously to fermentation and is known as simultaneous saccharification and fermentation (SSF). As was described in the previous section, this process can now be done at low temperatures and when done under these conditions it is referred to as raw starch hydrolysis or cold cooking.

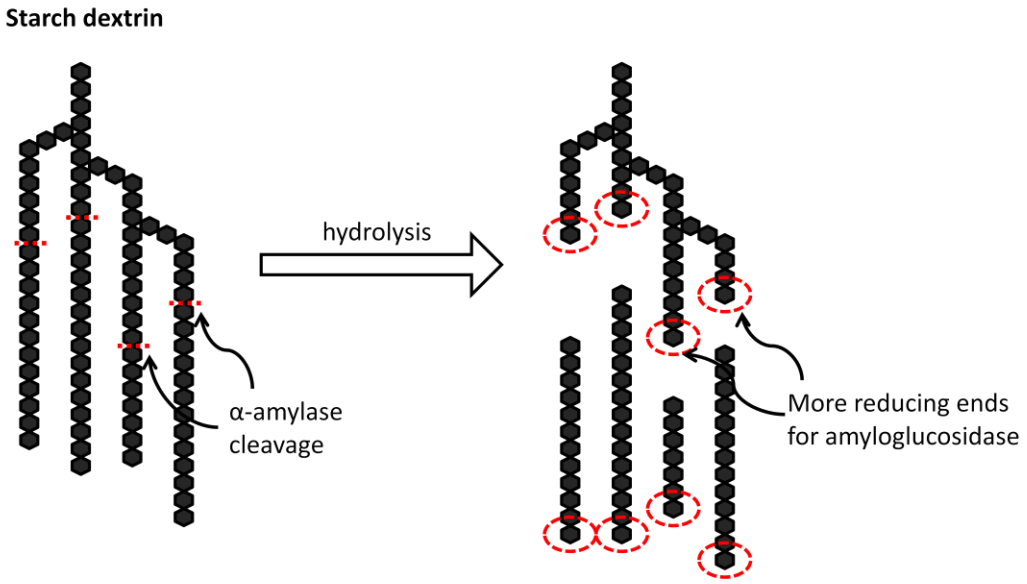

Figure 2-22: Synergism of α–amylase and amyloglucosidase

Commercial yeast is added to the large fermenters used for the SSF process; therefore, the temperature must be in a desirable range for yeast functioning and growth (~35-37°C). Prior to addition to the fermenters, the yeast is propagated to increase the cell concentration. During SSF it is important that a rate controlled release of glucose is maintained to ensure that yeast does not undergo osmotic shock (Albertyn *et al.*, 1994). Other benefits also arise from combining the processes. For example, the glucose produced is readily used by the yeast which limits the growth of contamination organisms (Matsumoto *et al.*, 1982). This becomes especially important for raw starch hydrolysis due to the lack of a heating step prior to fermentation. Current yields from very high gravity fermentation in conjunction with SSF range up to 24% v/v ethanol in laboratory settings (Thomas *et al.*, 1993) or up to 15-16% in industrial settings (Ingledew, 1999). It has also been reported that using very high gravity fermentation also lowers the level of contaminating bacteria (Bayrock and Ingledew, 2001; Thomas *et al.*, 1996); however, no specific mechanism or data was given to support this statement.

2.2.6 Distillation

Following fermentation, a range between 10-16% ethanol (v/v) is produced and must be separated from the fermentation media, also identified as beer (Monceaux and Kuehner, 2009). The beer contains ethanol and all of the nonfermentables which includes yeast biomass, water, protein, fibre, residual starch, sugars, and other solubles. The wide range of ethanol concentrations mentioned above is a result of using either low or high gravity fermentation processes. With higher solids loading, more ethanol can be produced which not only impacts alcohol production, but can lower plant operating costs (Earnest *et al.*, 2009). Cost savings are due to the extra time requirement of operating the still to remove larger concentrations of water at lower

ethanol concentrations (Earnest *et al.*, 2009). Alternatively, the still temperature could be increased to separate low ethanol concentrations faster, but this solution is also cost intensive (Earnest *et al.*, 2009).

Distillation columns are used to separate ethanol from the fermentation media; however, before describing the actual separation, it is important to understand how distillation columns are designed (see Figure 2-23). Steam used to heat the column enters near the bottom, or stripping section, of the distillation column. This feature is designed to create a gradient of heat that produces high temperatures near the bottom of the column and lower temperatures near the top of the column. The feed mixture, in this case beer, enters the distillation column near the midway point where gravity naturally forces the beer towards the hotter stripping section of the column. At these high temperatures both water and ethanol are vaporized and begin ascending towards the rectifying section of the column. Here is where the distillation column takes advantage of boiling point differences between water and ethanol. As the vapour rises it begins to cool due to the gradient heating. The temperature should be above 90°C but below 100°C ensuring that ethanol remains a vapour and exits the column, while a portion of the water condenses and remains in the column. The exiting vapour, or overhead product, is raised to an ethanol concentration of approximately 30% after one pass through a distillation column. It takes numerous passes through a series of distillation columns to raise the ethanol concentration to a point where spirit (a 190° proof/95% ethanol) is produced. To obtain anhydrous ethanol, the spirit must be dehydrated because the ethanol-water mixture reaches a stage (constant boiling mixture/azeotropic solution) where the vapour produced is the same composition as the liquid from which it is being generated (Madson, 2009). Dehydration can be achieved using chemical dehydration, membrane separation, adsorption processes, vacuum distillation, azeotropic distillation, extractive distillation, or diffusion distillation (Kumar *et al.*, 2010). Anhydrous ethanol is then commonly denatured with poisonous chemicals and/or blended with gasoline for use as a fuel.

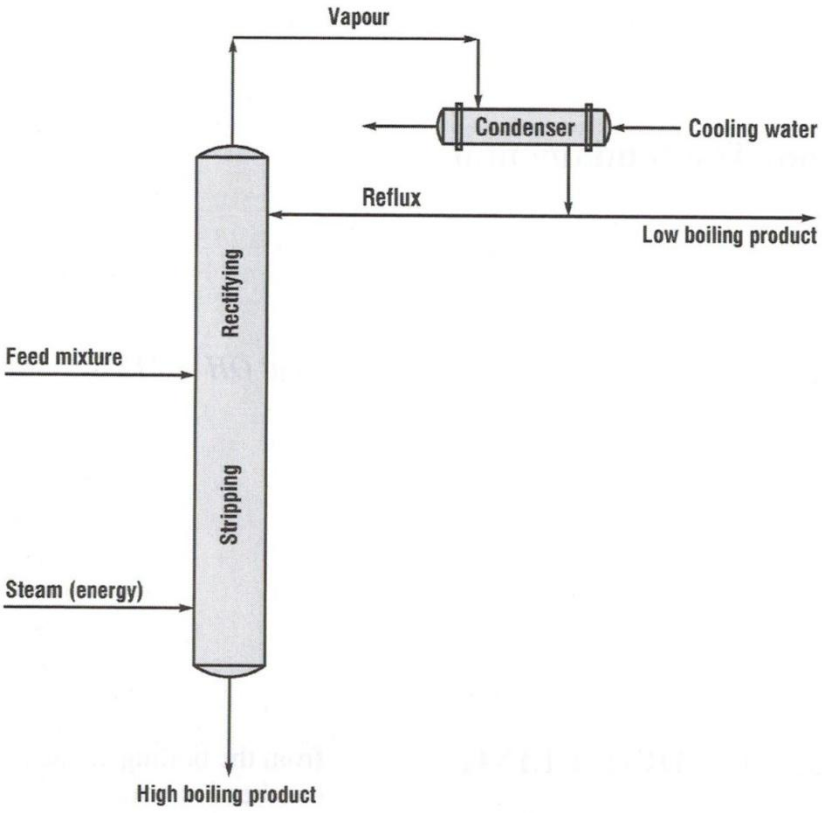

Figure 2-23: A simplified distillation column

"Reprinted from The Alcohol Textbook, Chapter 20, Madson PW, Ethanol distillation: the fundamentals, 290, Copyright (2009), with permission from Nottingham University Press."

2.2.7 Dryhouse technologies

The bottoms product from the distillation column, consisting of beer and nonfermentables, is now referred to as whole stillage. Between 25-50% (w/w) of the original grain components remain in the whole stillage after ethanol production (Monceaux and Kuehner, 2009). Various processing techniques are used to create products such as distillers' wet grains, distillers' dried grains, distillers' dried grains with solubles (DDGS), thin stillage and/or concentrated thin stillage (syrup) from whole stillage (Monceaux and Kuehner, 2009). Production facilities have the option of choosing downstream processes to produce the above products, but not all of these products will be generated because they typically involve only minor processing differences. For example, distillers' dried grains do not contain the condensed thin stillage syrup, but DDGS does. Another example is wet distillers' grains which are only centrifuged and not dried. Typically, dry-grind corn ethanol plants produce DDGS and thin stillage (Monceaux and Kuehner, 2009). DDGS is sold on the animal feed market and thin stillage is recycled into the mashing stage to reduce water consumption.

The first step used to produce DDGS and thin stillage typically involves either a continuous decanter or a solid-bowl centrifuge (Monceaux and Kuehner, 2009). The objective of this step is to separate water and water solubles from the insoluble solids. The soluble aqueous phase, containing mainly water soluble solids and a small portion of insolubles is designated thin stillage. Kim *et al.* (2008) report that thin stillage contains mainly fermentation by-products, soluble sugars, soluble proteins, and organic acids. Numerous evaporator technologies are available to condense the thin stillage, as well as to recycle water into the mashing process operation. The result of evaporation is an increase in solids concentration from 5-10% to 30-50%, resulting in a syrup-like consistency (Monceaux and Kuehner, 2009).

Centrifugation also produces a pellet referred to as wet cake which is comprised of yeast biomass, residual starch, insoluble protein, insoluble fibre, lipids, and other minor insoluble components. The wet cake can be sold directly as wet distillers' grains, further dried to produce dried distillers' grains, or combined with evaporated thin stillage to produce DDGS. Dryer technologies available to industry include drum drying, pneumatic conveyer drying, rotary drying, ring drying, and fluidized bed drying (Monceaux and Kuehner, 2009). Due to the high temperature of these processes, changes to starch structure are likely. High temperatures could lead to side reactions, such as previously described Maillard reactions, changing the overall composition of the DDGS (Izydorczyk, 2005).

2.3 DDGS composition

Dried distillers' grains with solubles (DDGS) are a by-product of ethanol fermentation and are commonly used as animal feed. As described above, DDGS is a mixture of wet cake and condensed thin stillage (or syrup). DDGS includes soluble and insoluble proteins, soluble and insoluble fibre, lipids, residual starch, soluble sugars, organic acids, yeast biomass, fermentation by-products, and other minor components (Belyea *et al.*, 2004; Kim *et al.*, 2008; Gibreel *et al.*, 2009 & 2011; Srichuwong and Jane 2011). Many studies have measured DDGS composition; however, analysis of DDGS focuses on nutritional characteristics to determine its value. One of the strongest drivers of DDGS value is the protein content and a significant amount of the research has been towards characterizing amino acids (Belyea *et al.*, 2004). Common measurements include: digestibility, total digestible nutrients, net energy, and amino acid and mineral profiles (Kim *et al.*, 2008). Quite often the carbohydrate content, or more specifically the starch content, of DDGS is not determined because it has little value as an animal feed. On the other hand, starch is the most valuable component for grain ethanol fermentation and is therefore an important evaluation tool for bioethanol production.

Table 2-6: The proximate composition of DDGS as determined by various studies

Grain	Fermentation	Protein	Lipid	Crude Fibre	Starch	Residual Starch Determination Method	Reference
		% dwb					
corn	Commercial	31.3	11.9	10.2	5.1	AOAC 1984 official method (enzyme or acid hydrolysis not specified)	Belyea *et al.*, 2004
corn	Commercial	27.3	14.5	ND	5.2	Various enzymatic methods; heat gelatinization only	Kim *et al.*, 2008
barley	Laboratory (jet-cooked)	37.2	5.6	3.3	0.2	Megazyme total starch kit (AOAC method 996.11)	Gibreel *et al.*, 2009
barley	Laboratory (raw starch hydrolysis)	40.1	6.9	2.9	0.5	Megazyme total starch kit (AOAC method 996.11)	Gibreel *et al.*, 2009
corn	Laboratory (jet-cooked)	32	12.5	4.6	0.4	Megazyme total starch kit (AOAC method 996.11)	Gibreel *et al.*, 2009
corn	Laboratory (raw starch hydrolysis)	30.8	15.5	4.1	2.8	Megazyme total starch kit (AOAC method 996.11)	Gibreel *et al.*, 2009
wheat	Laboratory (jet-cooked)	43.7	5.2	4.2	0.2	Megazyme total starch kit (AOAC method 996.11)	Gibreel *et al.*, 2009
wheat	Laboratory (raw starch hydrolysis)	43.1	4.9	5.1	0.6	Megazyme total starch kit (AOAC method 996.11)	Gibreel *et al.*, 2009
corn	Laboratory	37.4	11.1	ND	2.2	Hexane defatted DDGS; with DMSO solubilization prior to enzymatic hydrolysis	Srichuwong and Jane, 2011
corn	Commercial	25.3	14.6	ND	5.5	Hexane defatted DDGS; with DMSO solubilization prior to enzymatic hydrolysis	Srichuwong and Jane, 2011
triticale	Laboratory (jet-cooked)	45.3	3.5	5.1	0.1	Megazyme total starch kit (AOAC method 996.11)	Gibreel *et al.*, 2011
triticale	Laboratory (raw starch hydrolysis)	49	3.9	3.4	0.4	Megazyme total starch kit (AOAC method 996.11)	Gibreel *et al.*, 2011

2.3.1 Starch

A portion of starch escapes enzymatic hydrolysis during dry-grind ethanol production. This residual starch may be soluble or resistant in nature. The soluble starch is more easily hydrolyzed by enzymes into sugars, whereas the resistant starch is difficult to hydrolyze (Sharma *et al.*, 2007). Ideally, the majority of the cereal grain starch is transformed into ethanol during SSF, leaving little residual starch in the DDGS. However, in practice there is always some residual starch remaining after production. Reported values for commercial samples all have over 5% (w/w) residual starch (see Table 2-6), suggesting that the current ethanol production process has not been fully optimized. Improved analysis of residual starch in DDGS is of major importance to conduct optimization studies; if not the residual starch remains unreported. More details on the structure of residual starch will be detailed in this section, while analysis methods will be discussed in the following section.

2.3.1.1 Soluble starch

Soluble starch makes up the vast majority of the native cereal grain starch. Most of this starch is easily hydrolyzed into sugars and made available to yeast during fermentation. Both conventional enzymes and raw starch hydrolyzing enzymes are able to hydrolyze soluble starch, so the fraction of soluble starch in DDGS is expected to be low. Soluble starch in whole stillage should be separated into the thin stillage fraction because of its solubility in the aqueous fraction of fermentation media. Kim *et al*. (2008) has proven that a portion of starch is present in thin stillage, albeit a very small fraction (0.5% dwb). It would seem that even though this starch is available to amylase enzymes during liquefaction and saccharification, due to time constraints during industrial production some readily available starch escapes hydrolysis.

2.3.1.2 Resistant starch

Crystalline regions of starch are believed to be inherently more resistant to hydrolysis due to a compact structure that causes steric inhibition of amylase binding (Eerlingen and Delcour, 2005). These crystalline starch structures tend to precipitate out of solution and would almost certainly be present in the wet cake portion of whole stillage. Resistant starch is associated with a number of different structures, some that arise due to treatments used during ethanol production. For example, heating and cooling of starch is known to form one type of resistant starch known as retrogradated amylose (see Section 2.3.1.2.3). Other forms of resistant starch exist in the native starch granule, as was discussed in Section 2.1. Many of the ethanol production operations are used to make natural forms of resistant starch available to amylases during liquefaction and saccharification. For example, gelatinization can melt crystalline regions and make them more available for hydrolysis. The following subsections will describe both the structure

and if applicable, the operation used to make the starch accessible for conversion into ethanol.

2.3.1.2.1 Resistant starch type I

Resistant starch type I refers to the starch that is inherently inaccessible due to the structure of the cereal grain. The pericarp, seed coat, nucleus, and lipoid layers that form a protective barrier around the grain are responsible for enclosing this starch. Very limited transfer takes place between the outer regions of the grain kernel to the inner starchy endosperm. The amylase enzymes need to gain access to the starchy endosperm to hydrolyze the starch; therefore, ethanol producers must use wet-milling or dry-grinding to access resistant starch type I. Milling the grain also increases the surface area for amylase-starch interactions by reducing the particle size.

2.3.1.2.2 Resistant starch type II

Resistant starch type II is related to the granular structure of starch. Highly ordered crystalline regions containing many amylopectin double helices are located at the outer region of starch granules (see Figure 2-24). These regions differ from typical crystalline regions because of the interchain double helices between the amylopectin molecules. The resistant starch type II regions are so tightly packed that amylase enzymes cannot bind and hydrolyze the starch. Gelatinization of starch helps to melt resistant starch type II crystalline regions and makes them available to conventional amylase enzymes. On the contrary, raw starch hydrolysis enzymes drill holes into the starch granule and hydrolyze from the inner cavity of the granule (Shariffa *et al.*, 2009). Recent literature reviews have revealed no studies that report on the availability of resistant starch type II to raw starch hydrolyzing enzymes. The proposed mechanism of drilling into channels or existing pores on the outer surface of the starch granule even suggests that raw starch hydrolyzing enzymes bypass resistant starch type II altogether. Recently, it has been discovered that a raw starch hydrolyzing enzyme from *Rhizomucor* sp hydrolyzes crystalline regions of corn starch at faster rate than amorphous regions (Tawil *et al.*, 2011). Tawil *et al*. (2011) based this conclusion on the rapid decline in crystallinity during the first stages of hydrolysis. Although this is an interesting finding, there is little evidence to suggest that the rapid decline in crystallinity is related to the hydrolysis of resistant starch type II because other regions also contribute to crystallinity.

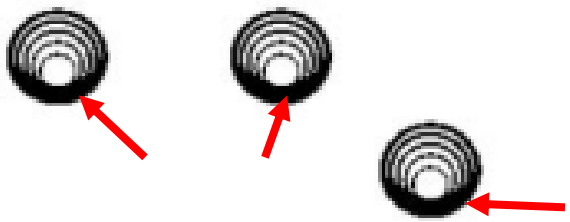

Figure 2-24: Highly ordered regions of amylopectin that constitute resistant starch type II; see arrows

"Resistant starch - a review. Sajilata MG, Singhal RS, Kulkarni PR. Comprehensive Reviews in Food Science and Food Safety 5: 1-17. Copyright (2006) John Wiley and Sons. Reprinted by permission of John Wiley and Sons via Rightslink."

2.3.1.2.3 Resistant starch type III

Resistant starch type III is unlike other resistant starch types discussed thus far because it is not present in the native starch granule. During processing the heating and cooling of starch results in retrogradation, with the end result being a reordering of amylose molecules into a highly compact crystalline structure held together with hydrogen bonding. The high number of hydrogen bonds order the amylose strands into tightly woven double helices within a continuous gel matrix (Leloup *et al*., 1992), thereby reducing the ability of amylase enzymes to bind to the starch (Ellis *et al*., 1998). The kinetics of amylose double helix formation favour shorter amylose strands (DP 80-100)- (Gidley and Bulpin, 1989). Gelatinization temperatures around 60-70°C are enough to melt amylopectin crystalline regions in resistant starch type II, but temperatures of 130-170°C are needed to melt amylose double helices in resistant starch type III (Sievert and Pomeranz, 1989). Due to these high melting temperatures, resistant starch type III formed during the ethanol production process is almost certainly unavailable to amylases used for hydrolysis.

It is believed that operations during ethanol production that reach high temperatures such as jet-cooking or DDGS drying can actually produce resistant starch type III. Cereal grain characteristics that may lead to increased formation of resistant starch type III are higher amylose content along with the processing conditions (temperature and water content) - (Berry, 1986; Sievert and Pomeranz, 1989). Based on these principles alone, a higher yield of resistant starch type III would be expected when high temperature processing, such as jet-cooking is used as compared to raw starch hydrolysis. However, another mechanism for resistant starch type III formation has recently been proposed. Lopez-Rubio *et al*. (2008) and Tawil *et al*. (2011) suspect that as linear amylose-like fragments are released by α-amylase and they too can organize into crystalline structures indicative of resistant starch type III. This would suggest that resistant starch

is potentially formed during any type of enzymatic hydrolysis, regardless of the exposure of starch to heating and cooling cycles. This is an important finding considering that resistant starch type III is well known to be highly resistant to enzymatic attack (Colonna *et al.*, 1992; Planchot *et al.*, 1997).

2.3.1.2.4 Resistant starch type IV

Resistant starch type IV is a chemically cross-linked starch and is also not present in the native starch granule. To produce cross-linked starch bi- or polyfunctional reagents like sodium trimetaphosphate, phosphorus oxychloride, or adipic acid are used to create side chains between starch polymers (Sajilata *et al.*, 2006). The cross-linked starch involves linkages with starch hydroxyl groups thereby resulting in resistant to amylolytic attack (Sajilata *et al.*, 2006). There is not expected to be any resistant starch type IV production during the wet-milling or dry-grinding processes, so further discussion of this type of resistant starch will not be undertaken as it is not relevant to industrial fuel fermentations.

2.3.1.2.5 Resistant starch type V

Resistant starch type V refers to a structural complex formed between amylose and lipids. These amylose-lipid complexes are further subcategorized as type I and type II (Jane, 2009). Native amylose-lipid complexes are referred to as type I, whereas type II amylose-lipid complexes are formed after heat treatments, when the leached amylose is in the presence of monoacylglycerides (Kowblansky, 1985; Czuchajowska *et al*., 1991; Tufvesson and Eliasson, 2000). When type I amylose-lipid complexes are heated at a temperature of at least 80°C, the native type I starch anneals to form semi-crystalline structures, associated with birefringence and a V-type x-ray pattern rarely seen in native cereal starch (Biliaderis *et al*., 1986; Jane, 2009). These annealed complexes are known as type II amylose-lipid complexes or as resistant starch type V. In another study, Tufvesson and Eliasson (2000) concluded that a temperature of at least 80°C was needed to form type II amylose-lipid complexes, but that higher yields would be formed at ≥90°C.

In regards to the accessibility of these amylose-lipid complexes, there are different melting points for the two types. Type I amylose-lipid complexes have a lower thermal transition peak (94-100°C) than type II amylose-lipid complexes (100-125°C) associated with resistant starch type V (Karkalas *et al*., 1995; Jane, 2009). This means that native amylose-lipid complexes are much more accessible to enzymes than the type II amylose-lipid complexes. The greater resistance of the type II amylose-lipid complex is why it is defined as resistant starch type V.

2.3.2 Protein

Protein accounts for 28-33% of the total weight of dry-grind corn DDGS (Belyea *et al.*, 2004). Results from Gibreel *et al*. (2011) confirm the protein range for corn DDGS samples reported by Belyea *et al*. (2004), but also found that wheat and triticale have higher protein contents of 37-44 and 39-49% respectively. An earlier study by Gibreel *et al*. (2009) reported hulless barley protein contents to have a similar range to wheat at 37-43%. A much higher protein content range of 35-40% was reported for corn DDGS in a study done by Srichuwong and Jane (2011), although a commercial corn DDGS sample in the same study was approximately 25%. Each of these studies used different drying techniques that could significantly alter the quantitative analysis of protein within DDGS samples. Gibreel *et al*. (2011) used a combination of rotary evaporation at 72°C and freeze drying at -60°C (at ~$4x10^4$ Pa), designed to preserve sensitive micronutrients. Srichuwong and Jane (2011) also dried their laboratory produced DDGS in a two stage process, but used a boiling water bath in combination with a convection oven at 55°C. It is also interesting to note that all of the commercial samples had lower protein contents. The high protein content of DDGS is a result of the concentration of nonfermentables and the increased yeast biomass during SSF. In fact, Belyea *et al*. (2004) reported that up to 50% of all proteins in DDGS could be from yeast origin based on the amino acid profiles of corn DDGS. These values are likely to vary significantly from plant to plant due to processing differences, but Belyea *et al*. (2004) concluded that the variation is not related to the variation in the corn grain values prior to fermentation.

One of the biggest impacts the residual protein and amino acids could have in regards to DDGS composition are due to Maillard reactions at high temperatures during drying. The high temperatures used to dry DDGS induce Maillard reactions between proteins, or amino acids, and reducing sugars. The initial stages of this complex reaction were described in Section 2.2.3. End products of the Maillard reaction are generated from the polymerization of furfurals and hydroxymethylfurfurals (Izydorczyk, 2005)-(see Figure 2-25 & 2-26). The resulting characteristic dark brown polymers are known as melanoidins (Izydorczyk, 2005)-(see Figure 2-27). It is likely that the high temperatures used in commercial drying would lead to Maillard reactions to produce melanoidins, but it has not been reported as a reason for the reduced protein content in commercial DDGS samples. Other reasons for lower protein in commercial samples could be due to less yeast biomass production or the use of protease to produce free amino nitrogen as yeast food.

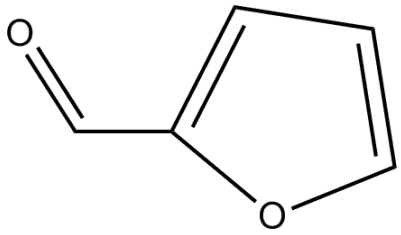

Figure 2-25: Structure of furfural

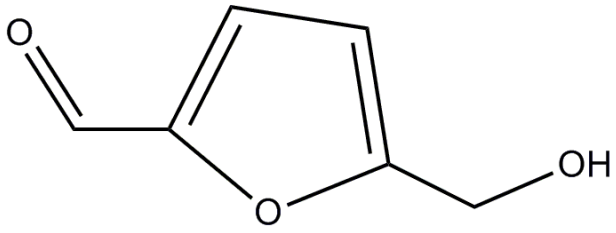

Figure 2-26: Structure of 5-hydroxymethylfurfural

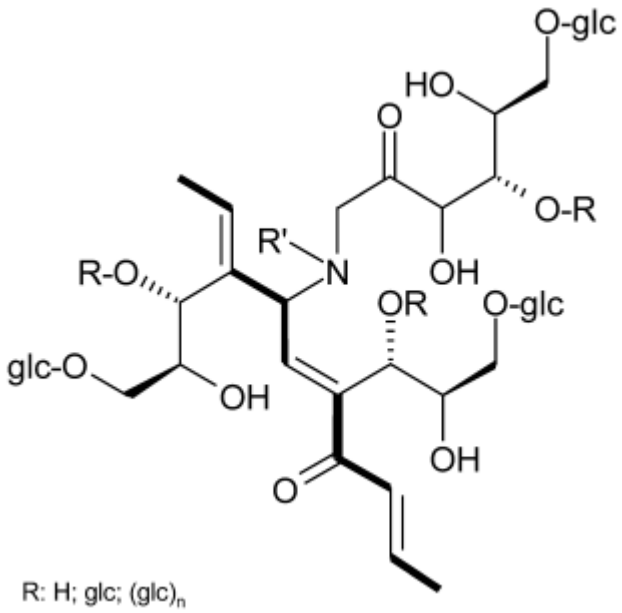

Figure 2-27: Proposed structure of melanoidins; glc = glucose

"Reprinted from International Congress Series, 1245, Cammerer B, Jalyschkov V, Kroh LW, Carbohydrate structures as part of the melanoidin skeleton, 269-273, Copyright (2002), with permission from Elsevier"

2.3.3 Lipids

The total lipid content of corn DDGS has been reported to range from 11-15% (Belyea *et al.*, 2004; Gibreel *et al.*, 2009 & 2011; Kim *et al.*, 2008; Srichuwong and Jane, 2011). Lipid contents in wheat, triticale, and barley are much lower than corn as would be

expected, due to their lower cereal grain lipid composition. Total lipids contents from wheat, triticale, and barley DDGS were reported as ranging between 4-7% (Gibreel *et al.*, 2009 & 2011). The studies by Gibreel *et al*. (2009 & 2011) further classified the free fatty acids and found that linoleic acid is the most abundant free fatty acids in the original cereal grain and in the DDGS regardless of cereal or DDGS type (corn, wheat, triticale, and barley). In the cereal grain and the DDGS, linoleic acid accounts for approximately 50% of all free fatty acids. Other free fatty acids making up a significant portion of the DDGS were oleic and palmitic acids. Further classification of lipids was not undertaken by any of the above studies.

Resistant starch type V, also known as a type II amylose-lipid complex, is also found in DDGS samples. The quantification of the lipid bound to starch has not been reported, but defatting DDGS prior to starch analysis leads to an increase in starch content (Srichuwong and Jane, 2011). The improved starch analysis reported by Srichuwong and Jane (2011) implies the presence of type II amylose-lipid complexes. The starch is unavailable when complexed to the lipid, but after defatting the DDGS the starch can be hydrolyzed and quantified. It should be noted that Srichuwong and Jane (2011) only reported the use of their defatting procedure on conventional jet-cooked DDGS. There may be no formation of type II amylose-lipid complexes in DDGS using the raw starch hydrolysis method because of the lack of high temperatures of 80-90°C that anneal native complexes into type II complexes (see Section 2.3.1.2.5).

2.3.4 Non-starch polysaccharides

Carbohydrate polymers, other than starch, are typically broadly classified as fibre or non-starch polysaccharides. Numerous forms of non-starch polysaccharides are found in DDGS. Cellulose and β-glucan are two major non-starch polysaccharides found in cereal grain cell walls (see Figure 2-28 & 2-29). Kim *et al*. (2008) reported cellulose values of 16% in commercial dry-grind corn DDGS, but other studies report crude fibre in the 4-10% range (Belyea *et al.*, 2004; Gibreel *et al.*, 2009). This is an odd occurrence because crude fibre is designated as cellulose, lignin, and hemi-cellulose which are all present in DDGS. The value of crude fibre should therefore be higher than the reported 16% value determined by Kim *et al*. (2008). No studies have reported the values of β-glucan in DDGS, but values within cereal grains range from 0.5-16% (Bhatty 1992; Skendi *et al.*, 2003). No other non-starch polysaccharides have been reported either because studies typically only report crude fibre.

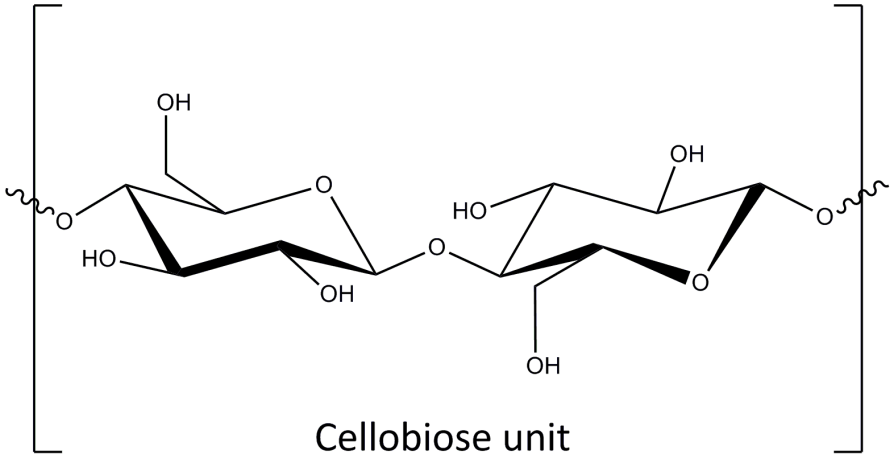

Figure 2-28: Structure of repeating β-glucan molecules (β-1-4 linkages) in cellulose

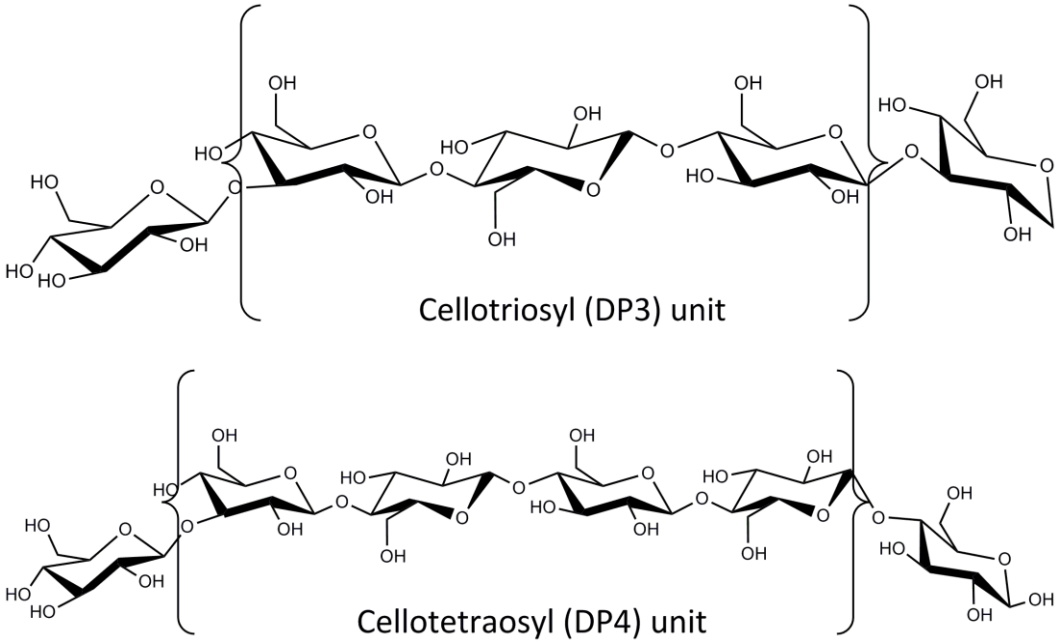

Figure 2-29: Structure of repeating β-glucan molecules (β-1-3 and β-1-4 linkages) in β-glucan cellotriosyl and cellotetraosyl units

Both cellulose and β-glucan are homopolysaccharides; that is they contain only one kind of monosaccharide which is glucose (Izydorczyk, 2005). β-glucan is a linear soluble fibre with β-1-3 linked cellotriosyl and cellotetraosyl units arranged randomly (Gomez *et al.*, 1997). On the other hand, cellulose is a linear, insoluble, and recalcitrant material consisting of β-1-4 linked glucan molecules designed to provide structural stability within plants. β-glucan polysaccharides differ from α-glucan chains in starch because of the alternating orientation of glucan residues. Amylase enzymes used in bioethanol production do not hydrolyze non-starch polysaccharides because of structural differences in their glycosidic linkages.

Another non-starch polysaccharide in DDGS is referred to as hemicellulose. Hemicellulose is included in the crude fibre measurements analyzed in DDGS composition studies. The hemicellulose chains are branched, contain various monosaccharides, have a low molecular weight, and are structurally associated with cellulose (see Figure 2-30). More specifically, hemicellulose is a heteropolysaccharide containing 500-3000 sugar monomers of both five and six-carbon sugars (Izydorczyk, 2005; Monceaux, 2009). The major sugar unit in hemicellulose is xylose, a five-carbon sugar (Monceaux, 2009). Cereals contain a specific class of hemicellulose, known as arabinoxylan (Monceaux, 2009). The arabinoxylan consists of a main chain of xylose with side chains of arabinose.

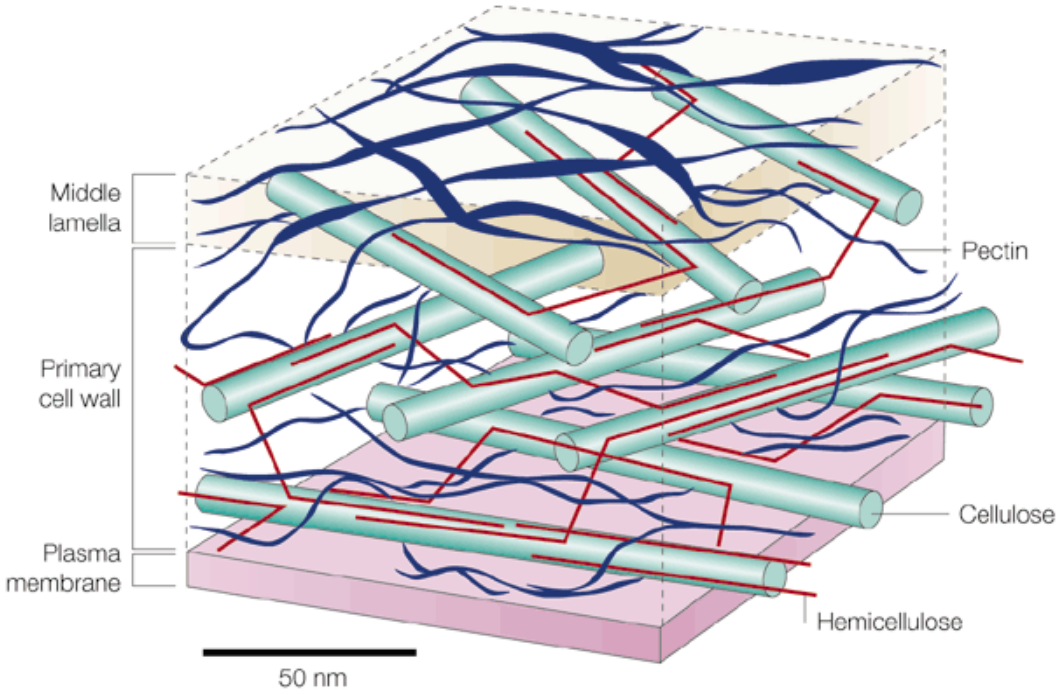

Figure 2-30: Interaction between cell wall polysaccharides

"Reprinted by permission from Macmillan Publishers Ltd: Nature Reviews Molecular Cell Biology, Smith LG, Plant cell division: building walls in the right places 2: 33-39, Copyright (2001)."

2.4 Starch determination

2.4.1 Enzymatic hydrolysis

Enzymatic analysis of starch was used as early as 1880 (Kearsley and Verwaerde, 1991). The principle of starch analysis is still the same today as it was over a century ago. Starch α-glucan units (anhydroglucose; MW=162) are hydrolyzed into free glucose (MW=180) followed by quantitative glucose determination. The glucose concentration

is determined with colourimetric assays or high performance liquid chromatography. The glucose concentration is then converted into starch content based on the molecular weight difference between anhydroglucose and free glucose. This indirect procedure creates a situation in which interfering substances in DDGS may affect the quantitative analysis of starch. For example, underestimation of starch may occur due to incomplete starch hydrolysis, isomerisation of glucose, or reactions between glucose and other compounds. Measurements that perceive interfering glucose or monosaccharides as starch-related glucose results in an overestimation of starch (Hall *et al.*, 2001). Other reasons for overestimation include if endogenous glucose is in the sample or if glucose is released by non-amylolytic enzymes.

When using enzymatic hydrolysis to measure total starch it is important to use enzymes of high purity. Contaminating enzymes could hydrolyze non-starch polysaccharides in DDGS and result in the overestimation of total starch. High purity bacterial enzymes used for the analysis of starch have been commercialized and are distributed under the trademark Megazyme. The total starch analysis kits sold by Megazyme employs two separate amylases for the purpose of hydrolyzing starch. The enzymes are produced from *Bacillus licheniformis* and *Aspergillus niger,* which produce the thermostable α-amylase and amyloglucosidase respectively. These amylases are similar in functionality as those used for SSF during ethanol production and the same synergism between the α-amylase and amyloglucosidase is utilized (see Figure 2-21). The actions of these amylases are very specific to starch glycosidic bonds, but the temperature and pH are major controls that enable the action of these enzymes. The analyst must take great care to ensure the proper temperature and pH is used for each step of the enzymatic hydrolysis method. It is also important when using enzymatic hydrolysis methods that positive controls are used. For example, a sample of corn starch with a known starch value should be analyzed in parallel to the unknown DDGS samples. Any disparity between the known starch value and the observed starch value determined by the analyst provides information about the reliability of their results.

Very limited research has been completed on the determination of residual starch in DDGS. It remains unclear whether an overestimation, underestimation, or accurate analysis is being reported. One might expect a large underestimation of starch because of the resistant starch forms discussed in the previous section. For the most part resistant starch type I, type II, and type IV are non-issues for the determination of residual starch in DDGS. Both resistant starch type I and type II are made available during the ethanol production process. Previous exposure to amylase enzymes has likely degraded any starch associated with resistant starch type I or type II. In the case of raw starch hydrolysis, which may not hydrolyze resistant starch type II, only mild heating is required during the starch analysis to make resistant starch type II available for hydrolysis (Sievert and Pomeranz, 1989). Moreover, resistant starch type IV is not expected in DDGS because no chemical cross-linking reagents are used during ethanol

production. Resistant starch type IV is produced for the food industry and requires specific processing conditions to be created. Therefore, based on starch structure alone, only resistant starch type III and resistant starch type V should create issues for the enzymatic hydrolysis of residual starch in DDGS.

Srichuwong and Jane (2011) have determined using gel permeation chromatography that the major fractions of residual starch in DDGS are made of linear molecules (average DP = 85) which have a lower molecular weight than native amylose. Earlier reports had already tied linear fragments in the DP 80-100 range as having a higher propensity to form resistant starch type III (Pfannemuller 1987). This could be problematic for analysis because high temperatures, such as those needed to melt resistant starch type III (130-170°C), are not reached during starch analysis. It is important that any methodology used for starch analysis has another mechanism to accurately measure resistant starch type III. Fortunately it has been discovered that chemical solvents can be used to dissolve resistant starch type III. The objective of using these solvents is to allow for a more complete hydrolysis of residual starch in DDGS by ensuring that resistant starch is hydrolyzed. The Megazyme total starch kit does recommend two chemical solubilization steps for samples containing resistant starch, those being dimethylsulfoxide (DMSO) and potassium hydroxide (KOH). One study has reported DDGS residual starch values using DMSO, but as of yet KOH remains untested.

The mechanism of resistant starch solubilization for DMSO is believed to be due to a disruption of hydrogen bonds. Srichuwong and Jane (2011) suggest that DMSO disrupts bonds between amylose chains due to DMSO's activity as a hydrogen bond acceptor. The DMSO is such a strong hydrogen bond acceptor that starch hydroxyl groups preferentially bind to DMSO instead of binding to each other (Craig *et al.*, 1989). Resistant starch type III and type V owe their resistant properties to strong hydrogen bonds involved; therefore, DMSO is possibly a useful solvent for both resistant starch type III and resistant starch type V. When DMSO was used in conjunction with enzymatic analysis of DDGS samples, Srichuwong and Jane (2011) found that DMSO was a useful solvent and it resulted in higher reported residual starch values. Additional improvements were made to their analysis methods which included defatting the DDGS with hexane prior to dissolution with DMSO. It was concluded that defatting the DDGS prevented the instantaneous reformation of resistant starch type V following the dilution of DMSO in subsequent steps involving enzyme-buffer solutions (Srichuwong and Jane, 2011).

Alkaline solutions such as KOH or NaOH also result in a disruption of hydrogen bonding between amylose chains in resistant starch. The mechanism is described as an ionization of starch molecules which causes a coulombic repulsion between the ionized hydroxyl groups (Craig *et al.*, 1989). The charged repulsion of these groups prevents the association of starch chains (Craig *et al.*, 1989) and should result in improved enzyme

access to the starch chains. A recent literature search found no research regarding the use of alkaline solutions for the improvement of residual starch analysis in DDGS.

2.4.2 Acid hydrolysis

In the presence of heat, starch glycosidic bonds are randomly hydrolyzed by hydrated protons (H_3O+) from aqueous hydrochloric acid (HCl) leading to saccharification and solubilization of starch granules (Brummer and Cui, 2005; Vasanthan and Bhatty, 1996). Small granules of corn and barley were found to be hydrolyzed by acid at a significantly higher rate than large granules (Xia 2010; Vasanthan and Bhatty, 1996). Quick hydrolysis of small starch granules has been attributed to the high surface area, hydration properties, and increased swelling of these granules (Vasanthan and Bhatty, 1996). Acid hydrolysis is an alternative method to enzyme hydrolysis, but it is still considered an indirect method because it requires released glucose to be quantified and back calculated into starch content.

Several studies have examined the mechanism of acid hydrolysis and it is widely believed that the amorphous regions of starch are preferentially hydrolyzed (Jenkins and Donald, 1997; Miao *et al.*, 2011). It was found by Xia *et al*. (2010) using scanning electron micrographs that acid hydrolyzes cereal starch from the outer regions of the granule. Other studies report increased crystallinity using x-ray diffraction indicating that crystalline regions are well preserved (Jenkins and Donald, 1997; Miao *et al.*, 2011). Miao *et al*. (2011) also analyzed the chain lengths of acid hydrolyzed waxy corn starch and observed that the long (DP > 33) and very short (DP < 13) chains were hydrolyzed by acid. It was concluded from these findings that the inner branch chains within crystalline regions of starch were resistant to acid hydrolysis. It should be noted that the above acid hydrolysis studies were done at low temperature over a number of days.

Dilute acid hydrolysis was used by Kim *et al*. (1988) to measure residual starch remaining in spent fermentation medium. The fermentation was conducted using an inoculation with mutant yeast cells into a 500mL flask containing 4% soluble potato starch. The mutant yeasts were capable of producing and secreting α-amylase and amyloglucosidase. Fermentation was conducted over a period of 5 days at a temperature of 30°C. It was reported by Kim *et al*. (1988) that a conversion efficiency of starch to ethanol of over 93% was achieved with the mutant yeasts based on residual starch analysis. The starch analysis method involves adding 1mL of 2M HCl to the spent medium and incubating in a boiling water bath for 35 minutes. The solution is then neutralized with the addition of 1mL of 2M sodium hydroxide (NaOH) followed by the quantitative analysis of glucose using the glucose-oxidase peroxidase reagent (GOPOD)- (see Section 2.4.4). The culture medium used in this study was a much less complex material than DDGS and interferences or other challenges may occur for DDGS residual starch analysis.

Another study has reported the use of acid hydrolysis for the measurement of pericarp fibre and corn germ residual starch. Similarly to DDGS, these ethanol by-products from enzymatic milling have relatively low starch content (Videl 2009). The residual starch analysis was completed using both enzymatic hydrolysis and acid hydrolysis. Enzymatic analysis involved using a standardized total starch analysis kit from Megazyme (Wicklow, Ireland). The acid hydrolysis was completed on 1g samples weighed into an autoclavable container and autoclaved for 1 hour at 127°C in the presence of 50mL of hydrochloric acid (0.4N). The germ and pericarp fibre samples were spiked with endosperm flour for enzymatic and acid hydrolysis methods. No significant difference was observed in residual starch values for either method unless the samples were spiked with endosperm flour. Enzymatic analysis using the Megazyme total starch kit was concluded to be underestimating the starch in these samples. The researchers deemed the acid hydrolysis method a suitable option for the residual starch analysis of corn germ and pericarp fibre produced from enzymatic milling.

The presence of resistant starch type III and type V in DDGS also creates a challenge for acid hydrolysis. It has been determined that when using sulphuric acid (16%) at 25°C only the amorphous sections of retrogradated amylose (resistant starch type III) are hydrolyzed (Jane and Robyt, 1984). In regards to resistant starch type V, it was reported by Vasanthan and Hoover (1992) that defatting starches did not improve acid hydrolysis rates versus native starch. This suggests that amylose complexed with lipid does not resist degradation by acid hydrolysis; however, it is possible that bound lipids were not removed with the defatting process and that type II amylose-lipid complexes resisted acid hydrolysis in both native and defatted starches.

Based on the inability of acid to hydrolyze crystalline regions of starch, we are suggesting that acid hydrolysis may slightly underestimate the amount of residual starch in DDGS. On the other hand, a methodology using higher temperatures may alter the hydrolysis mechanism reported previously in the literature and allow for an accurate measurement of residual starch. Acid hydrolysis at higher temperatures also increases the possibility that other glucose non-starch polysaccharides will be hydrolyzed because acid hydrolysis lacks the specificity of enzymatic hydrolysis.

2.4.3 Glucose analysis

2.4.3.1 Glucose oxidase peroxidise enzyme (GOPOD)

The GOPOD reagent is a colourimetric determination method for quantitative measurement of glucose. The enzyme is specific to glucose and works in two stages involving two separate enzymes: β D-glucose oxidase and peroxidase (see Figure 2-31). The initial reaction oxidises D-glucose to D-gluconate with the release of 1 mole of H_2O_2. For the second reaction there are numerous options for the composition and end colour of the indicator dye. The Megazyme kit used in this study makes use of a reaction

between H_2O_2 and an indicator dye made of ρ-hydroxybenzoic acid and 4-aminoantipyrine. This reaction yields a pink colour due to the formation of quinoneimine dye. The colour intensity is proportional to the glucose concentration in the sample and is measured spectrophotometrically at 510nm. The unknown sample concentrations are compared to a glucose standard and known starch controls. Detection limits noted by the Megazyme assay kit are as little as 2.0mg of D-glucose/L of sample solution. This level corresponds to 0.18% starch, which is much lower than the expected residual starch values in the DDGS.

1) D-glucose + O_2 $\xrightarrow{\beta \text{ D-glucose oxidase}}$ D-gluconate + H_2O_2

2) H_2O_2 + indicator dye $\xrightarrow{\text{peroxidase}}$ colour + H_20

Figure 2-31: GOPOD reactions

Interfering substances for the GOPOD reactions include mannose, galactose, and xylose (Kearsley and Verwaerde, 1991). However, the above substrates are oxidized at approximately 1, 0.1, and 0.4% of the rate of glucose, respectively (Kearsley and Verwaerde, 1991). These interferences should be minor to non-existent when considering the expected levels of these substrates in DDGS and the relative oxidation rates as compared to glucose. It was decided that GOPOD would provide reasonable specificity and precision for the analysis of residual starch in DDGS.

2.4.3.2 Calculation to convert sample absorbance to % starch

The absorbance of the sample is an arbitrary value that must be converted to a percentage starch basis. The calculation must first calculate the concentration of glucose in the sample, based on the absorbance of a known solution. Then the glucose concentration needs to be converted into starch content based on the molecular weight difference between anhydroglucose (MW = 162) and free glucose (MW = 180). Other calculations are also included for the extent of sample dilution, sample weight, and the absorbance of the [glucose] in the samples and the standards. Based on volume adjustments made in our methods to increase sample throughput, the calculation is slightly different than that used in the Megazyme assay kit. Please see the calculation in Equation 2-1.

$$\text{Starch \%} = \Delta A \times F \times \frac{FV}{0.005} \times \frac{1}{1000} \times \frac{100}{W} \times \frac{162}{180}$$

Where:

ΔA = sample absorbance (read against the reaction blank)

$F = \dfrac{5\mu g \text{ of glucose}}{\text{absorbance of } 5\mu g \text{ of glucose}}$

(conversion from absorbance to µg)

FV = final volume of dilution (mL)

0.005 = volume of sample analyzed (mL)

1/1000 = conversion from µg to mg

100/W = factor to express starch as a percentage

W = weight of the sample (mg)

162/180 = adjustment from free D-glucose to anhydrous D-glucose (as occurs in starch)

Equation 2-1: Calculation for conversion of sample absorbance into starch content

3. Materials and Methods

3.1 Materials

3.1.1 DDGS

The DDGS samples used for this thesis work were provided from a study done by Gibreel *et al*. (2009) and from unpublished work in our laboratory. The starch content and other information about the grain used to produce the DDGS in this thesis can be seen in Table 3-1. In general, high temperature jet-cooking or raw starch hydrolysis was used to hydrolyze and saccharify cereal starch (detailed methods are available in Appendix 1). The fermentations were conducted in duplicate using 5L high-performance bioreactors (Rose Scientific, Ltd., Mississauga, Ontario). The DDGS was then dried using a two stage process which involved the evaporation of the liquid phase in rotary evaporator at 72°C, followed by freeze-drying at -60°C at ~4 x 10^4Pa for 72 hours.

The study by Gibreel *et al.* (2009) intended on measuring sensitive nutritional compounds in DDGS, which required a delicate drying process. In order to simulate industrial drying conditions, freeze-dried DDGS was rehydrated to 30% (w/w) with distilled water in aluminum pans. A convection oven (Fisher Isotemp oven model 750F)

was used to dry the rehydrated DDGS for 24 hours at 105°C. After oven drying the pans were scraped and the collected sample was milled (IKA mill model M20S3). A general flow chart that illustrates the different processing and drying conditions is shown in Figure 3-1.

Table 3-1: Background information about the cereal grains used to produce DDGS

Grain type	Received from	Starch % (dwb)	Moisture %	Reference
AC Reed Wheat	Agriculture Canada Research Station (Lethbridge, AB)	61.7	7.7	Gibreel *et al.*, 2009
Hi-Bred Corn	Pioneer Hybrid, Ltd. (Chatham, ON)	62.1	10.1	Gibreel *et al.*, 2009
CDC Bold Barley	Kaun's seed farm (Red Deer, AB)	56.8	11.4	Gibreel *et al.*, 2009
Ultima Triticale	Alberta Agricultural Field Crop Development Centre (Lacombe, AB)	58.2	10.7	Gibreel *et al.*, 2011

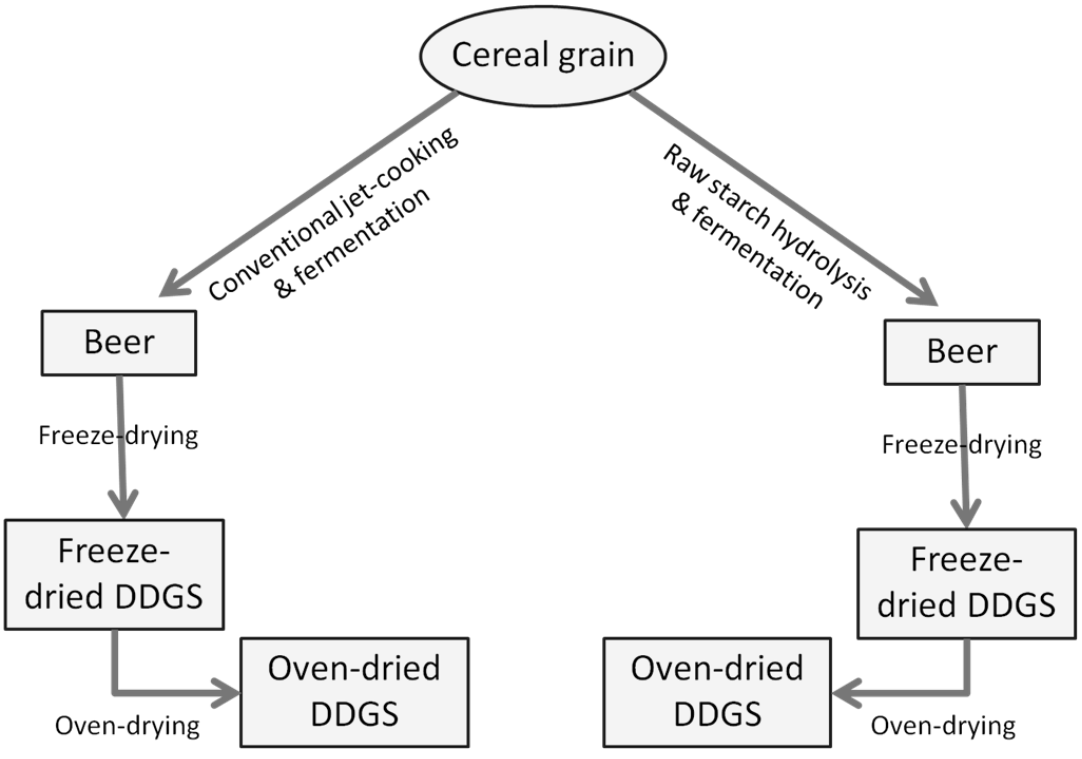

Figure 3-1: Generalized flow-chart of the processing and drying conditions used to produce DDGS samples

3.1.2 Chemicals and other materials

Starch analysis kits are commercially available, including the official AOAC method for analysis (Megazyme; AOAC official method 996.11). The starch analysis kits and all other materials used for my thesis experiments are summarized in Table 3-2.

Table 3-2: Chemicals and materials used for thesis experiments

Material	Catalogue Number (Year)	Manufacturer	Supplier
Megazyme total starch kit	K-TSTA (2010)	Megazyme	Cedarlane Burlington, ON
Hydrochloric acid	320331 (2008)	Sigma	Sigma-Aldrich Co. St. Louis, MO
Glacial acetic acid	A35 (2011)	Fisher Chemicals	Fisher Scientific Fair Lawn, NJ
Potassium hydroxide	P250 (2008)	Fisher Chemicals	Fisher Scientific Fair Lawn, NJ
Sodium hydroxide	S320 (2011)	Fisher Chemicals	Fisher Scientific Fair Lawn, NJ
Sodium azide	BP9221 (2011)	Fisher Chemicals	Fisher Scientific Fair Lawn, NJ
Dimethyl sulfoxide	471267 (2011)	Sigma	Sigma-Aldrich Co. St. Louis, MO
MOPS sodium salt	M-9381 (2010)	Sigma	Sigma-Aldrich Co. St. Louis, MO
Microcrystalline cellulose	191499 (2009)	MP Biomedicals	MP Biomedicals Solon, OH
β-glucan concentrate (~50% β-glucan)	Not commercially available	Cevena Bioproducts	Not commercially available
β-glucan concentrate (~70% β-glucan)	Not commercially available	Cevena Bioproducts	Not commercially available
Superstart instant dry yeast	6419-19 (2009)	Lallemand Ethanol Technology	Lallemand Ethanol Technology Milwaukee, WI

3.2 Experimental methods

3.2.1 DDGS sieving

DDGS from freeze or oven-dried samples was sieved on a US standard sieve #35 (500μm). Only fractions <500μm were used for starch analysis. Sieving was done to create a more uniform particle size during residual starch analysis, thereby reducing

variation. The particle size was selected based on procedures outlined by the official method of total starch analysis (Megazyme; AOAC method 996.11).

3.2.2 Benchmarking residual starch analysis methods

Commonly reported methods in the literature were used to benchmark the residual content in DDGS. By far the most frequently used method is the Megazyme total starch kit (AOAC official method 996.11). Another benchmarked method includes a slight variation of the Megazyme method that incorporates DMSO. This variation is also an AOAC official method, but it is intended for use on samples known to have resistant starch. Interestingly, even though DDGS is known to have resistant starch, this method is not as commonly used in the literature. The last method benchmarked in this thesis involves acid hydrolysis with HCl. Variations of this method are quite common in the literature, so it was decided to select one acid hydrolysis method that was commonly used in our laboratory. Reporting the residual starch using these methods allows for a baseline comparison between all methods evaluated in this thesis.

3.2.2.1 Megazyme method – AOAC Official Method 996.11

DDGS samples were analyzed for total starch content according to the AOAC Official Method 996.11 (Megazyme total starch kit - method B). DDGS samples (<500µm) were weighed to 100mg ± 5% using an analytical scale (Precisa XT 220A). The samples were then dispersed in 80% ethanol and vortexed to disperse the starch in the sample. Thermo-stable α-amylase (300U) and 3mL of MOPS buffer (50mM; pH =7.0) were added to each sample. Next, the samples were heated in a boiling water bath for 6 minutes. Test tubes were then transferred to a water bath (Shel Lab WS27) and stabilized at 50°C. Amyloglucosidase (326U) and 4mL of sodium acetate buffer (200mM; pH=4.5) were added to each test tube followed by vortexing. After an incubation period of 30 minutes, the samples were transferred to 10mL volumetric flasks and made up to volume with distilled water. Flasks were mixed by inverting 10 times before transferring a 1.5mL aliquot into microcentrifuge tubes. Each aliquot was centrifuged at 1610 x g for 10 minutes in a microcentrifuge (Eppendorf 5424). After centrifugation, only the supernatant was used for absorbance readings because any free glucose would be soluble in the aqueous solution.

The recommended procedure for absorbance readings was altered from the standard Megazyme method for a higher throughput. This was achieved by conducting the GOPOD reagent incubation step in 96 well microplates as a substitute for using test tubes. Microplates were loaded with 5µL of sample supernatant, starch control, glucose control, or a reagent control. Each microplate well then received 240µL of GOPOD reagent for the incubation step. Incubation at 50°C was completed using an incubator (Fisher Isotemp oven model 100FS). Absorbance values were read with a microplate

reader (Biotek SynergyMx) at 510nm. The absorbance wavelength is published in the Megazyme method and is based on the production of quinoneimine dye.

All absorbance values had sample blank absorbance readings subtracted, which accounts for the residual glucose in the DDGS samples and prevents the overestimation of residual starch in DDGS. Sample blanks were analyzed by weighing 100mg of DDGS sample into test tubes. Each tube received 10mL of distilled water and was vortexed. A 1.5mL aliquot was transferred into microcentrifuge tubes and centrifuged at 1610 x g for 10 minutes in a microcentrifuge (Eppendorf 5424). The supernatant was used to load 5µL of sample supernatant into microplate wells. Sample blanks then received 240µL of GOPOD reagent, followed by the incubation and microplate absorbance measurements used for all other measured samples.

3.2.2.2 Megazyme method (DMSO format) – AOAC Official Method 996.11

Samples were analyzed for total starch content according to the AOAC Official Method 996.11 (Megazyme total starch kit - method D). DDGS samples (<500µm) were weighed to 100mg ± 5% using an analytical scale (Precisa XT 220A). The samples were then dispersed in 80% ethanol and vortexed to disperse the starch in the sample. Next, 2mL of DMSO was added and the samples were heated in a boiling water bath for 5 minutes. Following this incubation, thermo-stable -amylase (300U) and 3mL of MOPS buffer (50mM; pH =7.0) were added to each sample. The test tubes were then incubated for another 6 minutes in the boiling water bath. Additional enzyme incubation steps in this procedure are outlined in Section 3.2.2.1, following the boiling water bath step (see Figure 3-2). Absorbance readings were completed in a microplate as described in Section 3.2.2.1. All absorbance values had sample blank absorbance readings subtracted to account for residual glucose in the DDGS samples.

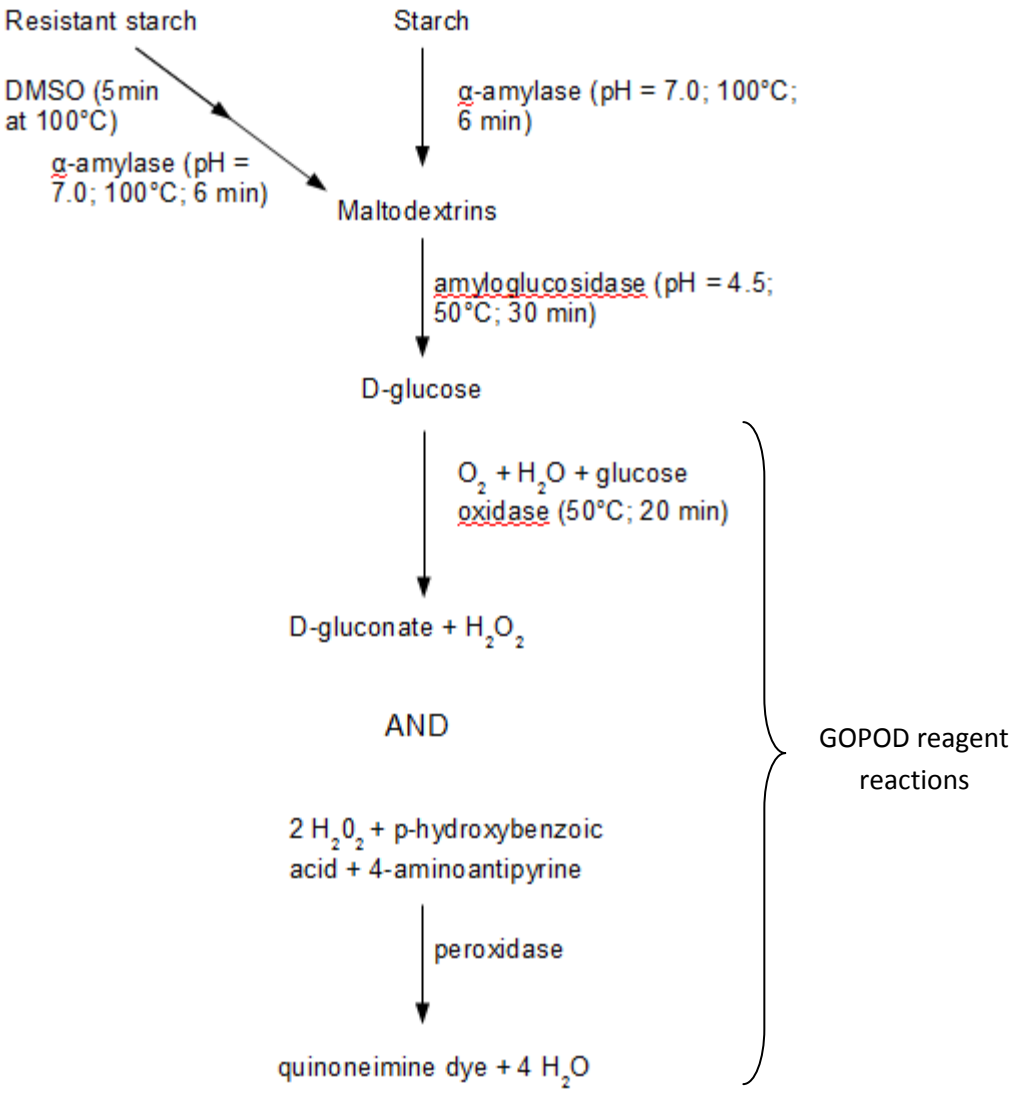

Figure 3-2: A flow-chart of two enzyme hydrolysis methods used for residual starch benchmarking

3.2.2.3 Acid hydrolysis

An acid hydrolysis method was developed by merging a protocol outlined by Kim *et al*. (1998) with the altered GOPOD incubation used in the outlined enzymatic methods (see Figure 3-3). DDGS samples (<500µm) were weighed to 100mg ± 5% using an analytical scale (Precisa XT 220A). Next, 2mL of 2M HCl was used to hydrolyze starch during a 35 minute boiling water bath incubation. Each test tube was then cooled on ice and neutralized with 2M NaOH. Each sample was then transferred to a 10mL volumetric flask and topped up to 10mL with distilled water. A 1.5mL aliquot of this solution was transferred into a microcentrifuge tube and centrifuged at 1610 x g for 10 minutes in a microcentrifuge (Eppendorf 5424). Samples then follow the same microplate incubation with GOPOD reagent used for enzymatic analysis. Finally, the microplate was analyzed

in a microplate reader (Biotek SynergyMx) at 510nm. All absorbance values had sample blank absorbance readings subtracted to account for residual glucose in the DDGS samples.

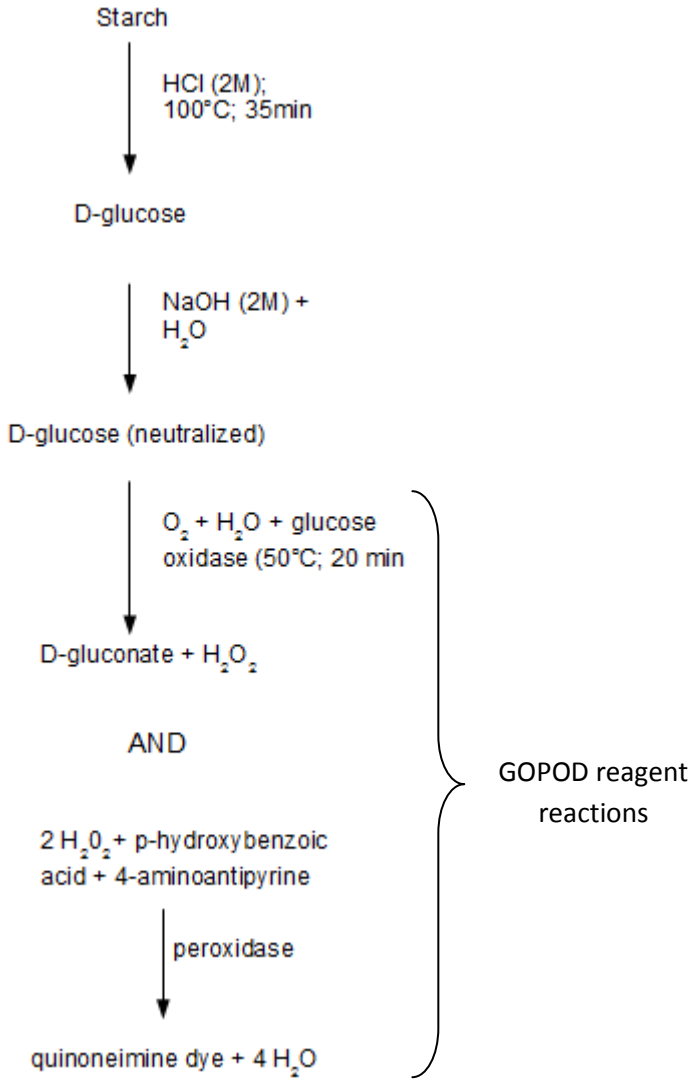

Figure 3-3: A flow-chart of the acid hydrolysis method used for residual starch benchmarking

3.2.2.4 Testing the effect of varying α-amylase concentration

An experiment was designed to determine if small fluctuations in α-amylase concentration alter the reported values for starch. This was necessary to eliminate possible extraneous factors and provide a fair evaluation of methods. The experiment tested two concentrations of α-amylase (20 and 32µL/mL). The concentrations were selected based on the difference in volumes between the benchmarked residual starch analysis methods. For example, an additional 2mL of DMSO is added prior to α-amylase

hydrolysis when using the Megazyme + DMSO method which dilutes the α-amylase incubation step. To differentiate effects caused by a possible chemical inhibition of α-amylase with and dilution effects, an additional sample diluted the α-amylase using 2mL of distilled water.

The experiment used pure starch weighed to 100mg ± 5% using an analytical scale (Precisa XT 220A). The advantage of using pure starch is that it has a known value. Three samples in total were analyzed: one sample was undiluted, the second sample was diluted using distilled water (2mL), and another sample was diluted using DMSO (2mL). The undiluted sample had an α-amylase concentration of 32µL/mL, while the diluted samples had concentrations of 20µL/mL. The samples were then hydrolyzed into D-glucose using the enzymatic hydrolysis steps outlined the Megazyme or Megazyme + DMSO methods shown in Figure 3-2. Of course only the sample diluted with DMSO was analyzed using the Megazyme + DMSO method. Following hydrolysis, samples were transferred into 100mL volumetric flasks and made up to volume with distilled water. A 1.5mL aliquot of this solution was transferred into microcentrifuge tubes and centrifuged at 1610 x g for 10 minutes in a microcentrifuge (Eppendorf 5424). Samples then followed the same microplate incubation with GOPOD reagent and spectrophotometric microplate analysis previously described.

3.2.3 Alternative methods for residual starch analysis

This section describes methods that have not previously been reported in the literature for residual starch determination in DDGS. Both of these alternative methods are variations of the Megazyme total starch analysis kit. One major difference is that the α-amylase and amyloglucosidase incubations are combined into one step. Another significant change is the use of aqueous alkaline solutions prior to α-amylase hydrolysis in an attempt to improve the hydrolysis and measurement of resistant starch. One method uses KOH and is a recommended, but unofficial, method for samples containing resistant starch. Another method uses NaOH at various pH levels and has never been attempted for residual starch determination in DDGS.

3.2.3.1 Buffer optimization experiments

To ensure a complete hydrolysis of starch it is important to carefully control the combined amylase incubation step. Specific enzyme requirements indicate a working temperature and pH range, which must be adhered to for proper functioning. Fortunately, there is some overlap in the pH range that can be used for these amylases. The range is fairly narrow (pH = 4.5-5.5), but can be achieved using a buffer solution following a pre-treatment step with either KOH or NaOH. Two separate experiments were conducted to determine appropriate buffers for each one of these methods. Appropriate buffer solutions were found through the trial and error of many different attempted buffer solutions. The pH of each solution was measured with a micro pH

probe (Lazar Research Laboratories PHR-146B) connected to a pH meter (Thermo Scientific Orion 4 Star).

It should be noted that a buffer solution already exists for the Megazyme + KOH method; however, addition of this buffer solution raised the volume of total solution past 10mL. Calculations then required the use of an approximate volume which creates variability within the results. Instead, it was decided to lower the pH of the buffer so a lower volume could be added. This change allowed the final volume to be accurately measured to 10mL in a volumetric flask and maintained consistency with all other methods evaluated in this thesis.

3.2.3.2 Megazyme method (KOH format)

Samples were analyzed for total starch content according to the Megazyme total starch kit (method C), with some minor modifications (see Figure 3-4). DDGS samples (<500µm) were weighed to 100mg ± 5% using an analytical scale (Precisa XT 220A). The samples were then dispersed in 80% ethanol and vortexed to disperse the starch in the sample. Next, the test tubes had magnetic stir bars added and were placed in an ice water bath over top of a magnetic stirrer (Corning PC-611). Each test tube then received 2mL of 2M KOH and was constantly stirred for 20 minutes in the ice water bath. While continuing to stir, 6mL of sodium acetate buffer (1.2M; pH=2.65), 0.1mL (300U) of α-amylase, and 0.1mL (326U) of amyloglucosidase were added. The test tubes were vortexed and then placed in a 50°C water bath (Shel Lab WS27). After 30 minutes, with vortexing at 15 and 30 minutes, the samples were transferred into 10mL volumetric flasks and made up to volume with distilled water. A 1.5mL aliquot of this solution was transferred into microcentrifuge tubes and centrifuged at 1610 x g for 10 minutes in a microcentrifuge (Eppendorf 5424). Incubation and absorbance readings for this analysis were also done in a microplate, as described in Section 3.2.2.1. The absorbance values of sample blanks were subtracted to account for residual glucose in the DDGS samples.

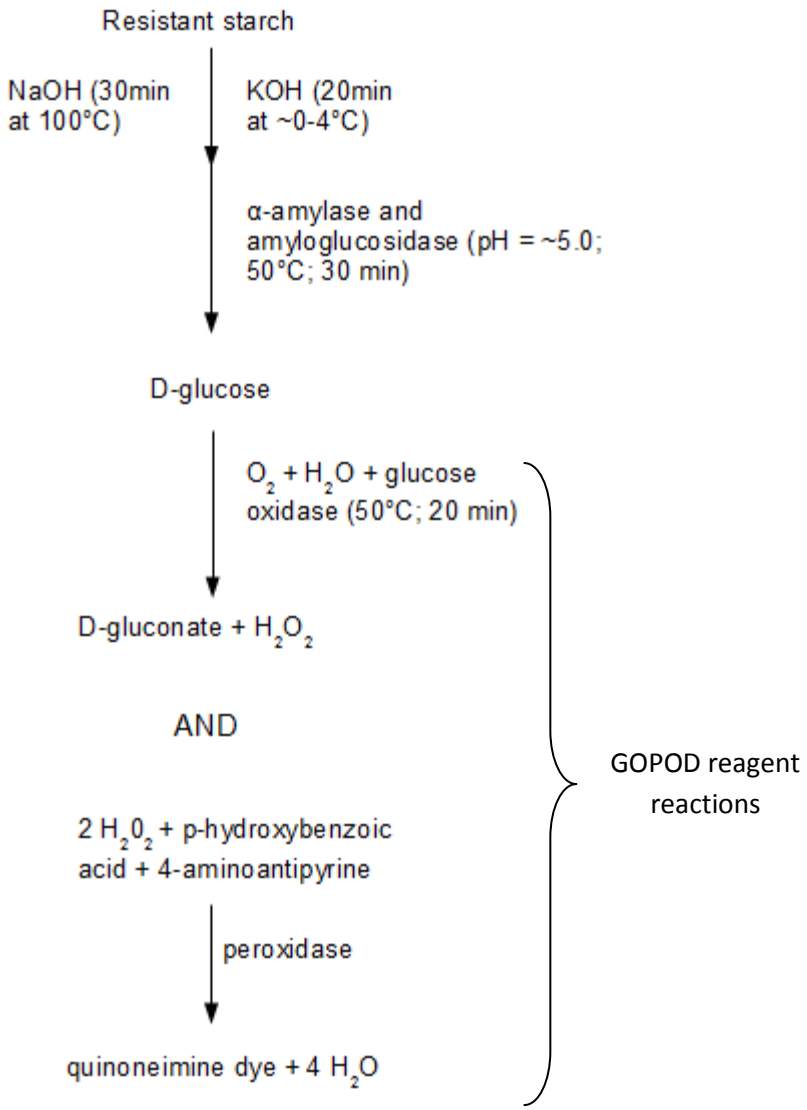

Figure 3-4: A flow-chart of the alternative residual starch analysis methods

3.2.3.2 Megazyme method + NaOH (pH 7, 10 & 12)

One of the main objectives of this thesis was to find an alternative method for residual starch analysis. The use of chemical reagents to improve resistant starch analysis is well documented, but no reports have attempted to use NaOH for this purpose. The amount of NaOH needed to provide an effect was unknown, so three various pH levels (7, 10, and 12) were used to treat DDGS samples prior to enzymatic analysis.

DDGS samples (<500µm) were weighed to 100mg ± 5% using an analytical scale (Precisa XT 220A). NaOH (0.5M) was added prior to enzyme exposure to adjust the sample pH to 7, 10, or 12. The pH values were measured using a micro pH probe (Lazer Research Laboratories PHR-146B) connected to a pH meter (Thermo Scientific Orion 4 Star). The test tubes were then heated in a boiling water bath for 30 minutes. Samples were then

transferred to a 50°C water bath (Shel Lab WS27) and sodium acetate buffer (200mM, pH = 4.5) was used to lower the pH to the optimal range for amylase addition. Only 1mL of buffer was required for pH 7 and 10, but 3mL of buffer was used for pH 12 samples (separate experiments were completed to determine the required volume of buffer addition). Next, both α-amylase (0.1mL; 300U) and amyloglucosidase (0.1mL; 326U) were added to each sample followed by incubation at 50°C for 30 minutes in a water bath (Shel Lab WS27). Each sample was then transferred to a 10mL volumetric flask and made up to volume with distilled water. A 1.5mL aliquot of this solution was transferred into microcentrifuge tubes and centrifuged at 1610 x g for 10 minutes in a microcentrifuge (Eppendorf 5424). Incubation and absorbance readings for this analysis were also done in a microplate, as described in Section 3.2.2.1. The absorbance values of sample blanks were subtracted to account for residual glucose in DDGS.

3.2.4 Moisture analysis

Moisture analysis was completed for all DDGS samples so that starch values could be reported on a dry weight basis (dwb). This analysis is required to eliminate the variation due to different moisture levels between samples. The standard AOAC 930.15 methodology was used to complete moisture analysis; however, when testing the high purity β-glucan sample the weight was reduced due to limited sample. This method involves weighing 2g of sample into an aluminum dish, drying in a convection oven at 135°C for 2 hours, cooling the samples in a desiccator, and then reweighing the samples. Moisture is calculated as shown in Equation 3-1.

$$\% \text{ Moisture (w/w)} = \left(\frac{\text{Weight of wet sample (g)} - \text{Weight of dry sample (g)}}{\text{Weight of wet sample (g)}} \right) \text{x } 100\%$$

Equation 3-1: Calculation to determine sample moisture content

3.2.5 Hydrolysis of non-starch polysaccharides

To rule out the possible hydrolysis of non-starch polysaccharides as a cause of increased residual starch values, various non-starch polysaccharides were exposed to water, 2M HCl, 2M KOH, or NaOH (pH 12). For the NaOH analysis only pH 12 was used because it is expected to result in the highest degree of hydrolysis. Released glucose would indicate the hydrolysis of the samples containing non-starch polysaccharides, which included cellulose, β-glucan, and yeast cells. The release of non-starch glucose would then result in an overestimation of residual starch in DDGS samples.

Each non-starch polysaccharide was weighed to 100mg ± 5% into test tubes using an analytical scale (Precisa XT 220A). Next, 2mL of water, 2M HCl, or 2M KOH were added to the respective test tubes. The NaOH sample required a pH adjustment which was measured with a micro pH probe (Lazar Research Laboratories PHR-146B) connected to

a pH meter (Thermo Scientific Orion 4 Star). Samples were then subjected to incubation periods in water baths. The KOH samples were each incubated for 20 minutes in an ice water bath to simulate the Megazyme + KOH format. All other samples were heated in boiling water baths for 30 minutes (35 minutes for HCl) to simulate their respective methodologies. After the incubations, the samples were transferred into 10mL volumetric flasks and made up to volume with distilled water. Samples then followed the same microplate incubation with GOPOD reagent and analysis in a microplate reader as previously described.

3.2.6 Glucose reactivity

As mentioned in Section 2.4.1, glucose can isomerise into other monosaccharides or react with other compounds. Pure glucose was tested under various conditions resembling the residual starch analysis methods above. For example, pure glucose was weighed to 100mg ± 5% using an analytical scale (Precisa XT 220A) and subjected to high temperatures in the presence of water, 2M HCl, or NaOH at pH 12. Glucose was also treated with 2M KOH in an ice water bath to mimic the KOH treatment. A control used only distilled water and glucose without incubation at high temperature. Following the above procedures, each sample solution was transferred into a 100mL volumetric flask and made up to volume with distilled water. The glucose samples in this experiment had higher concentrations of glucose than DDGS; therefore, they were diluted to a greater extent than was used for residual starch analysis. Centrifugation was also unnecessary in this analysis because no insoluble material was present. Direct aliquots of diluted sample were transferred into microplate wells and incubated with GOPOD reagent as described for residual starch analysis. The microplate was then analyzed in a microplate reader (Biotek SynergyMx) at 510nm. Any reduction in glucose values would indicate a potential issue in regards to starch analysis that would likely lead to an underestimation of residual starch.

4. Results and Discussion

4.1 Evidence of residual starch in DDGS

As discussed in Chapter 2, one major difference between native starch in grains and starch in DDGS is the amount of resistant starch expected. In order to determine what forms of resistant starch might be present in DDGS, it was visualized using confocal microscopy (see Figure 4-1). For comparison, confocal microscopy images of flour are also included. Unfortunately, the resolution provided from confocal microscopy cannot provide specific details about what form of resistant starch may be present. However, some insight into the residual starch structure can be gleaned, as will be discussed in more detail below. Other structures observed in DDGS, which are not seen in flour samples are mainly yeast cells (see Figure 4-1). Yeast cells are easily recognizable due to their uniform structure, but range in colour from yellow to bright green. Protein is

stained red, but a mixture of starch (labelled green) and protein (labelled red) is responsible for the range of colours seen in the micrograph images. These colours range from brown, which is mostly protein, to a bright green that consists of mostly starch. More detailed information on the staining methods and microscopy can be found in Appendix 2.

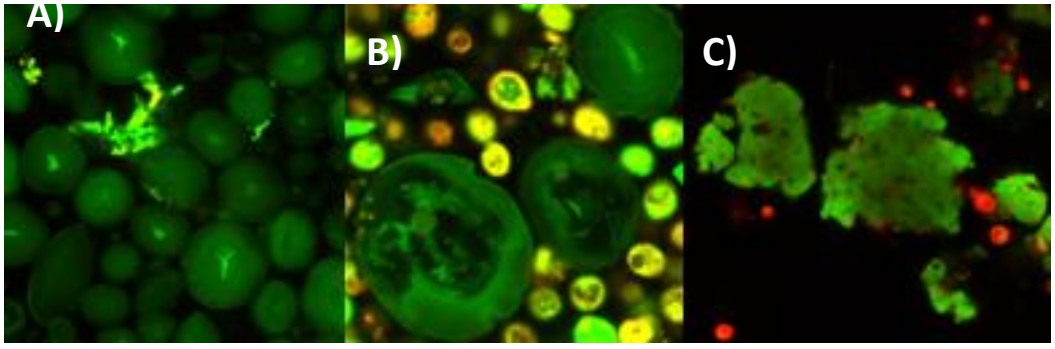

Figure 4-1: Confocal microscopy images of residual starch (labelled green) in wheat DDGS; A) wheat flour, B) raw starch hydrolysis DDGS, C) conventionally jet-cooked DDGS; green stain = starch, red stain = protein

The confocal microscopy image of wheat flour, shown in Figure 4-1a, shows native starch granules that have been released from cell walls and the starch-protein matrix existing in grain kernels (see Section 2.1.2). The starch granules are released due to milling during the production of the flour. Wheat starch is expected to have wide range of starch granular sizes (2-36µm), which can be generally observed in the image. The starch granules also remain intact after milling, so changes to starch structure seen in DDGS are not a result of milling. The limited amount of other grain-related structures in the image also suggests a high starch content, which is of course expected for a flour sample. Lastly, and most importantly, this image confirms that resistant starch type I, associated with the inaccessibility of starch granules, is limited or non-existent.

The residual starch in DDGS after raw starch hydrolysis has an appearance similar to native starch. The most notable differences in starch structure are the channels and enlarged cavities caused by hydrolysis (see Figure 4-1b). This observation supports Shariffa *et al*. (2009) in their proposition that amyloglucosidase provides access to the inner region of the cavity by "drilling" pinholes into the starch granules, followed by an expansion of the cavity by α-amylases. It can also be observed that the outer crystalline regions of starch granules remain intact. It is these outer regions that typically contain the amylopectin double helices responsible for resistant starch type II; therefore, it can be hypothesized that raw starch hydrolysis enzymes are unable to hydrolyze resistant starch type II.

Residual starch in jet-cooked DDGS samples has a unique structure that forms into clusters. It is clear that jet-cooking starch has disrupted the structure of native starch

granules (see Figure 4-1c). These clusters of starch are likely resistant in nature, but it is not possible to determine whether the clusters are a result of amylose gels (resistant starch type III) or amylose-lipid complexes (resistant starch type V). Both of these resistant starch structures are expected to be found in jet-cooked DDGS samples due to the exposure of starch granules to heating and cooling. Resistant starch type III is formed when starch is heated past gelatinization temperatures, resulting in the leaching and retrogradation (reordering) of amylose chains upon cooling. Resistant starch type V is formed when the amylose chains are in the presence of lipids at a temperature above 80°C, resulting in the form of an amylose-lipid complex.

It is clear that for both hydrolysis types (jet-cooking & raw starch hydrolysis) that starch has escaped hydrolysis. It should be noted that the imaged DDGS was freeze-dried to limit the changes in starch structure to the hydrolysis type only. Only so much information could be derived from the low resolution confocal microscopy images, but it is likely that both hydrolysis methods have a portion of soluble and insoluble starch. Due to different processing techniques the proportions of these starches are predicted to be vastly different. A higher level of resistant starch is expected for jet-cooked samples due to the heating and cooling of starch granules. In any case, all of these structures have already escaped hydrolysis from amylolytic enzymes during processing; therefore, the required hydrolysis for starch determination is a major challenge. Currently used methods for residual starch analysis are expected to be underreporting the actual amount of starch in DDGS because of resistant starch structures.

4.2 Challenges of residual starch analysis

Residual starch determination for DDGS samples has been reported by numerous other studies (Hall *et al.*, 2001, Belyea *et al.*, 2004, Kim *et al.*, 2008, Gibreel *et al.*, 2009 & 2011, Srichuwong and Jane 2011). Commonly used starch analysis methods were used in each study. Analysis methods were selected because they were considered to be an official method; however, in regards to starch determination, these methods were developed for high starch substrates with low levels of resistant starch. A problem arises in DDGS samples due to very low starch contents and the expected high levels of resistant starch. New methods for analysis of residual starch in DDGS need to consider the differences between high starch substrates (grain/food products) and low starch substrates (DDGS) to obtain higher accuracy and reliability.

Not all resistant starch types found in DDGS are created equal. As was previously discussed in chapter 2, resistant starch type I and type IV are non-issues for the determination of residual starch in DDGS. Resistant starch type I only refers to the inaccessibility of starch found in the endosperm of grains; however, after milling this starch is easily accessible to amylolytic enzymes. Another form of resistant starch, type IV, is not expected in our samples because it requires chemical modification using precise conditions, none of which were used in our processes.

Resistant starch types expected in DDGS samples used in this thesis are resistant starch type II, type III, and type V. Samples containing resistant starch type II will not be a major issue for residual starch analysis because only mild heating is required to disrupt the structure, making it available for hydrolysis (Sievert and Pomeranz, 1989). The issue arises when more complex structures, such as resistant starch type III and V are expected in the sample, which is the case for jet-cooked DDGS (see Figure 4-1c). It is very likely that official methods are underreporting residual starch values in samples containing these highly resistant structures. In the following sections, both official methods and methods used in the literature for residual starch analysis were benchmarked. In addition, alternative methods were conducted to specifically address the issues regarding resistant starch types III and V.

4.3 Benchmarking residual starch analysis methods

Three methods used in this study have previously been used to report residual starch in DDGS, or other low starch samples. For simplicity, these methods will be discussed separately from other residual starch analysis methods that were also evaluated in this thesis. By far the most common method reported in the literature is enzyme hydrolysis with α-amylase and amyloglucosidase (Hall *et al.*, 2001; Belyea *et al.*, 2004; Kim *et al.*, 2008; Gibreel *et al.*, 2009 & 2001; Srichuwong and Jane 2011). This method was described in detail previously (see Section 3.2.2.1), but briefly it uses heat gelatinization in combination with the amylases to hydrolyze starch into glucose. The glucose is then reacted with GOPOD reagent and develops a pink colour that is measured spectrophotometrically against a known glucose concentration. The protocol used for this analysis was AOAC method 996.11, also referred to in this thesis as the Megazyme method. Due to the extent this method is reported in the literature, this method was considered the standard methodology for comparison to all other methods.

Another method reported in the literature is a slight variation of the Megazyme method. The variation includes heating the sample in a chemical solvent (DMSO) prior to enzymatic hydrolysis (see Section 3.2.2.2). The DMSO is used in an attempt to improve the hydrolysis of resistant starch present in the sample, in fact using this method is recommended for samples known to contain resistant starch. Results using this method for residual starch analysis of DDGS samples were recently published by Srichuwong and Jane (2011).

The third method used to report residual starch analysis involves using acid to hydrolyze starch. This acid hydrolysis method was developed by merging a protocol outlined by Kim *et al*. (1988) with the altered GOPOD incubation used in the enzymatic methods (see Section 3.2.2.3). Originally this method was used to measure residual starch in a fermentation medium, but was slightly adapted for use on DDGS samples in our laboratory. One alternative acid hydrolysis method has been used to determine residual starch in DDGS (Vidal Jr. *et al.*, 2009); however, because our laboratory was already

using the outlined acid hydrolysis for some unpublished work, I decided to benchmark this particular method.

The majority of studies have only reported residual starch values of corn DDGS samples (Belyea *et al.*, 2004; Kim *et al.*, 2008; Srichuwong and Jane 2011), while two studies have also tested wheat, triticale, and barley (Gibreel *et al.*, 2009 & 2011). The results below measure the residual starch in all the grains mentioned above for both jet-cooking and raw starch hydrolysis produced DDGS (see Figures 4-2 to 4-5). This work is a significant improvement over the work done previously and is useful to understand residual starch determination for a wide range of DDGS samples produced from different grains and hydrolysis methods.

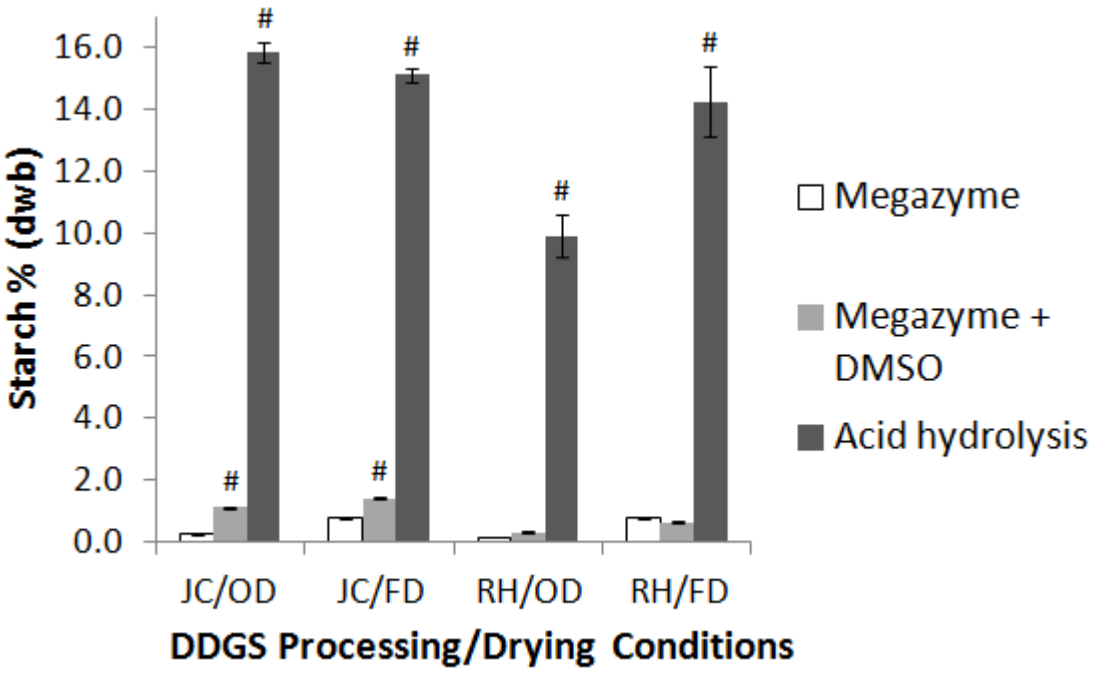

Figure 4-2: Benchmarking of residual starch analysis methods for barley DDGS samples; JC = jet-cooking, RH = raw starch hydrolysis, OD = oven-dried, FD = freeze-dried. N = 3; error bars represent ±1 standard deviation. Statistical significance was measured as the difference from the Megazyme value; P <0.001 = #.

The X-axis shown in Figure 4-2, and all following figures, are organized to show the most heat treated samples on the left and the least heat treated samples on the right. This was done purposely for easy recognition of processing and drying conditions that are expected to produce a lot of resistant starch. It is expected that improvements to the official methodology (ie. Megazyme) will measure both soluble and resistant starch, thereby producing higher and more accurate residual starch values. This increase is predicted to be greater for DDGS samples with elevated resistant starch levels, such as DDGS with more heat treatments, revealed on the left of the X-axis.

The residual starch values reported for barley DDGS using three benchmarked methods are shown in Figure 4-2. The values reported for acid hydrolysis are extremely high as compared to the enzymatic methods (Megazyme & Megazyme + DMSO) and the difference was found to be statistically significant ($P < 0.001$). A significantly higher starch value was reported with acid hydrolysis throughout all grain types regardless of the grain type, hydrolysis process, or drying method. Further investigation into this result and the reason for the increase is reported in the following sub-section (see Section 4.3.1) and will not be discussed further in this section to avoid repetition. The methodology used for stats analysis can be found in Appendix 3.

Another significant improvement versus the Megazyme method involves the increase in residual starch values observed when DMSO is used in addition to Megazyme enzymes ($P < 0.001$). As predicted, the improvements were only seen when heat treatments were used, more specifically jet-cooking heat treatments. More starch is available during jet-cooking with mash, so this is a likely reason for increased resistant starch production during jet-cooking versus high temperature oven-drying. It should also be pointed out that while the increase looks small on the graph, improvements of approximately 430 and 180% were observed for the jet-cooked/oven-dried and jet-cooked/freeze-dried DDGS samples respectively versus using Megazyme alone.

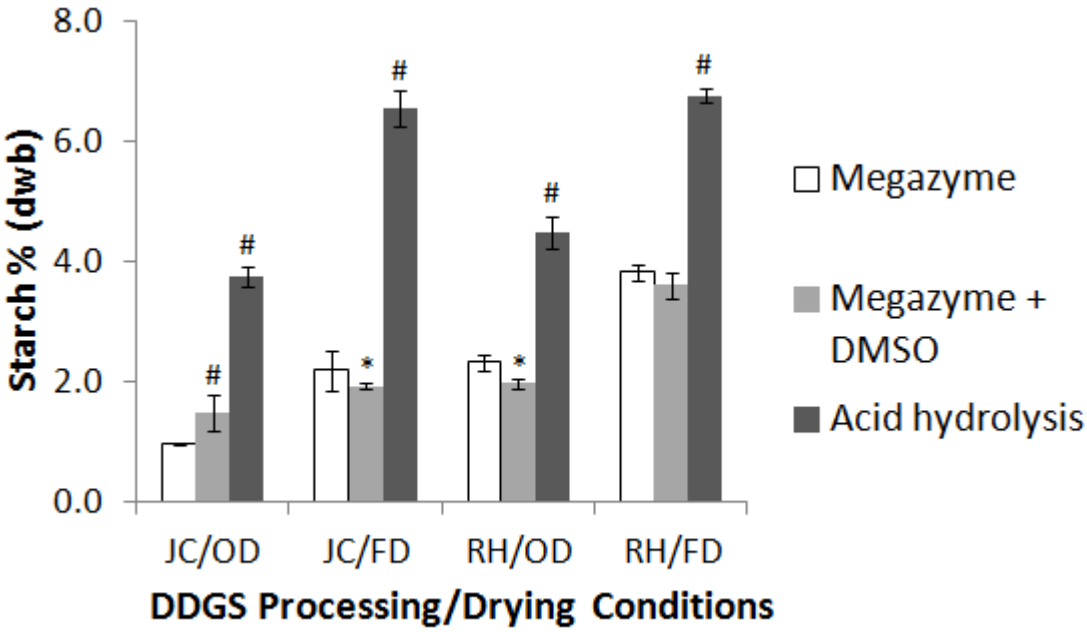

Figure 4-3: Benchmarking of residual starch analysis methods for corn DDGS samples; JC = jet-cooking, RH = raw starch hydrolysis, OD = oven-dried, FD = freeze-dried. N = 3; error bars represent ±1 standard deviation. Statistical significance was measured as the difference from the Megazyme value; $P < 0.05$ = *, $P < 0.001$ = #.

Benchmarking commonly used analysis methods on corn DDGS revealed a number of unique trends (see Figure 4-3). For example, using Megazyme + DMSO actually significantly reduced the residual starch value in the jet-cooked/freeze-dried and the raw starch hydrolysis/oven-dried samples ($P < 0.05$). It is important to note that this trend was not seen in any other DDGS samples, was only significant at the 0.05 level, and measured samples with a relatively high soluble starch content (as measured by Megazyme). Soluble starch content may be problematic for this analysis method due to the formation of microgels during DMSO solubilization (Schmitz *et al.*, 2009); however, this does not explain why the highest soluble starch sample (raw starch hydrolysis/freeze-dried) did not see a reduced starch value.

The Megazyme + DMSO method did report a significantly higher residual starch value for jet-cooked/oven-dried DDGS as compared to the Megazyme method ($P < 0.001$). This sample was hypothesized to show the greatest increase because of the exposure of the sample to two heat treatments. The heat treatments are responsible for forming resistant starches, specifically type III and type V, depending on the availability of monoacylglycerides. The higher lipid content in corn grain is likely responsible for the relatively low (~150%) increase observed from the solubilization of the sample in DMSO prior to hydrolysis. DMSO helps to disrupt hydrogen bonding (see Section 2.4.1) which exists in resistant starch type III, but is still likely underreporting resistant starch type V (amylose-lipid complexes). This result is confirmed in the study by Srichuwong and Jane (2011), which showed that defatting the DDGS lead to greater residual starch values reported by the Megazyme + DMSO method.

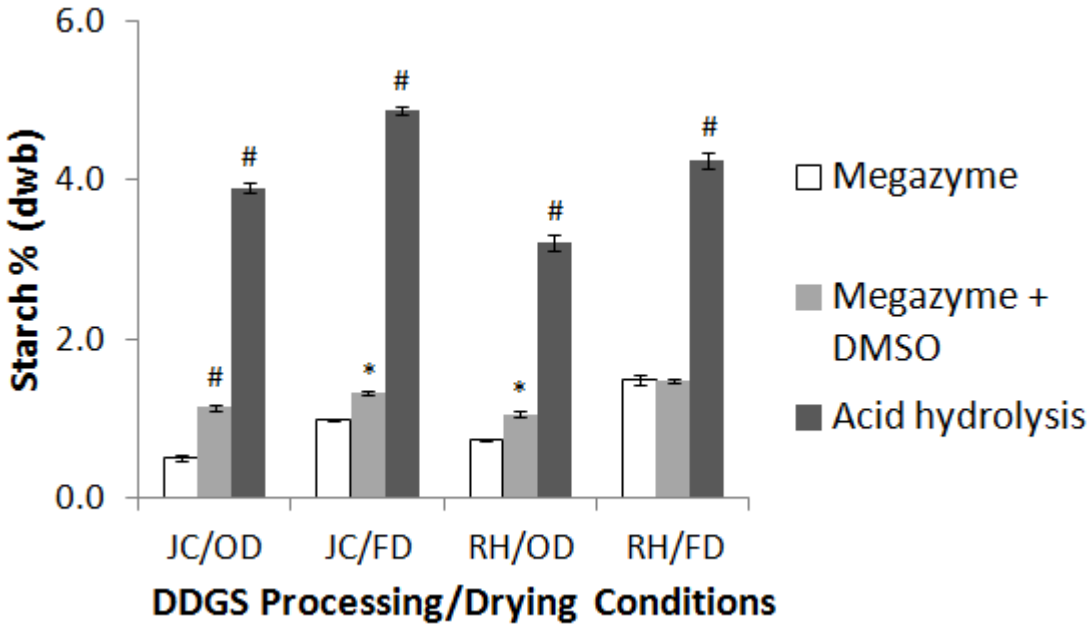

Figure 4-4: Benchmarking of residual starch analysis methods for triticale DDGS samples; JC = jet-cooking, RH = raw starch hydrolysis, OD = oven-dried, FD = freeze-dried. N = 3; error bars represent ±1 standard deviation. Statistical significance was measured as the difference from the Megazyme value; $P < 0.05$ = *, $P < 0.001$ = #.

Benchmarked methods tested on triticale DDGS samples revealed a significant improvement for the Megazyme + DMSO method in comparison to Megazyme alone for both jet-cooked samples (see Figure 4-4). The significance was found to be the greatest when two heat treatments were used ($P < 0.001$; ~230%), but was also significant for the jet-cooked/freeze-dried sample ($P < 0.05$; ~135%). These findings reveal that the Megazyme + DMSO method would be highly relevant to commercial samples, which are commonly exposed to jet-cooking heat treatments. This also suggests an additive effect of heat treatments, which has also been reported in a study that exposed starch to multiple autoclaving and cooling cycles (Yadav *et al.*, 2009).

For the first time in the entire data set, a raw starch hydrolysis produced DDGS sample (oven-dried) reported a significant improvement when using the Megazyme + DMSO analysis method ($P < 0.05$). It is not clear why this only occurs with triticale DDGS, especially if the soluble starch content is considered, which is much higher in corn for instance. One might expect that if more starch is available for gelatinization during oven-drying, that some resistant starch might be formed. One likely explanation for the observed improvement would be a higher amylose content in the triticale samples, but unfortunately amylose content was not tested prior to fermentation.

The only sample not showing a significant increase when using the Megazyme + DMSO method was the raw starch hydrolysis/freeze-dried sample. This sample was kept below the gelatinization point during processing and drying, so amylose leaching required for the formation of resistant starch type III and V would not have occurred. As predicted, a simple heat gelatinization step would make resistant starch type II available for enzymatic hydrolysis, which was the case for the Megazyme analysis.

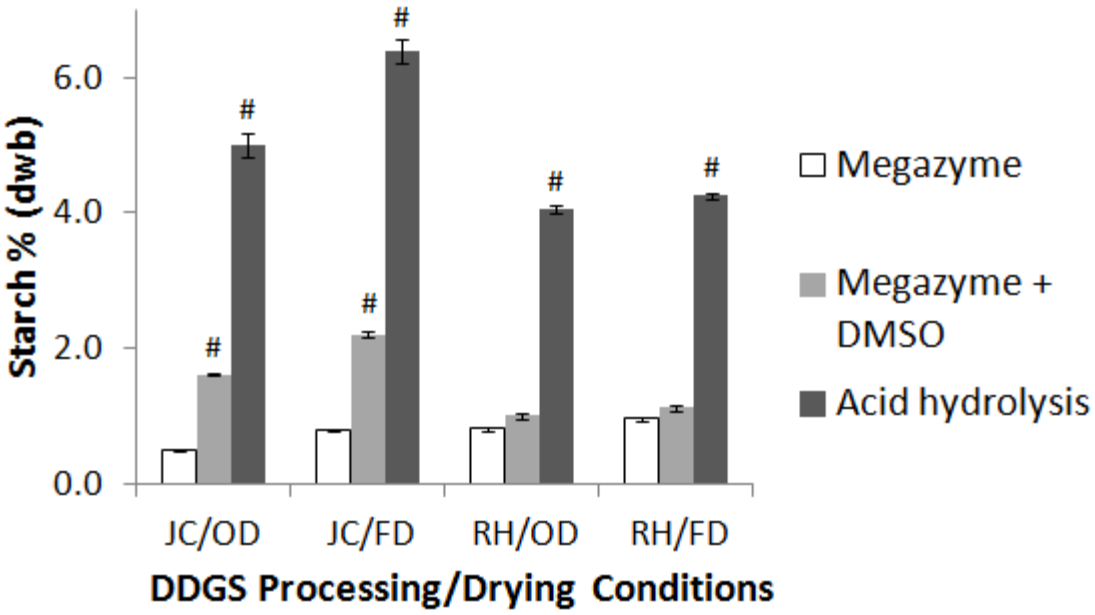

Figure 4-5: Benchmarking of residual starch analysis methods for wheat DDGS samples; JC = jet-cooking, RH = raw starch hydrolysis, OD = oven-dried, FD = freeze-dried. N = 3; error bars represent ±1 standard deviation. Statistical significance was measured as the difference from the Megazyme value; $P < 0.001$ = #.

For wheat DDGS, only two of the sample types exposed to heat treatments showed a significant increase in the residual starch values when using Megazyme + DMSO versus using Megazyme alone ($P < 0.001$). Both samples were jet-cooked, suggesting a higher formation of resistant starch when the high starch mash is heated. A similar trend was observed in barley DDGS, but the increase for barley DDGS samples was higher. Of all the grain types benchmarked with these methods the next highest improvement was reported for these jet-cooked wheat DDGS samples, which increased ~315 and 280% for oven-dried and freeze-dried samples respectively.

Wheat DDGS samples produced using the raw starch hydrolysis procedure did not see any improvement when measured with Megazyme + DMSO. It is likely that DMSO is not favourable when raw starch hydrolysis is used, regardless of drying type. The ability for raw starch hydrolyzing enzymes to work below gelatinization temperatures vastly reduces the amount of residual starch formation and provides little challenge for the accurate measurement of residual starch. This was expected due to the observation that only resistant starch type II was likely to exist in the raw starch hydrolyzed DDGS samples.

4.3.1 Acid hydrolysis of non-starch polysaccharides

The higher than expected values reported by acid hydrolysis throughout the benchmarking experiments was investigated further. It was hypothesized that acid was hydrolyzing non-starch polysaccharides. To test this hypothesis, the method was conducted on various non-starch polysaccharides expected in DDGS samples such as cellulose, concentrated cereal β-glucan, and yeast cells. In the case of cellulose and β-glucan, both are homopolysaccharides of glucose. On the other hand, yeast polysaccharides are a mixture of polysaccharides, ranging from cell wall materials to glycoproteins. In any case, the acid hydrolysis method will hydrolyze the susceptible polysaccharides which may include glucose. Following hydrolysis, only the glucose will be measured using a colourimetric analysis with the GOPOD reagent (see Section 3.2.2.1). The compounds releasing glucose are likely responsible for the over reporting of starch in the benchmarking experiment.

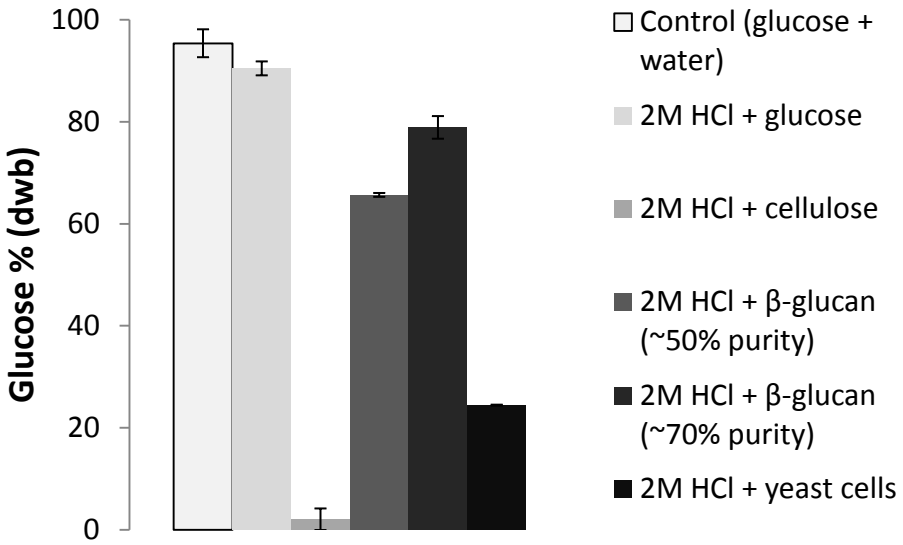

Figure 4-6: Measurement of glucose released from non-starch polysaccharides using acid hydrolysis (2M HCl); N = 3; error bars represent ±1 standard deviation.

It was determined that there are multiple sources of glucose being released during acid hydrolysis (see Figure 4-6). This result confirms that acid hydrolysis methods potentially overestimate the amount of residual starch in DDGS samples. It is recommended that if researchers intend to use acid hydrolysis methods, that a lower concentration than 2M HCl is used. At this concentration, glucose was released from all of the tested non-starch polysaccharides. Microcrystalline cellulose was only mildly hydrolyzed into glucose, but amorphous cellulose is expected to be more easily hydrolyzed. A high level of glucose was released from the β-glucan polymers, but these compounds were not of high purity so some starch was likely hydrolyzed as well. Interestingly, the yeast cells reported a high level of glucose release which is thought to be as a result of β-glucan

polymers within the yeast cell walls. These results also indicate the complexity of the matrix within DDGS and the challenges that exist when attempting to specifically hydrolyze residual starch.

4.3.2 Effect of α-amylase dilution

Various methods used for residual starch analysis in this thesis have varying amylase concentrations due to the addition of buffer or chemical solvents. It is important to verify that changes in starch values were a result of the actual treatments and not due to sample dilution for amylase incubations. An experiment was designed to test if amylase dilution is responsible for a change in the starch value of a control sample. High purity corn starch was used for the experiment because it has a known starch value. Megazyme analysis was then completed with and without dilution of the amylase enzymes (see Section 3.2.2.4). Alternatively, the Megazyme + DMSO method was also used because it also dilutes α-amylase. Starch values were determined colourimetrically (see Section 3.2.2.1) and it was observed that no changes resulted due to the different amylase concentrations (see Figure 4-7). The amount of α-amylase added (300U) is enough to hydrolyze 100mg of pure starch in combination with amyloglucosidase (326U). While both enzymes are slightly diluted this should be more than enough enzyme to hydrolyze the relatively low starch content in DDGS samples. It should be noted that the concentration changes also exist in the official methods published in the Megazyme kit.

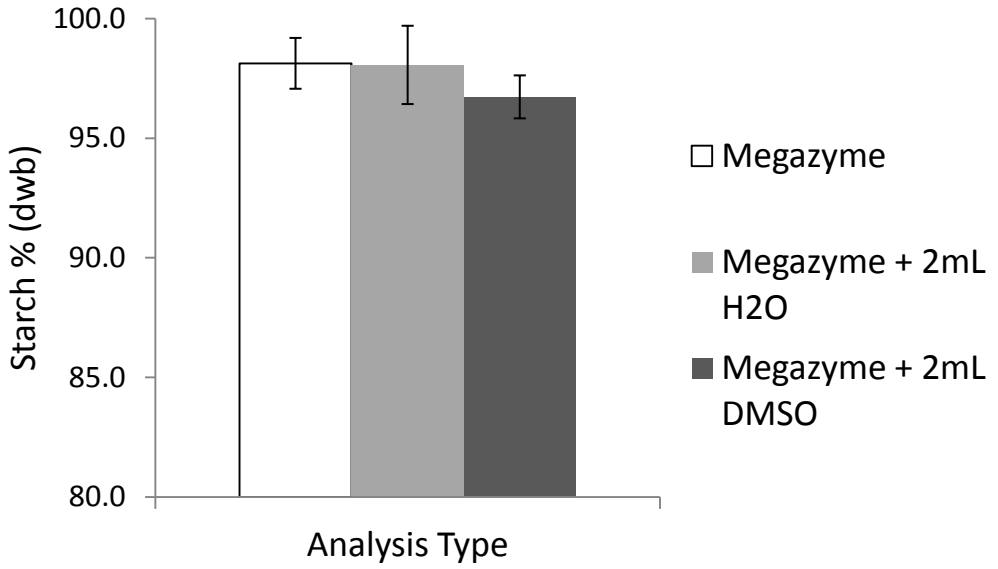

Figure 4-7**:** Effect of α-amylase concentration on starch hydrolysis of a known corn starch sample; N = 6; error bars represent ±1 standard deviation.

4.4 Alternative methods for residual starch determination

One major objective of this thesis was to find an alternative method for the measurement of residual starch in DDGS. Ideally, the method would provide enzyme access to resistant starch in DDGS samples. Chemical reagents that may provide this effect include basic substances. As described in Section 2.4.1, the ionization of starch molecules caused by aqueous alkali results in a coulombic repulsion between the ionized hydroxyl groups (Craig *et al.*, 1989). The charged repulsion of these groups then prevents the association of starch chains (Craig *et al.*, 1989). It remains unclear if resistant starch is disrupted using these methods, or if this only applies to starch pastes as described in the reported study. The Megazyme + KOH method attempted is recommended for use with resistant starch samples; however, results for this method have never been reported for residual starch determination of DDGS samples. Moreover, the Megazyme + KOH method is not an official method for starch analysis so it was not considered a benchmark.

In addition to the Megazyme + KOH method discussed above, a novel attempt was made to use Megazyme + NaOH. The pH level of the NaOH was controlled at three different levels (pH 7, 10, and 12) because at high temperatures the base would potentially hydrolyze non-starch polysaccharides as was seen with acid. It should be noted that pH 7 was tested, because DDGS is slightly acidic so NaOH addition was required to raise the sample to a neutral pH. Using a neutral pH tested the requirement of high pH values for the measurement of resistant starch, not just the addition of NaOH.

Another very different aspect of this methodology is the heat requirement (KOH uses an ice bath). The reason heat is used with NaOH is the much lower pH range tested for the methodology. When using 2M KOH, the sample pH raises to >14. Such a high pH would destroy nearly every compound in solution if it were heated; in fact it is even kept on ice to ensure that room temperature does not speed up the reactions too heavily.

4.4.1 Buffer optimization for the Megazyme + KOH method

A buffer solution is already recommended for this method; however, addition of this buffer solution raised the volume of total solution past 10mL. Calculations then required the use of an approximate volume which creates variability within the results. Instead, it was decided to lower the pH of the buffer so that a lower volume would be needed. This allowed the final volume to be accurately measured to 10mL in a volumetric flask and maintained consistency with all other methods evaluated in this thesis.

The published Megazyme + KOH method utilizes 8mL of sodium acetate buffer (1.2M; pH 3.8), but to lower the amount of buffer needed, a lower pH buffer was necessary. The pH is very critical at this stage, because a pH range of 4.5-5.5 is required for the functioning of both amylase enzymes simultaneously according to the manufacturers'

enzyme specifications. An experiment was conducted to reveal the combination of buffer pH and volume to achieve the desired pH range of 4.5-5.5 (see Section 3.2.3.1). A lower pH sodium acetate buffer (1.2M; pH 2.65), instead of the recommended buffer (1.2M; pH of 3.8), was added and measured at two volumes: 4 and 6mL (see Figure 4-8). The pH values obtained at the 6mL volume addition provided pH ranges of 5.06-5.21, which is within the manufacturers' specified range. The final buffer tested was the only experiment reported, many trials were completed before finding the optimal buffer pH.

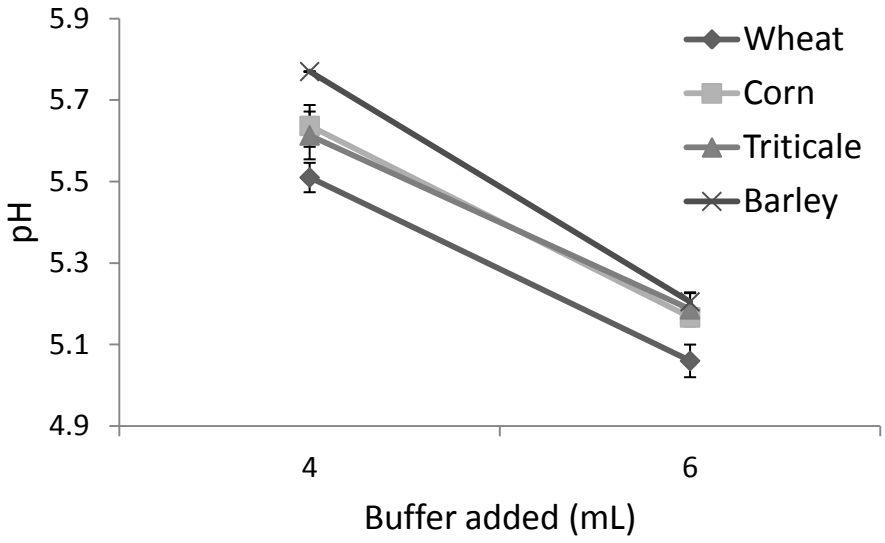

Figure 4-8: Buffer optimization experiment for the Megazyme + KOH method using different DDGS grain types; sodium acetate buffer (1.2M; pH 2.65); N = 3; error bars represent ±1 standard deviation.

4.4.2 Buffer optimization for the Megazyme + NaOH methods

No methodology currently exists for the use of NaOH prior to enzymatic hydrolysis, but to stay consistent with other methods, a final volume of 10mL was used. This method also used a procedure similar to the Megazyme + KOH method, where the amylase incubation is conducted simultaneously. The main difference between the methods is a heating step, which is used to help speed up the reaction.

A comparable experiment was conducted to ensure the optimal pH range for the functioning of both amylases after buffer addition (see Section 3.2.3.1). In this case a sodium acetate buffer (1.2M; pH 3.8 and 200mM; pH 4.5) was tested in this experiment, but only pH 4.5 is shown. Wheat DDGS samples had the pH measured after the addition of NaOH, after heating, and after the addition of 1mL of buffer. Additional buffer was used until the desired pH value was reached (see Figure 4-9). Final pH values for the NaOH methods (pH 7, 10, and 12) were 4.7, 5.1, and 5.2 respectively. These pH values

are within the manufacturers' requirements for efficient enzymatic hydrolysis. These findings indicate that 1mL of sodium acetate buffer (200mM; pH 4.5) is required for the NaOH methods at pH 7 & 10. A total of 3mL was required to reach the appropriate pH range for the NaOH method at pH 12.

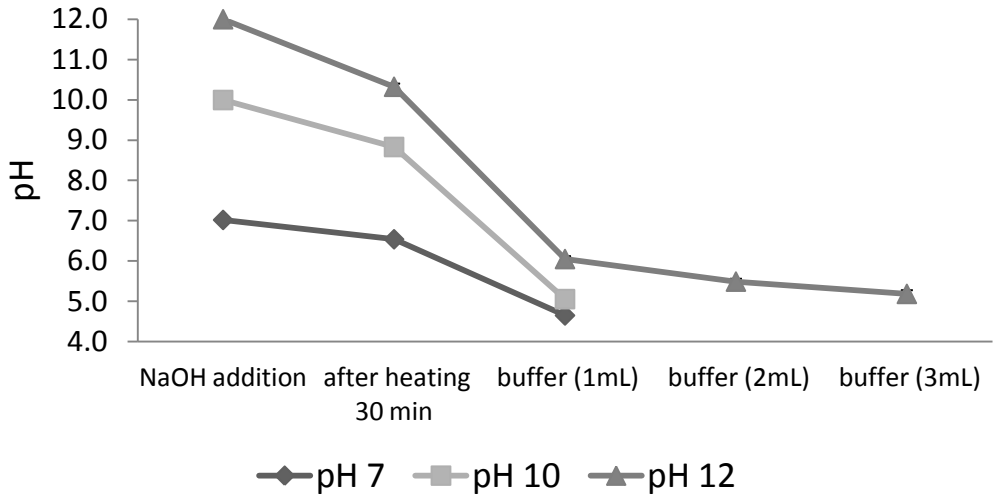

Figure 4-9: Buffer optimization experiment for the Megazyme + NaOH method (pH 7,10l and 12) using wheat DDGS; sodium acetate buffer (200mM; pH 4.5); N = 3; error bars represent ±1 standard deviation.

4.4.3 Alternative methods for residual starch analysis in DDGS

Following the buffer optimization studies completed for the Megazyme + KOH/NaOH methods, the analysis of DDGS samples was completed. The DDGS included the same benchmarked samples from barley, corn, triticale, and wheat. The DDGS samples were produced using jet-cooking or raw starch hydrolysis, followed by either oven or freeze-drying. These processing techniques (hydrolysis & drying) are expected to have a major impact on starch structure; therefore, they are also likely to impact analysis. Briefly, these analysis methods were attempting to improve enzymatic access to resistant starches type III and V (see Section 2.3.1.2 for structure details). Both of these structures involve the re-ordering of linear amylose molecules into crystalline entities. Type III resistant starch is formed due to the leaching of amylose molecules during gelatinization, followed by a cooling stage which enables amylose to align into a crystalline gel structure. Type V resistant starch involves leached amylose during gelatinization, but includes a formation of a complex between amylose and monoacylglycerides. Both forms of resistant starch are believed to cause an underestimation of residual starch in DDGS using official total starch analysis methods (ie. Megazyme). All of the results were compared to the original starch values reported by the Megazyme method in Section 4.3.

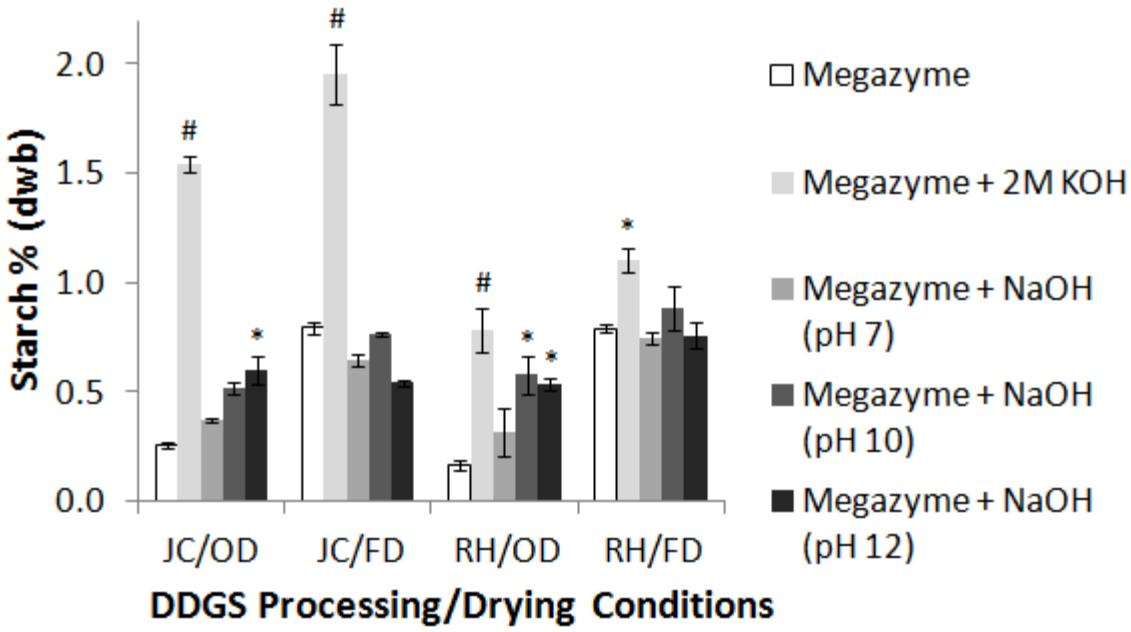

Figure 4-10: Measurement of residual starch in barley DDGS samples using alternative analysis methods; JC = jet-cooking, RH = raw starch hydrolysis, OD = oven-dried, FD = freeze-dried. N = 3; error bars represent ±1 standard deviation. Statistical significance was measured as the difference from the Megazyme value; $P < 0.05$ = *, $P < 0.001$ = #.

It is expected that high temperature processing and drying treatments produce more resistant starch in DDGS samples. Similarly to the benchmarked methods, these alternative methods are organized on the X-axis to reveal the most heat treated samples on the left and the least heat treated samples on the right.

Results for barley DDGS reveal a greater improvement for the alternative residual starch determination methods when heat treatments are used (see Figure 4-10). For example, the use of the Megazyme + KOH method drastically increased the reported starch values for jet-cooked barley DDGS samples. Residual starch values of jet-cooked barley DDGS were raised by 600 and 250% for oven-dried and freeze-dried samples respectively ($P < 0.001$). The use of two heat treatments in combination (jet-cooking & oven-drying) likely increased the amount of resistant starch formed, which was then made available by treating DDGS with KOH prior to enzymatic analysis.

Raw starch hydrolyzed barley DDGS samples also revealed higher residual starch values when measured by the Megazyme + KOH method. The oven-dried and freeze-dried DDGS samples were increased by 480 and 140% respectively ($P < 0.001$ & $P < 0.05$). Such large increases were not anticipated in these samples, due to lower levels of expected resistant starch. It is possible that 2M KOH is chemically hydrolyzing glycosidic bonds of non-starch polysaccharides, much like 2M HCl for the benchmarked analyses. Another possible reason for the observed increase could be an alternative resistant

starch mechanism that was reported by Lopez-Rubio *et al*. (2008) and Tawil *et al*. (2011). It was proposed that as linear amylose-like fragments are released by α-amylase, they can organize into crystalline structures indicative of resistant starch type III. This result will be further investigated in the next sub-section to rule out one of these possibilities.

The Megazyme + NaOH methods reported higher residual starch values for oven-dried barley DDGS ($P < 0.05$), but no significant difference for freeze-dried DDGS. More specifically, the jet-cooked/oven-dried barley DDGS required a pH of 12 to improve enzymatic hydrolysis of resistant starch. While for raw starch hydrolysis/oven-dried barley DDGS, a pH of 10 or 12 could improve hydrolysis of resistant starch. These results reveal that oven-drying, regardless of hydrolysis type, is responsible for a change in starch structure. The affected starch is then made available through exposure to NaOH at high temperatures at specific pH levels. It is unclear why the resistant starch formed by jet-cooking, which is measured with Megazyme + KOH, is not made available when treated with NaOH. It will be important to determine if the increased residual starch value measured by the Megazyme + KOH method is caused by the hydrolysis of non-starch polysaccharides.

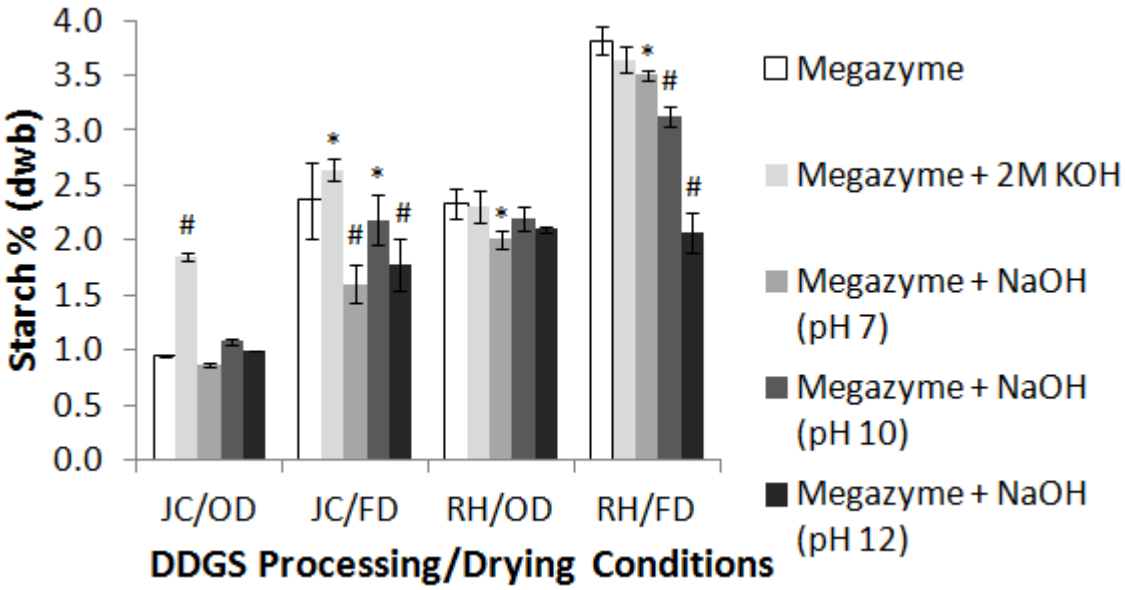

Figure 4-11: Measurement of residual starch in corn DDGS samples using alternative analysis methods; JC = jet-cooking, RH = raw starch hydrolysis, OD = oven-dried, FD = freeze-dried. N = 3; error bars represent ±1 standard deviation. Statistical significance was measured as the difference from the Megazyme value; $P < 0.05$ = *, $P < 0.001$ = #.

For jet-cooked corn DDGS samples, the Megazyme + KOH method increased the residual starch values significantly versus using Megazyme alone (see Figure 4-11). Smaller increases were observed in corn DDGS relative to barley. For instance, the jet-cooked/oven-dried and jet-cooked/freeze-dried samples were only increased by 190

and 110% respectively ($P < 0.001$ & $P < 0.05$). A possible reason for the smaller relative increase is the higher soluble starch measured in the corn DDGS samples. The soluble starch levels are indicated by the values determined by the Megazyme analysis. In the case of barley, Megazyme reported very small values of 0.26 and 0.76% starch (dwb) for jet-cooked samples, which allowed for high percentage increases even with a small increase in the reported residual starch value. On the other hand, Megazyme reported values of 1.55 and 2.36% starch (dwb) for jet-cooked samples, which required a much greater increase in the residual starch value to see a similar percentage increase.

It is interesting to note that no difference in residual starch values is reported between the Megazyme and Megazyme + KOH methods for analysis of raw starch hydrolysis DDGS samples. This suggests that non-starch polysaccharides are not being hydrolyzed by 2M KOH. It is unknown why raw starch hydrolyzed barley DDGS reported increases in residual starch values when measured with Megazyme + KOH, but the same trend does not hold with corn DDGS. Drastic changes observed between starches from different cereal grains imply a high level of complexity during raw starch hydrolysis which may or may not lead to resistant starch formation. Many factors could potentially impact the formation of resistant starch during raw starch hydrolysis. There is limited information regarding the possible formation of resistant starch during raw starch hydrolysis.

Another difference between barley and corn DDGS samples was observed for the analysis of residual starch with Megazyme + NaOH. Oven-dried barley samples showed some level of improvement when using the Megazyme + NaOH method; whereas, oven-dried corn DDGS did not significantly differ from Megazyme in nearly all cases. Only one significant difference from the Megazyme analysis was reported and it involved a significant decrease when Megazyme + NaOH (pH 7) was used to analyse raw starch hydrolysis/oven-dried DDGS ($P < 0.05$). It is unclear why a decrease in residual starch occurred, but further investigation was undertaken and will be reported in a following sub-section.

Lastly, the residual starch analysis of freeze-dried corn DDGS samples with the Megazyme + NaOH methods actually reduced the residual starch values significantly at every pH level as compared to the Megazyme analysis. The jet-cooked and raw starch hydrolyzed DDGS samples behave quite differently. For jet-cooked/freeze-dried DDGS the value reported when exposed to pH 7 significantly reduces the residual starch value, followed by a slight increase when using pH 10, and then another reduction at pH 12 (see Figure 4-11). Alternatively, for raw starch hydrolysis/freeze-dried DDGS the value reported continually decreases as the pH level rises. Further investigation into this result will be reported in the following sub-section.

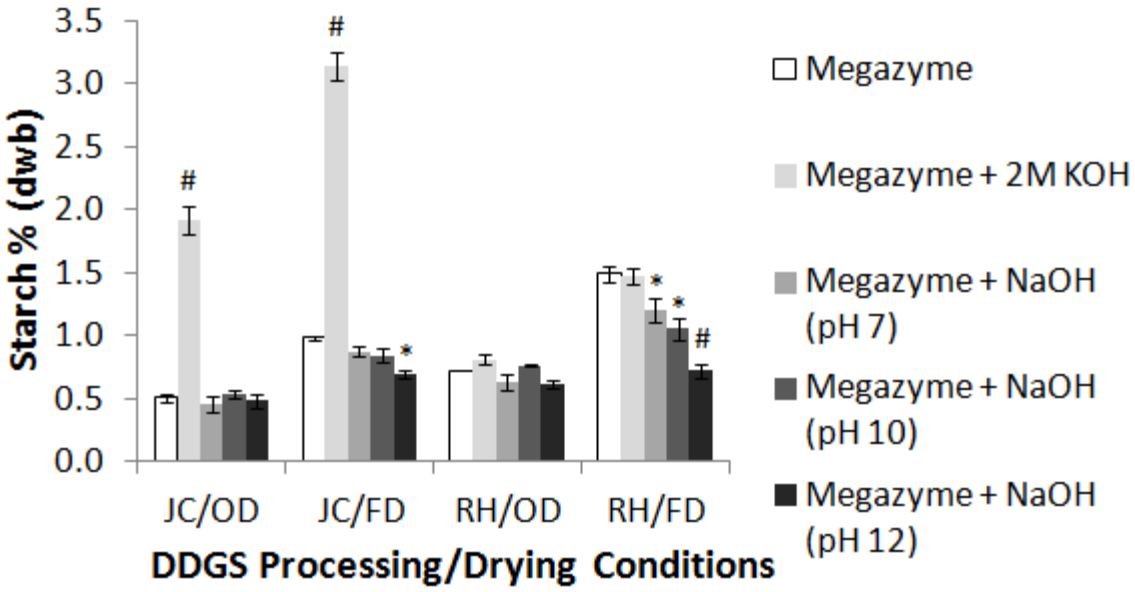

Figure 4-12: Measurement of residual starch in triticale DDGS samples using alternative analysis methods; JC = jet-cooking, RH = raw starch hydrolysis, OD = oven-dried, FD = freeze-dried. N = 3; error bars represent ±1 standard deviation. Statistical significance was measured as the difference from the Megazyme value; $P < 0.05$ = *, $P < 0.001$ = #.

In general, the triticale DDGS residual starch values reported by the alternative methods follow comparable trends to the corn DDGS samples. Starting again with the Megazyme + KOH method, residual starch values for jet-cooked/oven-dried and jet-cooked/freeze dried samples were increased by 380 and 320% respectively ($P < 0.001$). The continued effect of two heat treatments producing more residual starch was again observed for the jet-cooked/oven-dried triticale DDGS samples. This trend stayed consistent for all alternative analysis methods thus far.

Residual starch values reported by the Megazyme + KOH method for raw starch hydrolyzed triticale DDGS samples were not significantly different than the Megazyme analysis (see Figure 4-12). This result was also comparable to the corn DDGS samples, which also reported no significant increase in residual starch values for the Megazyme + KOH method. This result provides further evidence that 2M KOH is not hydrolyzing non-starch polysaccharides. It is becoming more apparent that structural features of starch are a major factor to consider for the analysis of residual starch in DDGS.

Yet another similarity to corn DDGS is observed during the Megazyme + NaOH analysis of oven-dried DDGS. The use of NaOH at any pH level does not significantly affect the residual starch value. The results suggest that resistant starch is not made available by NaOH for oven-dried triticale DDGS. It is unclear why resistant starch in oven-dried barley DDGS is made available for enzymatic hydrolysis, but not for similarly processed

and dried starch in corn or triticale DDGS. As mentioned previously, these results will be investigated further in the next sub-section.

Freeze-dried triticale DDGS samples had significantly lower residual starch values when using the Megazyme + NaOH method as compared to Megazyme alone (see Figure 4-12). For jet-cooked/freeze-dried DDGS, the significant decrease was only observed at the pH 12 level ($P < 0.05$). When testing raw starch hydrolysis/freeze-dried DDGS, all pH levels significantly decreased the residual starch values. As the pH value was raised, the residual starch value continued to decrease. It is quite evident that the pH has a large impact on the reduced residual starch values, which will be discussed in a following sub-section.

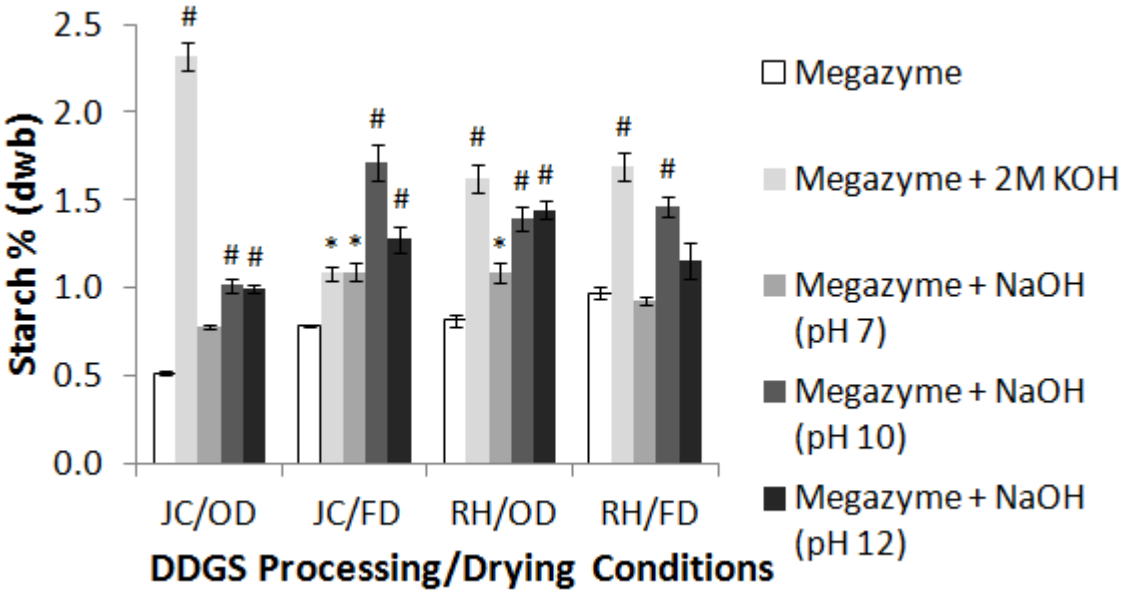

Figure 4-13: Measurement of residual starch in wheat DDGS samples using alternative analysis methods; JC = jet-cooking, RH = raw starch hydrolysis, OD = oven-dried, FD = freeze-dried. N = 3; error bars represent ±1 standard deviation. Statistical significance was measured as the difference from the Megazyme value; $P < 0.05$ = *, $P < 0.001$ = #.

The Megazyme + KOH method significantly increased the residual starch values reported in each wheat DDGS sample type (see Figure 4-13). The increase was expected for heat treated samples, such as the jet-cooked/oven-dried sample that reported a value 450% greater than that of the Megazyme value ($P < 0.001$). Some unexpected results were reported for the raw starch hydrolysis DDGS, which increased approximately 200 and 175% for oven-dried and freeze-dried samples respectively ($P < 0.001$). As was reported for raw starch hydrolyzed barley DDGS, this result may be due to an alternative mechanism for the formation of resistant starch type III. Details of this mechanism are described earlier in this section, as well as in Section 2.3.1.2.

Possibly the most interesting results for the Megazyme + NaOH method are observed in wheat DDGS. Some comparable trends have been reported in barley DDGS, but not with nearly as large of an effect. Significantly higher values are reported for each type of wheat DDGS when using the Megazyme + NaOH method versus using Megazyme alone (see Figure 4-13). Many of the increases are even at a high significance level ($P < 0.001$). For the first time throughout all of the DDGS samples analyzed, jet-cooked/freeze-dried DDGS analyzed using the Megazyme + NaOH method (pH 10) actually reports a residual starch value higher the Megazyme + KOH method.

Another interesting finding is the lower residual starch values observed for freeze-dried samples when the pH is raised from 10 to 12. This drop off was never reported for oven-dried samples of any DDGS type, yet it was commonly seen for freeze-dried samples. An unknown change is occurring during the drying process that has a profound effect on the Megazyme + NaOH method.

4.4.3.1 Effect of KOH and NaOH on non-starch polysaccharides

The use of basic reagents can potentially release glucose from other glucose polymers in DDGS samples. An erroneous release of glucose would cause an inaccurate reporting of starch, because starch determination requires an indirect method which quantifies glucose following hydrolysis. It will be important to rule out non-starch polysaccharides as a potential source of error in the alternative methods, especially since these methods have not been used for DDGS samples previously.

The most abundant non-starch polysaccharides in grain are cellulose, β-glucan, and hemicellulose. These fibres are concentrated during fermentation of grain starch to ethanol. A concentration factor of three is expected to occur in DDGS due to the removal of starch (Spiehs *et al.*, 2002). Another potential source of non-starch polysaccharides in DDGS are the yeast cells, which have grown throughout fermentation into a significant portion of the fermenter solids. Approximately 60% of yeast cell walls are made of β-glucans, which are the only glucose polymers in the cell wall (Aguilar-Ugcanga and Francois, 2003).

An experiment was conducted to test the hydrolysis non-starch polysaccharides exposed to KOH and NaOH (pH 12). Each sample followed a similar protocol to the methods outlined in Sections 3.2.3.2 and 3.2.3.3, with the exception of 100mg of non-starch polysaccharide sample being used in place of DDGS. For this experiment, a resistant form of cellulose, called micro-crystalline cellulose, was used. Two samples of β-glucan extracted from barley were also tested; however, using pure β-glucan was not possible. The purity of the concentrated barley β-glucan tested was determined to be approximately 50 and 70%. β-glucan extraction and measurement was conducted by another laboratory at the University of Alberta. Superstart yeast cells used for the fermentation of the DDGS used in this thesis was also subjected to both bases.

Unfortunately, hemicellulose samples could not be procured. Results of the non-starch polysaccharide hydrolysis using KOH and NaOH are shown in Figures 4-14 and 4-15.

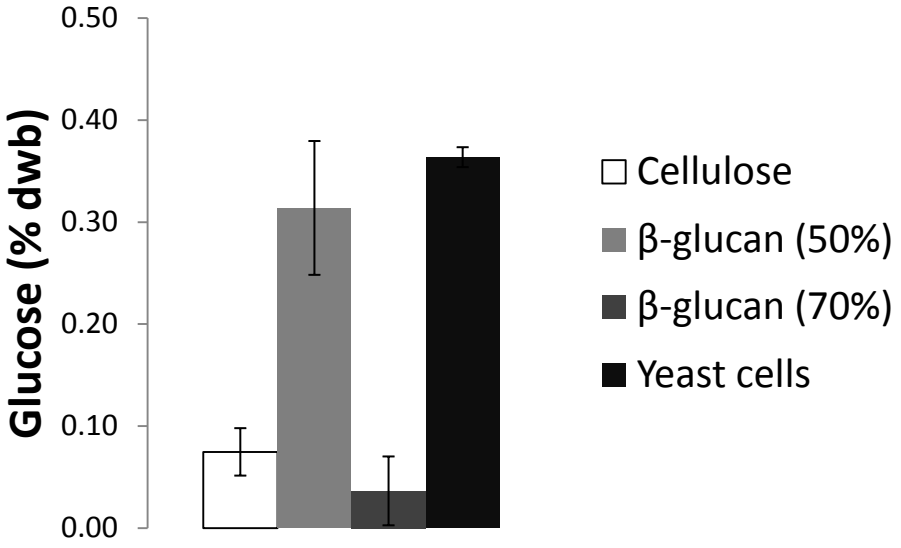

Figure 4-14: Amount of glucose released from non-starch polysaccharides exposed to 2M KOH; N = 3; error bars represent ±1 standard deviation.

The amount of glucose released from non-starch polysaccharides exposed to 2M KOH is extremely low, especially when considering the level of these compounds in DDGS. No methods exist that can single out the content of cellulose, β-glucan, and yeast cells in DDGS. Only crude estimations of soluble fibre (β-glucan) and insoluble fibre (cellulose) can be reported and even these values are not commonly reported in the literature. In any case, the amount of these compounds are expected to be much lower than what is reported in Figure 4-14, which means that an even smaller amount of glucose would be released from DDGS samples. It is also interesting to note the reduced glucose release from a higher purity β-glucan. This is likely due to a reduction in the amount of starch in the higher purity sample.

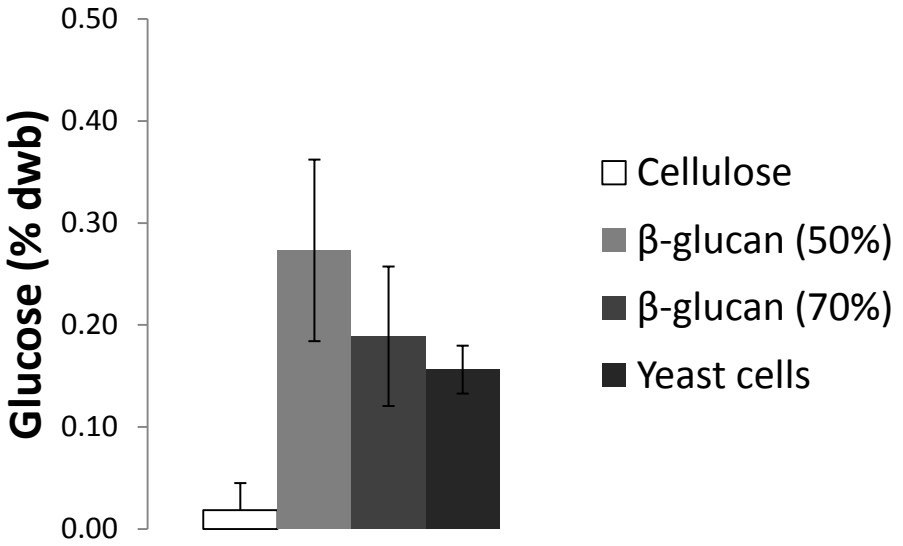

Figure 4-15: Amount of glucose released from non-starch polysaccharides exposed to NaOH (pH 12); N = 3; error bars represent ±1 standard deviation.

The amount of glucose released due to the hydrolysis of non-starch polysaccharides by NaOH (pH 12) is also very low. The β-glucan sample of higher purity is also releasing less glucose when exposed to NaOH, which follows the trend observed with KOH. As explained previously, this is likely due to reduced starch content in the sample. When assessing these results, it is important to consider the reduced content of these compounds in DDGS samples. Based on the limited amount of fibre in DDGS, it can be concluded that glucose released from non-starch polysaccharides using the Megazyme + NaOH method is very minimal.

4.4.3.2 Effect of KOH and NaOH on pure glucose

Some DDGS types reported a significant reduction in residual starch values when using the Megazyme + NaOH method at high pH (see Section 4.4.3). This result required further investigation and lead to an experiment that measured glucose reactivity with KOH and NaOH. Any reacted glucose would be unavailable for quantification and could negatively impact the determination of residual starch.

An experiment was conducted on 100mg samples of glucose. The glucose was incubated in an ice water bath for 20 minutes (KOH) or incubated in a boiling water bath for 30 minutes (NaOH) to simulate the experimental conditions used in the Megazyme + NaOH and Megazyme + NaOH methods (see Sections 3.2.3.2 & 3.2.3.3). Following each incubation period, the glucose was quantified colourimetrically using the GOPOD reagent (see Section 3.2.2.1). Results of this experiment are shown in Figure 4-16.

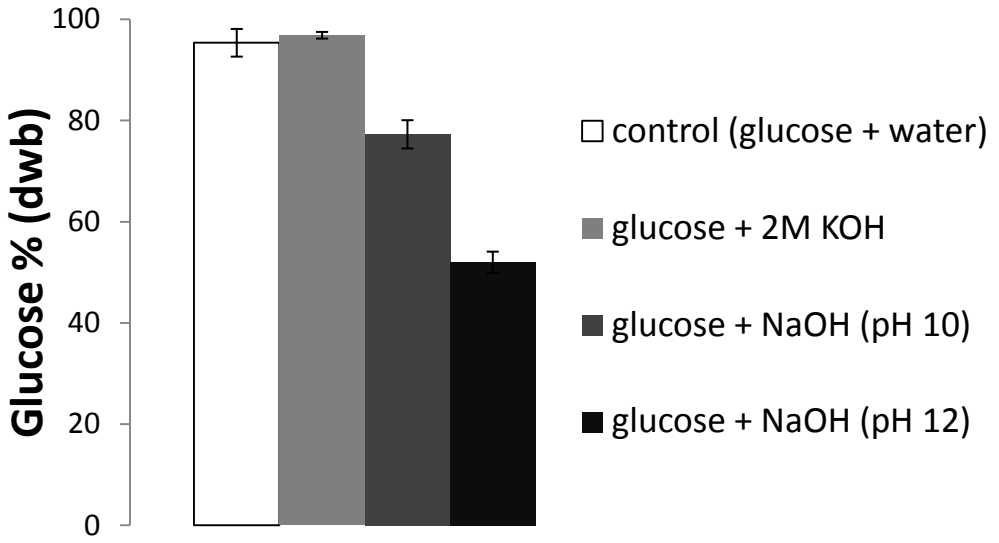

Figure 4-16: Reactivity of glucose with KOH and NaOH; N = 3; error bars represent ±1 standard deviation.

The glucose quantified after incubation with 2M KOH in an ice water bath was not significantly different than the control (see Figure 4-16). This result confirms that there is no interference of glucose measurement for residual starch determination using the Megazyme + KOH method. It is likely that the low temperature incubation halted any reactivity between the KOH and the glucose molecules.

A large reduction in the amount of glucose quantified was observed for NaOH at pH 10 and 12 (see Figure 4-16). Approximately half of the glucose was reacted into an unknown compound following incubation with NaOH at pH 12, which significantly impacted quantification. This result suggests that a significant portion of both free residual glucose in DDGS and glucose released during incubation with NaOH at high pH will be further reacted and become unavailable for quantification. These findings present a significant problem for the Megazyme + NaOH methods. As a result of either one of these scenarios, the residual starch value will be significantly reduced. The reactivity of glucose and NaOH explains, at least in part, the reason for the reduction in residual starch values reported at high pH levels (see Section 4.4.3).

4.5 Discussion

The reduced residual starch values reported for the Megazyme + NaOH method at high pH values are likely due to the destruction of residual glucose in DDGS samples. The residual glucose is measured by the sample blank. In some cases the residual glucose can be relatively high and if it was not accounted for, it could drastically overestimate the amount of starch in the sample. The problem occurs due to the subtraction of the sample blank, which in most cases stays constant. The reactivity of glucose with NaOH

during the incubation step reduces the glucose level in the sample, only to then have the full value of the blank subtracted for quantification. To fully demonstrate this impact, consider a residual glucose value of 1%. Assuming half of this glucose reacts with base, only 0.5% of the residual glucose is measured, but the full sample blank absorbance is subtracted from the final value. This equates to 0.5% glucose, or 0.4% starch based on the molecular weight difference of anhydrous glucose. Considering the low levels of starch in DDGS samples, 0.4% is a very significant value. Samples that reported the largest decreases were freeze-dried samples, which also had the highest residual glucose due to the lack of heating that contributes to Maillard reactions. Oven drying on the other hand would induce Maillard reactions between glucose and amino acids or proteins, thus reducing the residual glucose value of the DDGS and lowering the impact of NaOH.

In many cases it was discussed that two heat treatments (jet-cooking/oven-drying) resulted in the most resistant starch formation. This was indicated by the highest percentage increases when using chemical solvents in addition to the Megazyme enzymes. The large percentage increase in jet-cooked/oven-dried DDGS samples can also be attributed to the lower amount of starch available to the Megazyme analysis. The most important piece of information that can be taken away from these comparisons is that the reported residual starch values for DDGS samples that most closely resemble commercial samples (jet-cooking and oven-drying) are still being underreported. This is indicated by the larger residual starch values reported by the exact same jet-cooked samples (only freeze-dried). Theoretically, these samples have the same amount of starch, but in the case of oven-dried samples it remained unavailable and unreported. This result is expected to be caused by improved ordering of crystalline structures in oven-dried samples as a result of water being driven off at high temperatures and low moisture levels.

A very interesting finding was the formation of resistant starch in some raw starch hydrolyzed DDGS samples, but not for others. It is likely that starch characteristics are largely responsible for the discrepancy. Some starch properties of particular interest may include: the amylopectin chain length, the amylose content, the amylopectin chain length, and the distribution of amylopectin chains. Many other structural features can be examined by future studies, but the focus should consider characteristics responsible for the formation of linear starch molecules that are able to re-crystallize as resistant starch. Considering the nature and complexity of starch hydrolysis, it is entirely possible that random cleavage by α-amylase could produce varying effects within replicates of the same grain.

5. Conclusions

Benchmarked enzymatic analysis methods are underreporting the amount of residual starch in DDGS. This is particularly true for the Megazyme analysis that relies solely on

α-amylase and amyloglucosidase. The residual starch in DDGS has already escaped enzymatic hydrolysis during ethanol production which uses state of the art enzymes. When no attempt is made to improve enzymatic access to resistant starch it escapes hydrolysis a second time. While the Megazyme + DMSO method does make an effort to improve resistant starch measurement, it falls short of an alternative method reported in this thesis that utilizes Megazyme + KOH.

As already indicated, the Megazyme + KOH method can vastly improve the analysis of residual starch in DDGS samples. The largest improvements were observed for heat treated DDGS samples. In one case, the Megazyme + KOH reported a starch value six fold higher than when using Megazyme alone. Such drastic improvements lead to the further investigation of non-starch polysaccharide hydrolysis, which was determined to be insignificant. Without a doubt this alternative method for residual starch determination is reporting more accurate values of residual starch in DDGS; however, there is still room for improvement. Samples that most closely resemble commercial DDGS (jet-cooked/oven-dried) reported the largest relative increases with this method, yet they are still underreporting residual starch values. An insignificant difference is expected between jet-cooked samples exposed to oven or freeze-drying, so the fact that more starch was measured for the freeze-dried samples indicates that this method is underreporting oven-dried samples.

The Megazyme + KOH method was also determined to be necessary when measuring raw starch hydrolysis DDGS samples. While only barley and wheat DDGS reported increases, it was proven that resistant starch is formed during raw starch hydrolysis. The most likely scenario is an alternative mechanism proposed by Lopez-Rubio *et al*. (2008) and Tawil *et al*. (2011). The mechanism proposes that as linear amylose-like fragments are released by α-amylase and they too can organize into crystalline structures indicative of resistant starch type III. The interesting thing about the proposed mechanism is when the randomness of starch hydrolysis is considered, it is hard to know which samples might form resistant starch when exposed to raw starch hydrolyzing enzymes. For this reason, it is recommended that any DDGS samples generated using raw starch hydrolysis also measure residual starch using the Megazyme + KOH method.

Lastly, the use of acid hydrolysis methods for the measurement of residual starch in DDGS is not recommended. The lack of specificity was demonstrated by the significant release of glucose from various non-starch polysaccharides subjected to acid hydrolysis. As a result of the excess glucose released, mostly from β-glucans, the residual starch was vastly overestimated. Interestingly, the β-glucans in DDGS are from both cereal and yeast sources and both contribute to the overestimation of starch by acid hydrolysis.

Bibliography

Agu RC, Bringhurst TA, Brosnan JM, Jack FR. 2008. Effect of process conditions on alcohol yield of wheat, maize and other cereals. Journal of the Institute of Brewing 114(1): 39-44.

Aguilar-Uscanga B and Francois JM. 2003. A study of the yeast cell wall composition in response to growth conditions and mode of cultivation. Letters in Applied Microbiology 37: 268-274.

Albertyn J, Hohmann S, Thevelein JM, Prior BA. 1994. Characterization of osmotic-stress response in Saccharomyces cerevisiae: osmotic stress and glucose repression regulate glycerol-3-phosphate dehydrogenase independently. Current Genetics, 25: 12-18.

Ao Z and Jane J. 2007. Characterization and modeling of the A- and B- granule starches of wheat, triticale, and barley. Carbohydrate Polymers 67(2): 46-55.

Bayrock DP and Ingledew WM. 2001. Application of multistage continuous fermentation of fuel alcohol by very-high-gravity fermentation. Journal of Industrial Microbiology & Biotechnology 27: 87-93.

Belyea RL, Rausch KD, Tumbleson ME. 2004. Composition of corn and distillers dried grains with solubles from dry grind ethanol processing. Bioresource Technology 94: 293-298.

Berry CS. 1986. Resistant starch - formation and measurement of starch that survives exhaustive digestion with amylolytic enzymes during the determination of dietary fiber. Journal of Cereal Science 4(4): 301-314.

Bhatty RS. 1982. Distribution of lipids in embryo and bran-endosperm fractions of Risϕ 1508 and Hiproly barley. Cereal Chemistry 59: 154-155.

Bhatty RS. 1992. Beta-glucan content and viscosities of barleys and their roller-milled flour and bran products. Cereal Chemistry 69(5): 469-471.

Biliaderis CG, Page CM, Maurice TJ. 1986. On the multiple melting transitions of starch/monoglyceride systems. Food Chemistry 22(4): 279-295.

Brummer Y and Cui SW. 2005. Food carbohydrates: chemistry, physical properties, and applications. Chapter 2: edited by Cui SW. Taylor & Francis Group. Boca Raton, FL, USA.

Bulpin PV, Welsh EJ, Morris ER. 1982. Physical characterization of amylose-fatty acid complexes in starch granules and in solution. Starch/Starke 34(10): 335-339.

Cammerer B, Jalyschkov V, Kroh LW. 2002. Carbohydrate structures as part of the melanoidin skeleton. International Congress Series 1245: 269-273.

Colonna P, Leloup V, Buleon A. 1992. Limiting Factors of Starch Hydrolysis. European Journal of Clinical Nutrition 46: S17-S32.

Craig SAS, Maningat CC, Seib PA, Hoseney RC. 1989. Starch paste clarity. Cereal Chemistry 66(3): 173-182.

Czuchajowska Z, Sievert D, and Pomeranz Y. 1991. Enzyme-resistant starch - effects of complexing lipids. Cereal Chemistry 68(5): 537-542.

Dhital S, Shrestha AK, Gidley MJ. 2010. Relationship between granule size and in vitro digestibility of maize and potato starches. Carbohydrate Polymers 82: 480-488.

Donovon JN. 1979. Phase transitions of the starch-water system. Biopolymers 18(2): 263-275.

Duensing WJ, Roskens AB, Alexander RJ. 2003. Corn: chemistry and technology. Chapter 11. Edited by White PJ and Johnson LA. American Association of Cereal Chemists. St. Paul, MN, USA.

Earnest C, Snyder C, Westra S. 2009. The alcohol textbook 5th edition. Chapter 19. Edited by Ingledew WM, Kelsall DR, Austin GD, Kluhspies C. Nottingham University Press. Nottingham, UK.

Eerlingen RC and Delcour JA. 2005. Formation, analysis, structure and properties of type III enzyme resistant starch. Journal of Cereal Science 22(2): 129-138.

Ellis RP, Cochrane MP, Dale MFB, Duffus CM, Lynn A, Morrison IM, Prentice RDM, Swanston JS, and SA Tiller. 1998. Starch production and industrial use. J. Sci. Food Agric. 77: 289-311.

French D. 1984. Starch: chemistry and technology: Chapter 7. Edited by Whistler RL, BeMiller JN and Paschall JF. Academic Press. Orlando, FL, USA.

Gallant DJ, Bouchet B, Baldwin PM. 1997. Microscopy of starch: evidence of a new level of granule organization. Carbohydrate Polymers 32: 177-191.

Gibreel A, Sandercock JR, Lan J, Goonewardene LA, Zijlstra RT, Curtis JM, Bressler DC. 2009. Fermentation of barley using Saccharomyces cerevisiae: examination of barley as a feedstock for bioethanol production and value-added products. Applied and Environmental Microbiology 75(5): 1363-1372.

Gibreel A, Sandercock JR, Lan J, Goonewardene LA, Scott AC, Zijlstra RT, Curtis JM, Bressler DC. 2011. Evaluation of value-added components of dried distiller's grain with solubles from triticale and wheat. Bioresource Technology 102: 6920-6927.

Gidley MJ, Bulpin PV, Kay S. 1986. Gums and stabilizers for the food industry, vol 3. Elsevier. London, UK.

Gidley MJ. 1989. Molecular mechanisms underlying amylose aggregation and gelation. Macromolecules 22(1): 351-358.

Gidley MJ and Bulpin PV. 1989. Aggregation of amylose in aqueous systems: the effect of chain length on phase behavior and aggregation kinetics. Macromolecules 22: 341-346.

Gomez C, Navarro A, Manzanares P, Horta A, Carbonell JV. 1997. Physical and structural properties of barley (1→3),(1→4)-β-D-glucan. Part I. Determination of molecular weight and macromolecular radius by light scattering. Carbohydrate Polymers 32: 7-15.

Habibi Y and Dufresne A. 2011. Handbook of nanophysics: nanoparticles and quantum dots. Chapter 10. Edited by Sattler KD. Taylor & Francis Group. Boca Raton, FL, USA.

Haefele DM and Ross AJ. 2009. The alcohol textbook 5th edition. Chapter 4. Edited by Ingledew WM, Kelsall DR, Austin GD, Kluhspies C. Nottingham University Press. Nottingham, UK.

Hall M, Jennings JP, Lewis BA, Robertson JB. 2001. Evaluation of starch analysis methods for feed samples. Journal of the Science of Food and Agriculture 81: 17-21.

Hanashiro I, Abe J, Hizukuri S. 1996. A periodic distribution of the chain length of amylopectin as revealed by high-performance anion-exchange chromatography. Carbohydrate Research 283: 151-159.

Hizukuri S, Kaneko T, Takeda Y. 1983. Measurement of the chain-length of amylopectin and its relevance to the origin of crystalline polymorphism of starch granules. Biochimica et Biophysica ACTA. 760(1): 188-191.

Hizukuri S. 1986. Polymodal distribution of the chain lengths of amylopectins, and its significance. Carbohydrate Research 147: 342-347.

Huber KC and BeMiller JN. 1997. Visualization of channels and cavities of corn and sorghum starch granules. Cereal Chemistry 74(5): 537-541.

Imberty A, Chanzy H, Perez S. 1987. New three-dimensional structure for A-type starch. Macromolecules 20: 2636-2638.

Imberty A, Buleon A, Tran V, Perez S. 1991. Recent advances in knowledge of starch structure. Starch 43(10): 375-384.

Ingledew WM. 1999. Alcohol production by Saccharomyces cerevisiae: a yeast primer. In: The Alcohol Textbook 3rd edition, pp 49-87. Editors: Jacques KA, Lyons TP, and Kelsall DR. Nottingham University Press, UK.

Izydorczyk M. 2005. Food carbohydrates: chemistry, physical properties, and applications. Chapter 1: edited by Cui SW. Taylor & Francis Group. Boca Raton, FL, USA.

Jane J and Robyt JF. 1984. Structure studies of amylose-V complexes and retrograded amylose by action of alpha amylases, and a new method for preparing amylodextrins. Carbohydrate Research 132: 105-118.

Jane J, Xu A, Radosavljevic M, Sieb PA. 1992a. Location of amylose in normal starch granules I. susceptibility of amylose and amylopectin to cross-linking reagents. Cereal Chemistry 69(4): 405-409.

Jane JL, Shen L, Wang L, Maningat CC. 1992b. Preparation and properties of small-particle cornstarch. Cereal Chemistry 69: 280-283.

Jane JL, Kasemsuwan S, Leas S, Zobel H, Robyt JF. 1994. Anthology of starch granule morphology by scanning electron microscopy. Starch 46(4): 121-129.

Jane J. 2009. ScienceDirect (Online service). Starch: chemistry and technology: Chapter 6. Edited by BeMiller JN and Whistler RL. London: Academic.

Jenkins PJ, Cameron RE, Donald AM. 1993. A universal feature in the structure of starch granules from different botanical sources. Starch 45: 417-420.

Jenkins PJ and Donald AM. 1997. The effect of acid hydrolysis on native starch granule structure. Starch 49: 262-267.

Karkalas J, Ma S, Morrison WR, Pethrick RA. 1995. Some factors determining the thermal-properties of amylose inclusion complexes with fatty-acids. 268(2): 233-247.

Kasemsuwan T and Jane J. 1994. Location of amylose in normal starch granules II. locations of phosphodiester cross linking revealed by p-31 nuclear-magnetic-resonance. Cereal Chemistry 71(3): 282-287.

Kearsley MW and Verwaerde F. 1991. Advances in carbohydrate analysis. Edited by White CA. JAI Press Inc., UK.

Kelsall DR and Lyons TP. 1999. The alcohol textbook 3rd edition. Chapter 2. Edited by Lyons K and Kelsall TP. Nottingham University Press. Nottingham, UK.

Kelsall DR and Piggot R. 2009. The alcohol textbook 5th edition. Chapter 13. Edited by Ingledew WM, Kelsall DR, Austin GD, Kluhspies C. Nottingham University Press. Nottingham, UK.

Kiesselbach TA. 1999. The structure and reproduction of corn: 50th anniversary edition. Cold Spring Harbor Laboratory Press. Cold Spring Harbor, NY, USA.

Kim K, Park CS, Mattoon JR. 1988. High-efficiency, one-step starch utilization by transformed Saccharomyces cells which secrete both yeast glucoamylase and mouse α-amylase. Applied and Environmental Microbiology 54(4): 966-971.

Kim Y, Mosier NS, Hendrickson R, Ezeji T, Blaschek H, Dien B, Cotta M, Dale B, Ladisch MR. 2008. Composition of corn dry-grind ethanol by-products: DDGS, wet cake, and thin stillage. Bioresource Technology 99: 5165-5176.

Kindred DR, Verhoeven TMO, Weightman RM, Swanston JS, Agu RC, Brosnan JM, Sylvester-Bradley R. 2008. Effects of variety and fertiliser nitrogen on alcohol yield, grain yield, starch and protein content, and protein composition of winter wheat. Journal of Cereal Science 48: 46-57.

Kohl S. 2009. The alcohol textbook 5th edition. Chapter 14. Edited by Ingledew WM, Kelsall DR, Austin GD, Kluhspies C. Nottingham University Press. Nottingham, UK.

Kowblansky M. 1985. Calorimetric investigation of inclusion complexes of amylose with long-chain aliphatic compounds containing different functional groups. Macromolecules 18: 1776-1779.

Kumar S, Singh N, Prasad R. 2010. Anhydrous ethanol: a renewable source of energy. Renewable and Sustainable Energy Reviews 14(7): 1830-1844.

Li C, Li W, Lee B, Laroche A, Cao L, Lu Z. 2011. Morphological characterization of triticale starch granules during endosperm development and seed germination. Can. J. Plant Sci. 91: 57-67.

Li L, Blanco M, Jane J. 2007. Physiochemical properties of endosperm and pericarp starches during enzyme development. Carbohydrate Polymers 67: 630-639.

Liu JJ, Ding WT, Zhang GC, Wang JY. 2011. Improving ethanol fermentation performance of Saccharomyces cerevisiae in very high-gravity fermentation through chemical mutagenesis and meiotic recombination. Applied microbiology and biotechnology. 91: 1239-1246.

Lindeboom N, Chang PR, Tyler RT. 2004. Analytical, biochemical and physiochemical aspects of starch granule size, with emphasis on small granule starches: a review. Starch 56: 89-99.

Lopez-Rubio A, Flanagan BM, Shrestha AK, Gidley MJ, Gilbert EP. 2008. Molecular rearrangement of starch during in vitro digestion: toward a better understanding of

enzyme resistant starch formation in processed starches. Biomacromolecules 9(7): 1951-1958.

Macrae R, Robinson RK, Sadler MJ (editors). 1993. Encyclopedia of food science and food technology and nutrition. Volume 7. Academic Press, Inc. San Diego, CA, USA.

MacGregor AW and Bhatty RS. 1993. Barley: chemistry and technology. American Society of Cereal Chemists, Inc. St. Paul, MN, USA.

Madson PW. 2009. The alcohol textbook 5th edition. Chapter 20. Edited by Ingledew WM, Kelsall DR, Austin GD, Kluhspies C. Nottingham University Press. Nottingham, UK.

Matsumoto N, Fukushi O, Miyanaga M, Kakihara K, Nakajima E, Yoshizumi H. 1982. Industrialization of a noncooking system for alcoholic fermentation from grains. Agricultural and Biological Chemistry 46(6): 1549-1558.

Matz SA. 1991. The chemistry and technology of cereals as food and feed. Pan-Tech International, Inc. McAllen, TX, USA.

Miao M, Jiang B, Zhang T, Jin Z, Mu W. 2011. Impact of mild acid hydrolysis on structure and digestion properties of waxy maize starch. Food Chemistry 126: 506-513.

Miles MJ, Morris VJ, Ring SG. 1985a. Gelation of amylose. Carbohydrate Research 135: 257-269.

Miles MJ, Morris VJ, Orford PD, Ring SG. 1985b. The roles of amylose and amylopectin in the gelation and retrogradation of starch. Carbohydrate Research 135: 271-281.

Monceaux DA. 2009. The alcohol textbook 5th edition. Chapter 6. Edited by Ingledew WM, Kelsall DR, Austin GD, Kluhspies C. Nottingham University Press. Nottingham, UK.

Monceaux DA and Kuehner D. 2009. The alcohol textbook 5th edition. Chapter 21. Edited by Ingledew WM, Kelsall DR, Austin GD, Kluhspies C. Nottingham University Press. Nottingham, UK.

Morrison WR, Law RV, Snape CE. 1993. Evidence for inclusion complex of lipids with V-amylose in maize, rice and oat starches. Journal of Cereal Science 18: 107-109.

Narendranath NV and Brey S. The alcohol textbook 5th edition. Chapter 23. Edited by Ingledew WM, Kelsall DR, Austin GD, Kluhspies C. Nottingham University Press. Nottingham, UK.

Newman RK and Newman CW. 2008. Barley for food and health: science, technology, and products. John Wiley & Sons, Inc. Hoboken, NJ, USA.

Perez S, Baldwin PM, and Gallant DJ. 2009. ScienceDirect (Online service). Starch: chemistry and technology. Chapter 5: edited by BeMiller JN and Whistler RL. London: Academic.

Peterson RF. 1965. Wheat: botany, cultivation, and utilization. Interscience Publishers Inc. New York, NY, USA.

Pfannemuller B. 1987. Influence of chain length of short monodisperse amyloses on the formation of A- and B-type X-ray diffraction patterns. International Journal of Biological Macromolecules. 9(2): 105-108.

Pilgram C and Wright S. 2009. The alcohol textbook 5th edition. Chapter 36. Edited by Ingledew WM, Kelsall DR, Austin GD, Kluhspies C. Nottingham University Press. Nottingham, UK.

Planchot V, Colonna P, Buleon A. 1997. Enzymatic hydrolysis of alpha-glucan crystallites. Carbohydrate Research 298(4): 319-326.

Qiang L. 2005. Food carbohydrates: chemistry, physical properties, and applications. Chapter 7: edited by Cui SW. Taylor & Francis Group. Boca Raton, FL, USA.

Rausch KD, Belyea RL, Ellersieck MR, Singh V, Johnston DB, Tumbleson ME. 2005. Particle size distributions of ground corn and DDGS from dry grind processing. Transactions of the Society of Agricultural Engineers 48: 273-277.

Renewable Fuels Association. 2007. Ethanol industry outlook: building new horizons. Washington, D.C. [online]: http://www.ethanolrfa.org/page/-/objects/pdf/outlook/RFA_Outlook_2007.pdf?nocdn=1

Ring SG, l'Anson KJ, Morris VJ. 1985. Static and dynamic light scattering studies of amylose solutions. Macromolecules 18: 182-188.

Robertson GH, Wong DWS, Lee CC, Wagschal K, Smith MR, Orts WJ. 2006. Native or raw starch digestion: a key step in energy efficient biorefining of grain. Journal of Agricultural and Food Chemistry 54: 353-365.

Sajilata MG, Singhal RS, Kulkarni PR. 2006. Resistant starch - a review. Comprehensive Reviews in Food Science and Food Safety 5: 1-17.

Salmanowicz BP and Nowak J. 2009. Diversity of monomeric prolamins in triticale cultivars determined by capillary zone electrophoresis. Journal of Agricultural and Food Chemistry 57: 2119-2125.

Sandhu KS and Singh N. 2007. Some properties of corn starches II: physiochemical, gelatinization, retrogradation, pasting and gel textural properties. Food Chemistry 101: 1499-1507.

Schmitz S, Dona AC, Castignolles P, Gilbert RG, Gaborieau M. 2009. Assessment of the extent of starch dissolution in dimethyl sulfoxide by ^{1}H NMR spectroscopy. Macromolecular Bioscience 9(5): 506-514.

Schwartz D. 1982. Amylose distribution in the starch granule of maize endosperm. Maydica 27: 54-57.

Shariffa YN, Karim AA, Fazilah A, Zaidul ISM. 2009. Enzymatic hydrolysis of granular native and mildly heat-treated tapioca and sweet potato starches at sub-gelatinization temperature. Food Hydrocolloids 23(2): 434-440.

Sharma V, Rausch KD, Tumbleson ME, Singh V. 2006. Starch fermentation characteristics for different proportions of amylose and amylopectin. American Society of Agricultural and Biological Engineers Meeting Presentation (Paper number 066066).

Sharma V, Rausch KD, Tumbleson ME, Singh V. 2007. Comparison between granular starch hydrolyzing enzyme and conventional enzymes for ethanol production from maize starch with different amylose:amylopectin ratios. Starch 59: 549-556.

Shetty JK, Lantero OJ, Dunn-Coleman N. 2005. Technological advances in ethanol production. International Sugar Journal 107: 605-610.

Sievert D and Pomeranz Y. 1989. Enzyme-resistant starch - characterization and evaluation by enzymatic, thermoanalytical, and microscopic methods. Cereal Chemistry 66(4): 342-347.

Singh V and Johnston DB. 2009. The alcohol textbook 5th edition. Chapter 15. Edited by Ingledew WM, Kelsall DR, Austin GD, Kluhspies C. Nottingham University Press. Nottingham, UK.

Siriamornpun S, Wootton M, Schultheiss J. 2004. Potential of capillary electrophoresis for identification of Australian triticale varieties. Australian Journal of Agricultural Research 55: 595-598.

Skendi A, Biliaderis CG, Lazaridou A, Izydorczyk MS. 2003. Structure and rheological properties of water soluble beta-glucans from oat cultivars of Avena sativa and Avena bysantina. Journal of Cereal Science 38(1): 15-31.

Spiehs MJ, Whitney MH, Shurson GC. 2002. Nutrient database for distiller's dried grains with solubles produced from new ethanol plants in Minnesota and South Dakota. Journal of Animal Science 80(10): 2639-2645.

Srichuwong S and Jane J. 2011. Methods for characterization of residual starch in distiller's dried grains with solubles (DDGS). Cereal Chemistry 88(3): 278-282.

Stenvert NL and Kingswood K. The influence of the physical structure of the protein matrix on wheat hardness. J. Sci. Fd. Agric. 1977. 28, 11-19.

Swanston JS, Smith PL, Gillespie TL, Brosnan JM, Bringhurst TA, Agu RC. 2007. Associations between grain characteristics and alcohol yield among soft wheat varieties. Journal of the Science of Food and Agriculture 87: 676-683.

Tawil G, Viksø-Nielsen A, Rolland-Sabaté A, Colonna P, Buléon A. 2011. In depth study of a new highly efficient raw starch hydrolyzing α-amylase from Rhizomucor sp. Biomacromolecules 12: 34-42.

Tester RF, Karkalas J, Qi X. 2004. Starch-composition, fine structure and architecture. Journal of Cereal Science 152: 151-165.

Thomas KC, Hynes SH, Jones AM, Ingledew WM. 1993. Production of fuel alcohol from wheat by VHG technology; effect of sugar concentration and fermentation temperature. Applied Biochemistry and Biotechnology 43: 211-226.

Thomas KC, Hynes SH, Ingledew WM. 1996. Practical and theoretical considerations in the production of high concentrations of alcohol by fermentation. Process Biochemistry 31(4): 321-331.

Tufvesson F and Eliasson AC. 2000. Formation and crystallization of amylose-monoglyceride complex in a starch matrix. Carbohydrate Polymers 43: 359-365.

Ullrich SE. 2011. Barley: production, improvement, and uses. John Wiley & Sons, Inc. Chichester, WS, UK.

Vasanthan T and Bhatty RS. 1996. Physiochemical properties of small- and large-granule starches of waxy, regular, and high-amylose barleys. Cereal Chem. 73(2): 199-207.

Vasanthan T and Hoover R. 1992. Effect of defatting on starch structure and physicochemical properties. Food Chemistry 45: 337-347.

Vidal Jr. BC, Rausch KD, Tumbleson ME, Singh V. 2009. Kinetics of granular starch hydrolysis in corn dry-grind process. Starch 61: 448-456.

Wang Q and Cui SW. 2005. Food carbohydrates: chemistry, physical properties, and applications. Chapter 5: edited by Cui SW. Taylor & Francis Group. Boca Raton, FL, USA.

Wang P, Singh V, Xue H, Johnston DB, Rausch KD, Tumbleson ME. 2007. Comparison of raw starch hydrolyzing enzyme with conventional liquefaction and saccharification enzymes in dry-grind corn processing. Cereal Chemistry 84(1): 10-14.

Watson SA. 2003. Corn: chemistry and technology 2nd edition. Chapter 3. Edited by White PJ and Johnson LA. American Association of Cereal Chemists. St. Paul, MN, USA.

Whitworth S, Coward-Kelly G, Clark, S. 2011. *Abstracts of Papers*, the 7th International Starch Technology Conference. Urbana, IL, USA.

Wong DWS, Robertson GH, Lee CC, Wagschal K. 2007. Synergistic action of recombinant α-amylase and glucoamylase on the hydrolysis of starch granules. The Protein Journal 26(3): 159-164.

Wu X, Zhao R, Wang D, Bean SR, Seib PA, Tuinstra MR, Campbell M, O'Brien A. 2006. Effects of amylose, corn protein, and corn fiber contents on production of ethanol from starch-rich media. Cereal Chem. 83(5): 569-575.

Yadav BS, Sharma A, Yadav RB. 2009. Studies on the effect of multiple heating/cooling cycles on the resistant starch formation in cereals, legumes, and tubers. International Journal of Food Sciences and Nutrition 60(S4): 258-272.

Yamaguchi M, Kainuma K, French D. 1979. Electron microscopic observations of waxy maize starch. Journal of Ultrastructure Research. 69(2): 249-261.

Yaylayan VA, Huyghues-Despointes A, Feather MS. 1994. Chemistry of Amadori rearrangement products: analysis, synthesis, kinetics, reactions, and spectroscopic properties. Critical Reviews in Food Science and Nutrition 34(4): 321-369.

Yu L and Chen L. 2009. Biodegradable polymer blends and composites from renewable resources: Chapter 1. Edited by Yu L. John Wiley & Sons, Inc. Hoboken, NJ, USA.

Zhao R, Wu X, Seabourn BW, Bean SR, Guan L, Shi YC, Wilson JD, Madl R, and Wang D. 2009. Comparison of waxy vs nonwaxy wheats in fuel ethanol fermentation. Cereal Chemistry 86(2): 145-156.

Zhao R, Wu X, Bean S, Wang D. 2010. Industrial crops and uses. Chapter 5. Edited by Singh BP. CAB International. Oxfordshire, UK.

Appendix 1 - Methods used for the fermentation of cereal grains

I) Conventional jet-cooking method:

A 35% (w/w) solids mash was obtained by mixing ground grain with water. The pH of the mash was adjusted to pH 4.8 using HCl (12M). Mash was then heated to 55°C with frequent stirring in a Groen kettle (model TS/9). During heating, Viscozyme (viscosity reducing enzyme - 300µL/kg grain) and Fermgen (protease - 940µL/kg grain) were added and the mash was incubated for 1 hour. At the end of this treatment, the pH was raised to 5.25 using 5N NaOH. A small dosage of Liquozyme SC (α-amylase - 21µL/kg grain) was added to the mash and the temperature was increased to 85°C. This incubation was carried out for 30 minutes. This mash was then passed through a laboratory jet-cooker five times at a flow rate of 1.9L/min. During jet-cooking the mash was heated to 110-120°C by direct injection of high-pressure clean steam. After jet-cooking, water was added back to the mash for an adjustment back to the original mass. This mash was then transferred back into the Groen kettle and incubated at 85°C with more Liquozyme SC (63µL/kg of grain). This incubation was carried out for 90 minutes.

To conduct fermentation, the mash was transferred into sterile 5L bioreactors and diluted to achieve a final concentration of 30% solids. The temperature was adjusted to 30°C with stirring set at 200-300rpm. Urea was then added to achieve a concentration of 16mM. Next, Spirizyme fuel (amyloglucosidase - 600µL/kg grain) was added, followed by a 15 minute incubation step. Finally, the pre-hydrated and incubated yeast (Superstart instant dry yeast) was used to inoculate the fermenter to a concentration of approximately 2×10^7 CFU/mL.

After 72 hours of fermentation, the remaining solids in the fermenter were dried using a two stage process which involved the evaporation of the liquid phase in rotary evaporator at 72°C, followed by freeze-drying at -60°C at ~4×10^4Pa for 72 hours. This produced the DDGS samples analyzed in this thesis.

II) Raw starch hydrolysis method:

A 35% solids mash was obtained by mixing ground grain with water. The mash was heated to 55°C and adjusted to pH 4.0 using HCl (12M). During heating, Optimash TGB (viscosity reducing enzyme - 80µL/kg grain) and Fermgen (protease - 940µL/kg grain) were added and the mash was incubated for 1 hour with frequent stirring.

To conduct fermentation, the mash was transferred into sterile 5L bioreactors and diluted to achieve a final concentration of 30% solids. The temperature was adjusted to 48°C with stirring set at 200-300rpm. Next, Stargen 001 (raw starch hydrolyzing enzyme - 2.8mL/kg of grain) was added and incubated for 1 hour. The temperature was then reduced to 30°C and urea was added to achieve a concentration of 16mM. Finally, the

pre-hydrated and incubated yeast (Superstart instant dry yeast) was used to inoculate the fermenter to a concentration of approximately 2 x 10^7 CFU/mL.

After 72 hours of fermentation, the remaining solids in the fermenter were dried using a two stage process which involved the evaporation of the liquid phase in rotary evaporator at 72°C, followed by freeze-drying at -60°C at ~4 x 10^4Pa for 72 hours. This produced the DDGS samples analyzed in this thesis.

Appendix 2 - Methods used for confocal microscopy of cereal flour and DDGS

Samples of flour or DDGS (10-15mg) were stained in 10µL of freshly made APTS solution (20mM APTS in 15% acetic acid) and 10µL of 1M sodium cyanoborohydride at 30°C for 15 hours. This was followed by a series of centrifugation and rinsing steps to remove excess dye. The samples were then dispersed in 0.5mL of Pro-Q Diamond solution (Molecular Probes, Eugene, OR) at room temperature for 1 hour. After washing with deionized water five times, the stained samples were suspended in 0.5mL of 50% glycerol for observation.

Stained samples were dropped into a glass bottom culture dish (MatTek, Ashland, MA), mixed with 0.1mL of deionized water, covered with a glass slip, and then observed with a confocal laser scanning microscope (LSM 710, Carl Zeiss MicroImaging GmbH, Jena, Germany). The microscope used a x40 1.3 oil objective lens and samples were excited using 488 and 561nm wavelengths (operating at 1 and 4% of power capacity, respectively) with an emission light interval of 490-560nm. Images were recorded with ZEN 2009 software (Carl Zeiss MicroImaging GmbH, Jena, Germany).

Appendix 3 - Statistical analysis methods

All samples were analyzed in triplicate using SAS statistical software (SAS version 9.2). A general linear model was used to test the main effects of grain type (barley, corn, triticale, and wheat); processing (jet-cooking, raw starch hydrolysis, oven-drying, and freeze-drying); treatment (Megazyme, Megazyme + DMSO, Megazyme + KOH, Megazyme + NaOH [at each pH level], and acid hydrolysis) and any interactions. The data was organized into separate groups based on these variables (see Table 1 below).

Table 1: Statistical grouping of the DDGS samples into variables (see the level descriptions above)

Variable	Levels
Grain	4
Processing	4
Treatment	7

The total number of observations used for the stats analysis can be calculated by multiplying the levels of each variable by the number of replicates. This study used three replicates, so:

Equation 1: Calculating the number of observations (n)

4 (grain type)*4 (processing)*7 (treatment)* 3(replicates) = 336 total observations

Using the SAS software (version 9.2) an ANOVA table was generated. The ANOVA table calculates the degrees of freedom, sum of squares, mean squares, and an F value.

Table 2: ANOVA table

Source	Degrees of Freedom	Sum of Squares	Mean square	F value
Model	111	2367.04	21.32	752.54
Error	223	6.32	0.03	
Corrected total	334	2373.36		

Following the ANOVA analysis an unprotected Fishers LSD test was used to analyze the differences between means. The Fishers LSD test uses the pooled standard deviation, or the square root of the mean square error, determined by ANOVA to determine a standard error (SE):

Equation 2: Calculating standard error

$$SE = \frac{\sigma}{\sqrt{n}}$$

Where: σ = the pooled standard deviation of the mean

n= the number of observations in the populations being compared

The denominator used to calculate standard error is based on the populations being compared. Population values within variables can vary, so different standard error values need to be calculated for each variable. An example of this calculation for the treatment variable (7 levels) is provided below.

Example 1: Calculation of standard error for the treatment variable

$$SE = \frac{\sqrt{0.3}}{\sqrt{(336/7)}}$$

$$SE = 0.024$$

This standard error calculation used the total number of observations (336) and divided it by the number of treatment levels (7). In other words, each treatment level measured a total of 48 samples. In the case of grain or processing type the number of levels equals 4, which indicates that 84 samples are within each grouping.

The standard error (SE) is used to calculate a t-value.

Equation 3: T-value calculation

$$t\text{-}value = \frac{[\chi_1 - \chi_2]}{SE}$$

Where: χ = mean of sample populations being compared

SE = standard error

Significant differences are then calculated between the observed values by converting the t-value into P-values, which is calculated automatically using the SAS software. Alternatively, this can be done manually using tables. Significance for this analysis was declared at both $P < 0.05$ and <0.001.